Design Guidance for Electrospun Nylon 6 Nanofiber Morphology through Design of Experiment and Statistical Analysis Method and Mechanical Properties Characterization

by

Feng Pan

A thesis submitted in partial fulfillment of the requirements for the degree of

Master of Science

Department of Mechanical Engineering
University of Alberta

© Feng Pan, 2014

Abstract

Electrospinning is an efficient and versatile technique to fabricate polymer nanofibers. In this study, ultrafine Nylon 6 nanofibers were successfully fabricated by the electrospinning technique. The electrospinning voltage, solution concentration and flow rate are three parameters that have been reported to have effects on nanofiber morphology and will be further investigated in this study. The design of experiment and statistical analysis methods were successfully applied to investigate the effects of electrospinning parameters on nanofiber diameters and uniformity, and whether the effects are linear or nonlinear. In addition, interaction effects between the parameters were studied. The mechanical properties of fiber strips, i.e., elongation at break, elongation at maximum stress, tensile strength and elastic modulus, were analyzed. Moreover, the relationship between the mechanical properties and the Nylon 6 solution concentration was examined. The significant findings from this study are: (1) solution concentration, electrospinning voltage, flow rate all have significant effects on Nylon 6 fiber diameter and uniformity; (2) the solution concentration has the most significant effect on fiber diameter and the effect is nonlinear; (3) the average fiber diameter increases with increasing solution concentration and the decrease of both electrospinning voltage and flow rate; (4) the fiber diameter is most consistent when both electrospinning voltage and flow rate are chosen at the highest possible levels for a certain fixed solution concentration; and (5) tensile strength and elongation at break of fiber strips increase with increasing Nylon 6 solution concentration.

Acknowledgements

I would like to take this opportunity to acknowledge to the people who have assisted me finish this thesis project and help me during my master study at the University of Alberta. My primary thanks go to my supervisors: Dr. Pierre Mertiny and Dr. Cagri Ayranci. Thank you very much for your leadership, advice and the thesis project funding. Thank you very much for your effort of reviewing my thesis. During my master study under your supervision, I learned how to become a good researcher. I also would like to thank Dr. Kajsa Duke who gave me a lot of useful advice for the design of experiment of my thesis project. In addition, I want to thank my friend, Tamran Hughen Lengyel, who provided me many useful suggestions not only in research but also in my life during my master study in Edmonton.

Table of Contents

Abstract ii

Acknowledgements iii

Table of Contents iv

List of Tables vi

List of Figures vii

List of Abbreviations x

Chapter 1 - Introduction 1

1.1 Background and applications of the electrospinning technique 1

1.2 Electrospinning process 3

1.3 The effects of electrospinning parameters on electrospun nanofibers 5

1.4 Different types of nanofibers that can be fabricated by electrospinning 7

1.5 Objective of the thesis project 8

1.6 Structure of the thesis 11

Chapter 2 - Experimental Methodology 12

2.1 Solution and electrospinning preparation 12

2.2 SEM characterization of electrospun Nylon 6 nanofibers 14

2.3 Viscosity measurements 15

2.4 Mechanical properties characterization of electrospun Nylon 6 nanofibers 16

Chapter 3 - Design of Experiment for Electrospinning Nylon 6 Nanofibers 19

Chapter 4 - Results and Discussions 24

4.1 Viscosity measurements 24

4.2 SEM analysis results 26

4.2.1 SEM analysis of electrospun Nylon 6 nanofibers with 10wt% solution concentration 26

4.2.2 SEM analysis of electrospun Nylon 6 nanofibers with 25wt% solution concentration 29
4.2.3 SEM images analysis for DOE screening test 31
4.2.4 SEM images analysis for the second step of the DOE study (original group) 33
4.3 Statistical analysis results 35
4.3.1 Statistical analysis for the screening test of the DOE study 35
4.3.2 Statistical analysis for the second step of the DOE study 42
Chapter 5 - Mechanical Properties Characterization of electrospun Nylon 6 fibers 64
Chapter 6 - Conclusions and Future Work 69
6.1 Summary of the thesis 69
6.2 Future directions 71
1. Mechanical property of single fibers 71
2. Adding nanoscale fillers to polymer solution 72
3. Increasing the number of tensile testing fiber mat specimens 72
Bibliography 74
Appendix A 78
Appendix B 80
Appendix C 85
Appendix D 86

List of Tables

Table 1. Advantages and disadvantages of major nanofiber formation techniques. Adopted from [3,4,5]. 2
Table 2. Synthetic and natural polymers with solvents and their concentrations used commonly during electrospinning. Adopted from [4]. 3
Table 3. Applications of electrospun Nylon 6 nanofiber. 9
Table 4. Properties of electrospun Nylon 6 fiber mats with concentrations of 15wt%, 17.5wt% and 20wt%. 19
Table 5. Coded levels and real level values of variables for the screening test. 22
Table 6. Coded levels and real level values of variables for the mixed two- and three-level design in the second DOE step. 23
Table 7. 2^3 full factorial design table with the results from the screening test of DOE study. 36
Table 8. Mixed two- and three-level full factorial design table with all results for the second step of the DOE study. 43
Table 9. Regression model predicted fiber diameter values and absolute difference between experimental fiber diameter and regression model predicted values for all 36 test runs. 49
Table 10. Regression model predicted standard deviation values and absolute difference between experimental values and regression model predicted standard deviation values for all the 36 runs. 57
Table 11. Experimental average standard deviation values of the two groups and the regression model predicted values. 59
Table 12. Elongation at maximum stress and at break, tensile strength and elastic modulus of Nylon 6 fiber mat tensile specimens for different electrospinning solution concentrations. 66
Table 13. The average Nylon 6 fiber diameter and electrospinning parameters for the three different groups of tensile test samples. 69

List of Figures

Figure 1.Schematic of the electrospinning process. 4
Figure 2.Schematic drawing of the electrospinning process. 4
Figure 3. Schematic figure of solid, porous, core/shell, hollow nanofiber. 7
Figure 4. Number of publications on electrospinning since 1995 (search was conducted in SCOPUS) [34]. 8
Figure 5. Chemical formulation of Nylon 6 [38]. 9
Figure 6. Electrospinning setup. 13
Figure 7. Gold-coated SEM samples cut from fiber mats. 14
Figure 8. BROOKFIELD RVDV-III Ultra programmable rheometer. 15
Figure 9. Measureable range of the SC4-21spindle. 16
Figure 10. Nylon 6 fiber strip for tensile testing with Parafilm cover at both extremities. 17
Figure 11. BOSE ES Series III ElectroForce test instrument. 18
Figure 12. Tensile test specimen that broke in the gauge section center during tensile testing. 18
Figure 13. Viscosity of Nylon 6 solution versus shear rate for solution concentrations ranging from 10wt% to 20wt%. 25
Figure 14. SEM images of electrospun Nylon 6 fibers with 10wt% solution concentration for different electrospinning voltages and flow rates: (a) 12kV, 2µl/min; (b) 20kV, 2µl/min; (c) 12kV, 5µl/min; and (d) 20kV, 5µl/min. 27
Figure 15. SEM image of electrospun Nylon 6 fibers with solution concentration of 10wt%, electrospinning voltage of 12kV and flow rate of 2µl/min. 28
Figure 16. SEM image of electrospun Nylon 6 fibers with solution concentration of 10wt%, electrospinning voltage of 12kV and flow rate of 5µl/min. 28
Figure 17. SEM images of electrospun Nylon 6 fibers with 25wt% solution concentration at electrospinning voltages of 16, 20, 24kV and flow rates of 2 and 5 µl/min. 30
Figure 18. SEM images with average fiber diameters for the screening test of DOE study at different levels of solution concentration, flow rate and electrospinning voltage. 32
Figure 19. Nylon 6 fiber diameter distribution plots for samples prepared with 20wt% solution concentration, flow rate of 5µl/min and electrospinning voltage of (a) 12kV and (b) 24kV. 33

Figure 20. SEM images with average fiber diameters for electrospun Nylon 6 nanofibers made with different solution concentrations and electrospinning voltages and a fixed flow rate of 2µl/min. 34
Figure 21. SEM images with average fiber diameters for electrospun Nylon nanofibers made with different solution concentrations and electrospinning voltages and a fixed flow rate of 5µl/min. 35
Figure 22. Mean plots of fiber diameter versus, correspondingly, solution concentration, electrospinning voltage and flow rate for the screening test. 38
Figure 23. Mean plots of standard deviation of fiber diameter versus solution concentration, electrospinning voltage and flow rate for the screening test. 41
Figure 24. Pareto Chart for the effect of electrospinning parameters on fiber diameter in the second step of the DOE study. 45
Figure 25. Mean plots of fiber diameter versus, correspondingly, solution concentration, electrospinning voltage and flow rate for the second step of the DOE study. 46
Figure 26. Relationship between fiber diameter and solution concentration for electrospinning voltage levels of -1, 0 and 1. 47
Figure 27. Relationship between fiber diameter and electrospinning voltage for solution concentration levels of -1, 0 and 1. 47
Figure 28. Regression model predicted fiber diameters versus experimental fiber diameters. 48
Figure 29. Fitted surface response plots showing the nanofiber diameter as a function of (a) electrospinning voltage and solution concentration for a fixed flow rate, and (b) flow rate and solution concentration for a fixed electrospinning voltage. 50
Figure 30. (a) Normal probability plot of residuals, (b) plot of residual values versus predicted values and (c) plot of predicted values versus the observed values for the fiber diameter. 51
Figure 31. Pareto Chart for the effect of the electrospinning parameters on the standard deviation of fiber diameter in the second step of the DOE study. 53
Figure 32. Mean plots of standard deviation of fiber diameter versus solution concentration, electrospinning voltage and flow rate for the second step of the DOE study. 54
Figure 33. Relationship between the standard deviation of fiber diameter and electrospinning voltage for solution concentration levels of -1, 0 and 1 55

Figure 34. Relationship between the standard deviation of fiber diameter and electrospinning volate for flow rate levels of -1 and 1. 55
Figure 35. Relationship between the standard deviation of fiber diameter and solution concentration for flow rate levels of -1 and 1. 56
Figure 36. Fitted surface response plots showing the standard deviation of fiber diameter as a function of (a) electrospinning voltage and solution concentration for a fixed flow rate, and (b) flow rate and solution concentration for a fixed electrospinning voltage. 61
Figure 37. Surface response plots showing the standard deviation of fiber diameter as a function of (a) electrospinning voltage and flow rate for a fixed solution concentration at level: 0 (b) electrospinning voltage and flow rate for a fixed solution concentration at level: 1 (c) electrospinning voltage and flow rate for a fixed solution concentration at level:-1 63
Figure 38. (a) Normal probability plot of residuals and (b) plot of residual values versus predicted values for fiber diameter standard deviation in the second step of the DOE study. 64
Figure 39.Tensile stress/strain curves of Nylon 6 nanofiber mats electrospun from solutions with concentrations of 15wt%, 17.5wt% and 20wt%. 65
Figure 40. Elongation at break versus solution concentrations for electrospun nanofiber mat specimens. 68
Figure 41. Tensile strength versus solution concentrations for electrospun nanofiber mat specimens. 68
Figure 42. Elastic modulus versus solution concentrations for electrospun nanofiber mat specimens that failed in the gauge section center. 68
Figure 43. Elastic modulus versus solution concentrations for all the electrospun nanofiber mat specimens. 69

List of Abbreviations

CVD: Chemical Vapor Deposition

SEM: Scanning Electron Microscopy

DOE: Design of experiment method

D: Fiber diameter

S: Standard deviation of fiber diameter

C: Solution concentration of Nylon 6

V: Electrospinning Voltage

F: Flow rate

$ø_{mat;}$ Mat porosity

$\rho_{mat:}$ Mat density

T: Tensile force

σ: Tensile stress

A: Cross sectional area

δ: Average thickness of fiber mat

W: Average width of the tensile testing fiber mat strip

Chapter 1 - Introduction

1.1 Background and applications of the electrospinning technique

Ultrafine polymer nanofibers exhibit unique characteristics such as high surface-to-volume ratio and small pore sizes between nanofibers within fiber mats. These properties are useful in a variety of applications, such as the fields of nanocomposite materials, separation membranes, and biomedical systems [1,2].

Several manufacturing techniques are available to fabricate nanofibers, including wet spinning, dry spinning, solution electrospinning, melt spinning, needleless electrospinning and centrifugal electrospinning. For the above techniques, except the melt spinning, solvent is needed to dissolve the polymer to make the polymer dope, which consists of a polymeric material and a mixed solvent as a whole system. In addition, compared to thermoset polymers, thermoplastic polymers are more commonly used for these techniques. Polyurethane is one example of thermoset polymers used for the spinning technique. In wet spinning, the spinneret is immersed in a polymer bath. The polymer which is dissolved in the solvent is extruded directly into a liquid. The solidification of fibers occurs during their precipitation [3]. In dry spinning, fibers are solidified under a stream of hot air and the solvent is removed by heating. Solution electrospinning is a dry spinning technique. The difference between solution electrospinning and dry spinning is that solution electrospinning does not require heating to remove the solvent. In solution electrospinning, ultrafine fibers are solidified due to simple solvent evaporation under ambient conditions [3]. Needleless electrospinning is based on the basic electrospinning principle except that no needle is used for discharging the solution [4]. Melt spinning involves a similar spinneret extrusion process as dry spinning; however, unlike dry spinning, the polymer melt is used as the spinning dope [3]. For centrifugal electrospinning, the spinneret is rotated during electrospinning and aligned nanofibers are collected on a circular collector enclosing the rotating spinneret [3, 5]. Advantages and disadvantages of these methods are summarized given in Table 1.

Based on the comparison of the different fiber manufacturing techniques in Table 1, it can be concluded that the electrospinning technique is an effective method for fabricating nanofibers from a wide range of different polymers. The electrospinning technique is also a rather efficient

way to generate various kinds of nanofibers, including conductive polymer nanofibers and composite nanofibers, e.g. ceramic and metal particles based nanofibers [6,7].

Table 1. Advantages and disadvantages of major nanofiber formation techniques. Adopted from [3,4,5].

Process method	**Advantage**	**Disadvantage**
Wet spinning	Non-solvent for fiber solidification	Slow
Dry spinning	Fast, large-scale production	Not applied for thermoplastics
Solution electrospinning	Fast, setup is very simple, very wide range of polymer solution can be electrospun	Bending instability limit the deposition precision, scale up has been challenging
Melt spinning	No solvent is used in melt spinning	Need proper machine for melt spinning; high heat input during the process
Melt electrospinning	No solvent is used in melt electrospinning	Expensive setup needed to maintain elevated temperature of the melt during the process
Needleless electrospinning	No clogging of syringe needle	Very small amount of solution can be electrospun; solution at the tip may solidify quickly
Centrifugal electrospinning	Fabricate highly aligned nanofibers at a large scale	Setup is more complicated compared to the solution electrospinning

Electrospinning is a very versatile process. A wide range of materials can be electrospun to fabricate nanofibers with great control over the end properties [7,8]. Compared to other fiber fabrication methods, the electrospinning technique is more suitable to produce long and thin polymer nanofibers [6, 9]. In addition, the electrospinning technique can create aligned continuous polymer fibers [10]. In addition to round nanofibers, electrospinning can produce thin nanofibers with a variety of cross-sectional shapes, such as flat ribbon, bent ribbon and ribbon with two tubes [11,12]. Another characteristic of electrospinning is the rapid formation of nanofiber structures, which may form in time periods of less than a millisecond [13,14].

A broad range of polymers have successfully been electrospun for many different applications [1,15]. Because of the unique properties of the electrospinning process, many synthetic and natural polymers have been electrospun into nanofibers for a variety of applications such as filtration and thermal insulation, sensors, tissue engineering, wound dressing, and enzyme immobilization[16,17]. Some of the examples of synthetic polymers and natural polymers that have successfully been electrospun are given in Table 2.

Table 2. Synthetic and natural polymers with solvents and their concentrations used commonly during electrospinning. Adopted from [4].

Synthetic Polymer	**Solvent**	**Concentration**
Nylon 4,6	Formic acid	10wt%
Nylon 6	1,1,1,3,3,3 hexafluoro-2-2-propanol	15wt%
Nylon 6, 6	Formic acid	12.1wt%
Nylon 12	1,1,1,3,3,3 hexafluoro-2-2-propanol	15wt%
Nylon 6	Formic acid	34%(w/v)
Nylon 6	Formic acid	22%(w/v)
Polycarbonate	Dichloromethane	15wt%
Polystyrene	Chloroform/Dichloroethane/Chlorobenzene	30%(w/v)
Polyurethane	Tetrahydrofuran (THF) and N,N-Dimethylformamide (DMF)	13wt%
Poly(vinyl alcohol) (PVA)	Water	25wt%
Poly(vinyl chloride) (PVC)	THF and DMF	13wt%
Poly(vinyl pyrrolidone) (PVP)	Ethanol /Ethanol and DMF	4wt%
Poly(vinylidene fluoride) (PVDF)	N,N-Dimethylacetamide	25wt%
Poly(etherimide) (PEI)	1,1,2-Trichloroethane	14wt%
Poly(ethylene oxide)	Water	10wt%
Bombyx mori silk fibroin	Formic acid	9-12wt%
Cellulose Acetate	N,N-dimethylacetamide and Acetone	15wt%
Collagen Type I	1,1,1,3,3,3 Hexafluoro-2-propanol	0.083g/ml
Wheat Gluten	1,1,1,3,3,3 Hexafluoro-2-propanol	10%(w/v)
Gelatin Type A	2,2,2-trifluorethanol	10-12.5wt%

1.2 Electrospinning process

The electrospinning technique is commonly used to fabricate polymeric nanofibers with diameters ranging from less than 3nm to over 1μm [6]. There are three basic components in the electrospinning process: a high voltage supply, a syringe and a needle that hosts the polymeric solution, and an electrically grounded collector [6]. A schematic of the electrospinning process is shown in Figure 1. Polymer nanofibers are electrospun by creating an electrically charged jet of polymer solution [15]. When the electrospinning voltage reaches a critical value at which the repulsive electric force overcomes the surface tension force of the solution, a charged polymer solution jet is ejected from the tip of the needle [1]. The polymer solution droplet acquires the stable shape when the electrical charge between the needle tip and collector is set at a certain critical value. In this case, an equilibrium exists between the electric forces and surface tension of polymer solution at the tip of the needle. Any further increase above the critical potential value will cause the equilibrium to vanish. Under the critical electrical potential, the polymer solution droplet will form a stable conical shape at the tip of the needle. This conical shape is

referred to as the Taylor cone having a distinct half angle. The half angle does not depend on fluid properties. The reason is that the increase of surface tension is always accompanied by an increase of the critical electric field [15,18]. The schematic Taylor cone at the tip of the needle during the electrospinning process is shown in the Figure 2. After the Taylor cone, the electrically charged polymer solution jet travels for a short distance in a straight line. This is known as the stable region. Then, at the end of the straight line, an unstable region is present prior to deposition on the collector. In this unstable region, the charged solution jet describes a conical helix due to so-called bending instability [14].

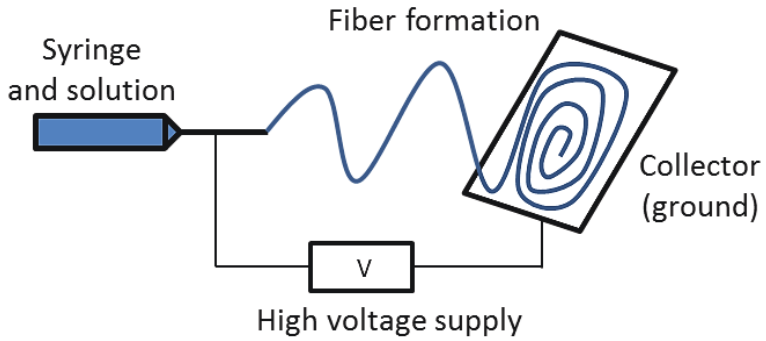

Figure 1.Schematic of the electrospinning process.

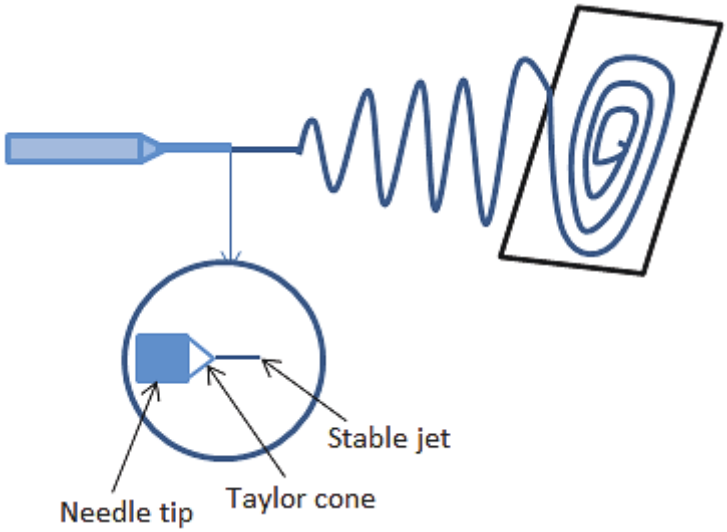

Figure 2.Schematic drawing of the electrospinning process.

The polymer solution jet undergoes an elongation due to the applied high voltage between the needle and the collector [6]. Meanwhile, the solvent evaporates, leaving behind polymer nanofibers, which lay randomly on the collecting metal plate, which is grounded [1,15].

1.3 The effects of electrospinning parameters on electrospun nanofibers

Users have great control over the end product by tailoring the parameters that affect the electrospinning process. These parameters include the (1) solution concentration, (2) applied voltage to form the electric field, (3) the distance between the tip of the needle and the grounded collector, and (4) the flow rate of the solution [19]. These four electrospinning parameters affect the nanofiber morphology and properties. In the following, a brief introduction about the effects of these parameters on the electrospinning process is given.

As mentioned above, the electrospinning voltage is the electrical potential applied between the needle and the collector. The electrospinning voltage must set within an appropriate range. When the voltage is low, not enough electric force can be generated to overcome the surface tension of polymer solution to form nanofibers [1]. Electrospun nanofibers can only be fabricated when the applied electrospinning voltage is above a critical value [20]. However, when voltage is too high, the electric force will be much larger than the surface tension of the solution, leading to instabilities in Taylor cone formation. The solution jet may spray out quickly, which negatively affects nanofiber morphology. Therefore, determining a suitable range for the electrospinning voltage is an important step for the design of an electrospinning process. Deitzel et al. [21] found that increasing the electrospinning voltage from 5.5kV to 9kV affects the shape of the initiating jet at the tip of needle, and thus on the structure and morphology of electrospun poly (ethylene oxide) (PEO) fibers. Megelski et al. [22] ascertained that the polystyrene (PS) fiber diameter decreases with the increase of the electrospinning voltage from 5kV to 12kV. Buchko et al. [23] also found that the Nylon 6,6 fiber diameter decreases with the increase of the electrospinning voltage from 4kV to 8kV. In addition, generally, it has been accepted that an increase in electrospinning voltage will generate higher mass flow from the needle tip, which will increase the deposition rate [19].

The flow rate is the rate of electrospinning solution emanating from the charged needle tip [24]. The flow rate affects the jet velocity and material transfer rate [19]. For electrospinning poly(D,L-lactic acid) (PDLA) nanofibers, it was observed that the electrospun nanofiber with relatively large fiber diameter was fabricated at a higher flow rate [20]. Clearly, the flow rate affects the nanofiber morphology. When the flow rate is too high, however, some large beads may form in the collected fiber mats. The reason for this is that the droplet forming at the needle

tip will be larger and the solution jet will move faster at a higher flow rate [20]. Also, solvent may not evaporate before reaching the collector, resulting in large beads in the fiber mat [20].

The electrospinning solution concentration is the polymer concentration in the solvent-based solution. Consequently, the solution concentration affects the solution viscosity. Viscosity plays an important role in determining the range of concentration to obtain electrospun fibers [21]. When the solution concentration is too low, the electrospinning solution jet will be unstable and the jet will break down [1]. However, when the solution concentration is too high, it will be difficult to form electrospun fiber as the solution would dry at the needle tip due to the high viscosity [1]. The solution concentration also controls the electrospun fiber structure and morphology [19]. Both Deitzel et al. [21] and Megelski et al. [22] found that the electrospun fiber diameter increased with increasing solution concentration.

The electrospinning distance is the distance between the needle tip and the collector. For different kinds of polymer, the range of electrospinning distance to obtain good nanofiber morphology is different. An appropriately larger electrospinning distance provides the electrospun fibers with more time to evaporate the solvent [24]. But, when the distance is higher than the electrospinning distance range, not sufficient amount of fibers can be collected on the collector. Since the needle to collector distance affects the deposition time and evaporation rate, it also affects the structure and morphology of electrospun fibers [19]. An insufficient needle to collector distance, which is lower than the electrospinning distance range, will produce wet fibers and bead structures in the electrospun fiber mats. Megelski et al. [22] found that the beads structures started to form for a distance lower than 5cm when electrospinning polystyrene (PS) nanofibers. Buchko et al. [23] also ascertained that an insufficient distance can produce wet fibers and bead structures.

Finally, also the collector will have an effect on the electrospinning process. For most electrospinning setups, the collector is made of a conductive material that is electrically grounded to guarantee a stable potential difference between the needle and collector. The most commonly used conductive collector for electrospinning is aluminum foil [4]. When a non-conductive material is used as collector, fibers are more loosely packed because the electric charge on the electrospinning jet is accumulated on the collector and the charge causes fibers to repel each other [4,25]. On the other hand, when a conductive material is used as the collector,

the electric charge on the fibers is dissipated and the repulsion among fibers is reduced, leading to a thick fiber mat and fibers being closely packed together. Furthermore, it was found that collectors of varying conductivity and geometry influence fiber arrangement and pore morphology [25]. Whether the collector is stationary or rotating will further affect the electrospinning process. A rotating collector enables collecting aligned nanofibers, and also provides more time for solvent to evaporate [4]. Therefore, a rotating collector can produce more well-aligned and uniform electrospun fibers [26].

1.4 Different types of nanofibers that can be fabricated by electrospinning

As shown by the schematic in Figure 3, different types of nanofibers can be produced, including solid, core/shell, hollow and porous fibers that can fulfill the requirements for applications in the fields of tissue engineering scaffolds, drug delivery, microfluidics, photonics and energy storage [27,28,29]. This versatility and ease in tailorability of the end product properties has attracted much research attention.

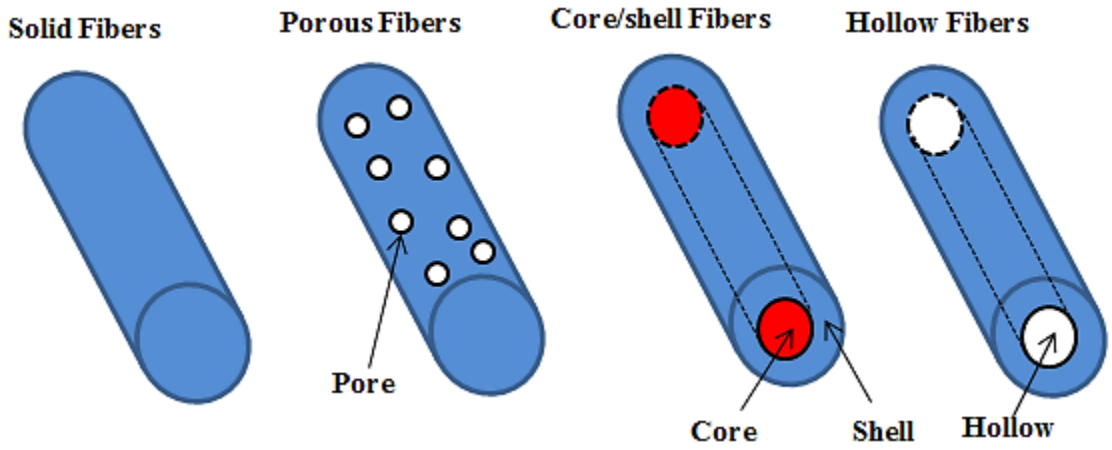

Figure 3. Schematic figure of solid, porous, core/shell, hollow nanofiber.

It was found that the humidity of the electrospinning environment played an important role in the formation of porous nanofibers. In addition, the type of polymer, solvent and electrospinning conditions affected the pore size of the porous nanofibers [4]. Megelski et al. [22] successfully fabricated electrospun porous polystyrene nanofibers and poly (methyl methacrylate) (PMMA) nanofibers. Bognitzki et al. [30] successfully electrospun porous polycarbonate (PC) nanofibers and poly (L-lactic acid) (PLLA) nanofibers.

Bognitzki et al. [31] used a chemical vapor deposition (CVD) method to fabricate poly (p-xylylene) (PPX) hollow nanofibers, and McCann et al. [29] applied the direct co-axial spinning method to fabricate polyvinylpyrrolidone (PVP)–TiO_2 hollow nanofibers. Another unique application of the co-axial electrospinning process is to fabricate the core-shell nanofibers. Zhang et al. [32] and Sun et al. [33] successfully applied the co-axial electrospinning method to fabricate polycaprolactone (PCL)-r-Gelatin and poly (ethylene oxide) (PEO)/ polysulfone (PSU) core-shell nanofibers respectively.

In general, the interest in electrospinning is growing dramatically, indicated by the number of scientific publications, which is exponentially increasing since early 1990's. The database SCOPUS lists over 11,969 publications since 1995 (see Figure 4) [34].

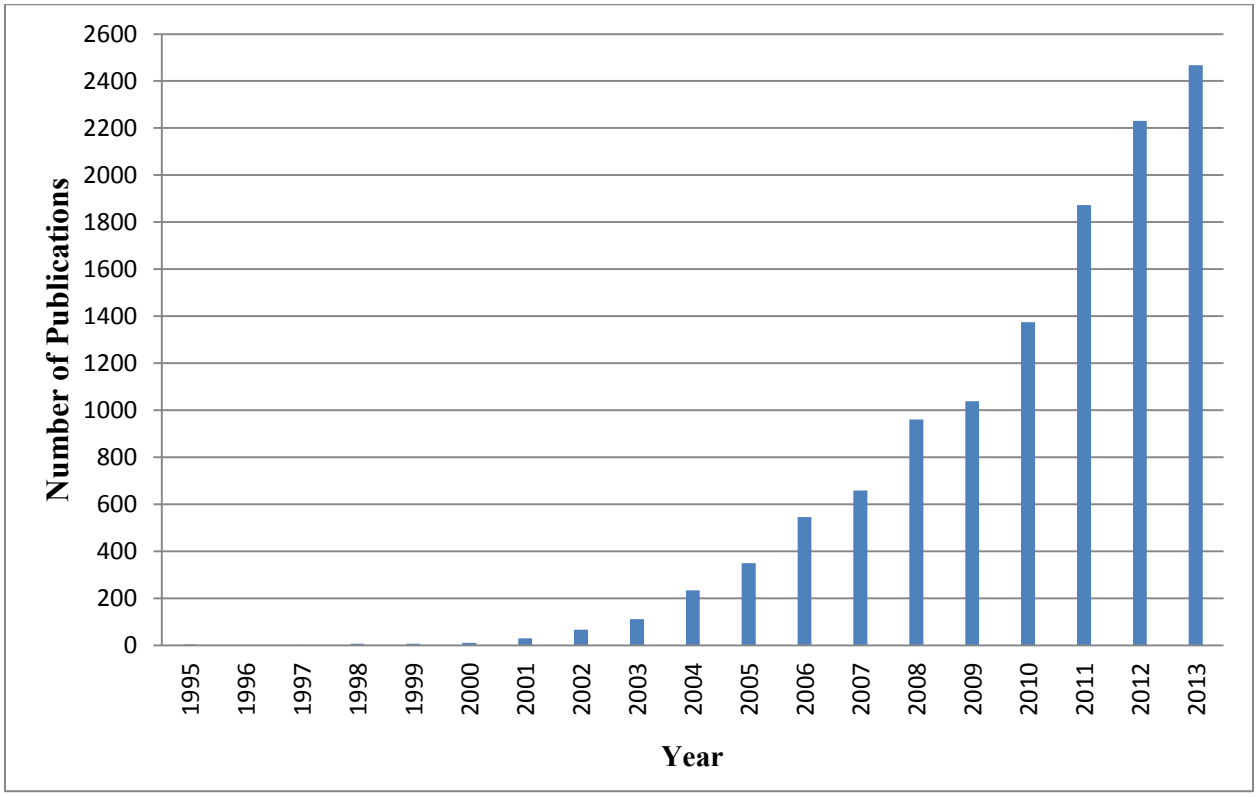

Figure 4. Number of publications on electrospinning since 1995 (search was conducted in SCOPUS) [34].

1.5 Objective of the thesis project

As can be seen from the preceding information and Table 2 above, there is a broad range of polymers and solvents that can be used for electrospinning. Amongst these, the polymer 'Nylon'

(Nylon 6, Nylon 6,6, Nylon 12 and Nylon 4,6) is commonly used in a broad range of applications. Some of examples for applications of electrospun Nylon 6 fibers are given in Table 3.

Nylon 6 is a synthetic semicrystalline polyamide, which is biodegradable and biocompatible and has good mechanical and physical properties [35,36]. The chemical formulation of Nylon 6 is given in Figure 5. Nylon 6 has high resistance against a variety of chemicals such as acids and some weak base for the initial substrate and matrix in the biomedical field [37]. As such, electrospun Nylon 6 nanofibers have widely been applied in the biomedical fields as shown in Table 3.

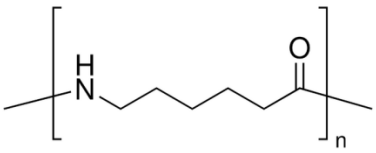

Figure 5. Chemical formulation of Nylon 6 [38].

In addition to its biomedical applications, Nylon 6/carbon nanotube nanocomposite fibers were successfully electrospun by different research groups [39,40,41]. It was found that these composite nanofibers were promising for strain sensor and electronic textiles applications [39,41].

Table 3. Applications of electrospun Nylon 6 nanofiber.

Polymer	**Solvent**	**Applications**	**Reference**
Nylon 6	1,1,1,3,3,3-hexafluoro-2-propanol	Tissue engineering devices	[35]
Nylon 6	Formic acid	Ultrafine nanofibers	[2]
Nylon 6,6	Formic acid	Biocompatible thin films	[23]
Nylon 6	1,1,1,3,3,3-hexafluoro-2-propanol	Electronics and sensor applications	[42]
Nylon6/Gelatin	Formic acid and acetic acid	Biomedical applications	[36]
Nylon 6	Formic acid	Medical applications	[37]
Nylon 6	Formic acid	Nano device applications	[43]
Nylon 6	Formic acid	Nanofibrous membranes as air filters	[44]
Nylon 6	Formic acid	Wound-healing applications	[45]
Nylon 6/ SWNTs	Formic acid	Strain sensor	[39]
Nylon6/ MWNTs	Formic acid	Electronic textiles applications	[41]

Although Nylon 6 is a commonly used polymer for electrospinning, only a limited number of publications [46,47,48,49] report on the effects of electrospinning parameters on the formation of Nylon 6 nanofibers and fiber morphology.

Chowdhury et al. [46] investigated the effects of voltage, concentration, flow rate and tip to collector distance on the diameter of electrospun Nylon 6 fibers. They found that fiber diameter increased with increasing concentration and flow rate. Conversely, the fiber diameter decreased with the increase in voltage and tip to collector distance. Sohrabi et al. [47] investigated the effect of the applied electric field on fiber diameter with the Nylon 6 concentration fixed at 15wt%. They found that the distribution of Nylon 6 nanofibers was finest with the narrowest size distribution when the applied electric field was 1kV/cm. Bazbouz et al. [48] investigated the effects of solution concentration and electrospinning voltage on Nylon 6 nanofiber morphology. They found that the solution concentration played an important role in the fiber morphology. They also found that the fiber diameter increased with the increase of concentration and the decrease of electrospinning voltage. Zargham et al. [49] investigated the effect of flow rate on the Nylon 6 nanofiber morphology. They found that there were a large number of branched and splitting fibers and beads when the flow rates were 1ml/hr and 1.5ml/hr. They suggested that the high flow rate may have caused the fiber to be collected without sufficient time for solvent evaporation. In addition, they also ascertained that the deposition area increased with increasing flow rate.

Heikkilä et al. [50] applied the orthogonal experimental design and the Analysis of the Mean (ANOM) methods to analyze the mean effect of electrospinning parameters, e.g. electrospinning voltage, viscosity, distance and needle size on Nylon 6 nanofiber morphology. They found that the main parameters affecting the fiber diameter were viscosity of solution and the strength of electric field, and the fiber diameter increased with the increase of viscosity from 500cp to 1500cp. But, without using some advanced statistical analysis methods, such as Analysis of Variance (ANOVA) analysis, effect estimate analysis, regression model analysis, mean plot analysis and surface response method, no conclusive result could be obtained, that is, no parameter was identified to have the most significant effect on fiber diameter and fiber uniformity, and whether or not effects of the interactions between these parameters are significant. In addition, without giving the effect coefficients of each parameter by the effect

estimate analysis, they could not accurately conclude the importance of the effect of all the parameters. Currently, there are no publications investigating the effects of electrospinning parameters on the Nylon 6 fiber diameter and fiber uniformity using the Design of Experiment (DOE) method and multiple advanced statistical analysis methods, such as effect estimate analysis, regression model analysis, mean plot analysis and surface response method. In addition, based on the potential applications of electrospun Nylon 6 nanofibers, determining the mechanical properties of the electrospun Nylon 6 nanofibers is important.

Based on the motivations behind this study discussed above, the six objectives of this study are summarized as follows: (1) To fabricate fine Nylon 6 nanofibers by electrospinning technique; (2) To determine the effects of three important electrospinning parameters, i.e., electrospinning voltage, solution concentration and flow rate, and their interactions on the nanofiber diameter and its standard deviation by DOE method and statistical analysis method; (3) To investigate whether these effects are linear or nonlinear; (4) To identify levels of parameters to electrospin uniform Nylon 6 nanofibers; (5) To characterize the Nylon 6 fiber mat mechanical properties, i.e., elastic modulus, tensile strength, elongation at break and elongation at maximum stress, and investigate the relationship between mechanical properties of fiber mat strips and solution concentration; and (6) To provide design guidance for electrospun Nylon 6 fiber morphology by DOE and statistical analysis methods.

1.6 Structure of the thesis

The thesis is divided into five parts. Chapter 2 concentrates on the experimental methodology used during the study. This includes the electrospinning solution preparation, electrospinning preparation and characterization of electrospun Nylon 6 nanofibers. Chapter 3 introduces the DOE and statistical analysis methods. For the DOE of electrospun Nylon 6 nanofibers, the choice of factors, the test range of factors, levels and specific DOE methods are discussed. Chapter 4 presents the result and their discussion. Results with respect to viscosity measurements, analysis of SEM photos for the screening test and second step of the DOE study, fiber diameter distribution analysis and the statistical analysis of screening test and second step of the DOE study are herein discussed. In the statistical analysis part, the average diameter of Nylon 6 nanofibers and standard deviation of average diameter under different parameters were compared. The effects of solution concentration, electrospinning voltage and flow rate on the average fiber

diameter and the standard deviation of fiber diameter were analyzed. In Chapter 5, results pertaining to the mechanical characterization of three kinds of samples with three different concentrations (15wt%, 17.5wt% and 20wt%) are analyzed and compared. This includes the elongation at break, elongation at the maximum stress, tensile strength and elastic modulus. Finally, in Chapter 6, a summary of the research is given, and possible future directions for this research are discussed.

Chapter 2 - Experimental Methodology

The present chapter 2 describes the experimental methods employed in this study. This includes the electrospinning solution preparation, electrospinning setup, viscosity measurements, SEM and mechanical properties characterization for Nylon 6 nanofibers.

2.1 Solution and electrospinning preparation

Nylon 6 pellets were purchased from Sigma Aldrich Canada (Oakville, Ontario). The density and approximate molecular weight of Nylon 6 is 1.084 g/mL and 10,000 g/mol, respectively. The solvent used for electrospinning, formic acid with the purity of 88%, was obtained from Fisher Scientific Canada (Ottawa, Ontario). Formic acid was chosen as the solvent since it is the most commonly used solvent for Nylon 6 as shown in Table 3. To prepare the electrospinning solution, Nylon 6 pellets were first added into the formic acid. Then, the mixture was stirred with a Cole-Parmer (Montreal, Quebec) magnetic stirrer until the Nylon 6 pellets were completely dissolved in the formic acid and a homogenous and transparent solution was obtained. Various concentrations of Nylon 6 in formic acid were prepared for the experiments, i.e., 10wt%, 15wt%, 17.5wt%, 20wt% and 25wt%.

The final Nylon 6 solution was loaded into a 10ml syringe (BD - Canada, Mississauga, Ontario) fitted with blunt needles (gauge 20 precision glide needle type, 305175, by BD - Canada, Mississauga, Ontario). The blunt needles were cut using a rotary cutting tool with different grade sanding discs (100 series, by Dremel, Mount Prospect, Illinois, USA). The flow rate of the Nylon 6 electrospinning solution was controlled by a syringe pump (Legato 101, by GENEQ Inc., Montreal, Quebec). The electrospinning voltage was controlled and adjusted by a high voltage

supply (model ES30P-5W/DDPM, by Gamma High Voltage Research, Inc., Ormond Beach, Florida, USA). The positive polarity electrode was connected to the syringe needle and the ground electrode was connected to the aluminum foil collector. The laboratory electrospinning setup is shown in Figure 6.

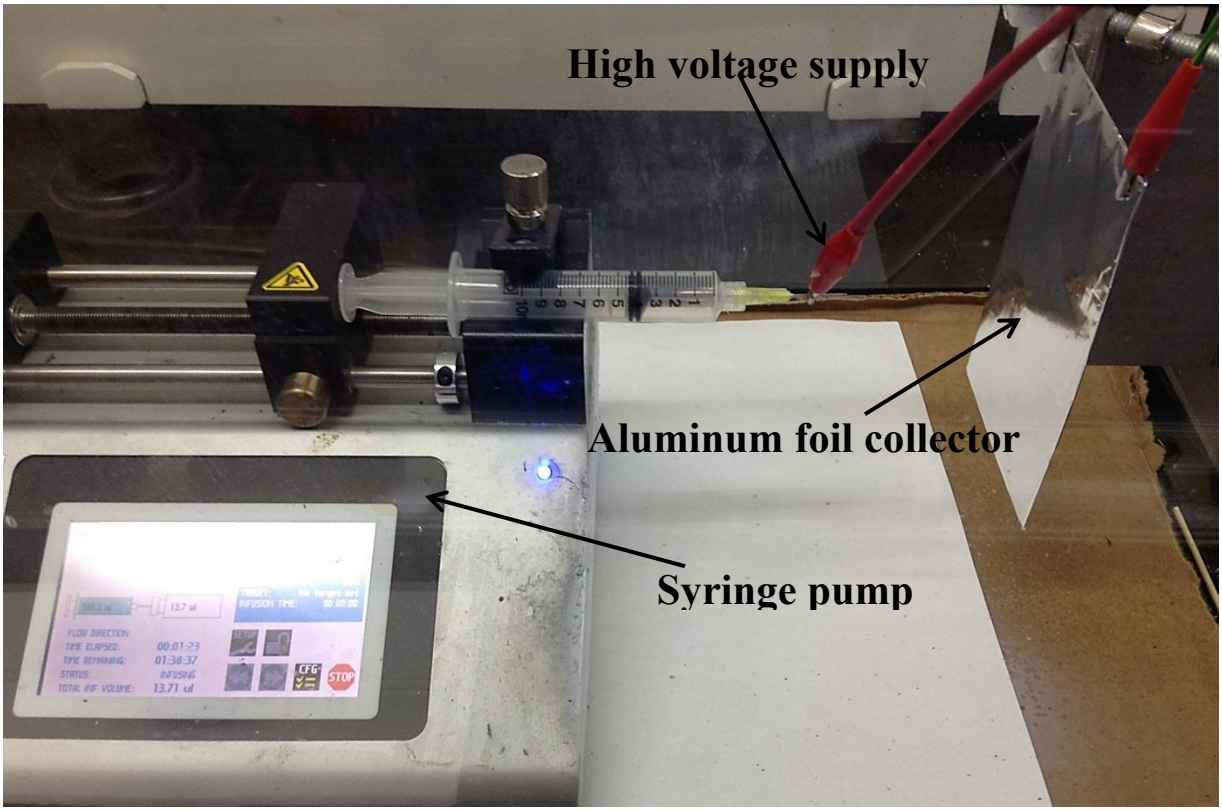

Figure 6. Electrospinning setup.

For the Nylon 6 electrospinning experiment, the electrospinning voltage was adjusted between 12kV and 24kV. The solution concentration was ranged between 10wt% and 25wt% and the flow rate from 2µl/min to 5µl/min. The tip to collector distance between the tip of the needle and the collector remained constant at 10cm because it was found that more electrospun Nylon 6 fibers could be collected at this distance and the solution jets were more stable. Nylon 6 nanofibers were collected on a stationary grounded collector covered by aluminum foil. During the electrospinning process, nanofibers were collected on the surface of the aluminum foil. All the electrospinning experiments were carried out in a fume hood at a temperature of 27ºC and humidity of 34%.

2.2 SEM characterization of electrospun Nylon 6 nanofibers

The diameters of electrospun nanofibers were investigated by Scanning Electron Microscopy (SEM) using a VEGA-3 instrument (TESCAN Brno, s.r.o., Brno-Kohoutovice, Czech Republic). The electrospun Nylon 6 nanofiber samples were coated with gold prior to the SEM analysis. The SEM samples were cut from the middle of the electrospun fiber mats. A fiber mat after cutting of a SEM sample and gold-coated SEM samples are shown in Figure 7. To determine the average fiber diameter and the size distribution of the Nylon 6 nanofibers, a total of three SEM photos from three different locations were taken and analyzed for the three solution concentrations (15wt%, 17.5wt% and 20wt%). For each SEM photo, 20 nanofibers were randomly chosen to measure their diameters. Therefore, for each sample, a total of 60 nanofibers were used to calculate the average nanofiber diameter and the standard deviation. The diameter of Nylon 6 nanofiber was measured using the ImageJ software (version 1.49a, public domain).

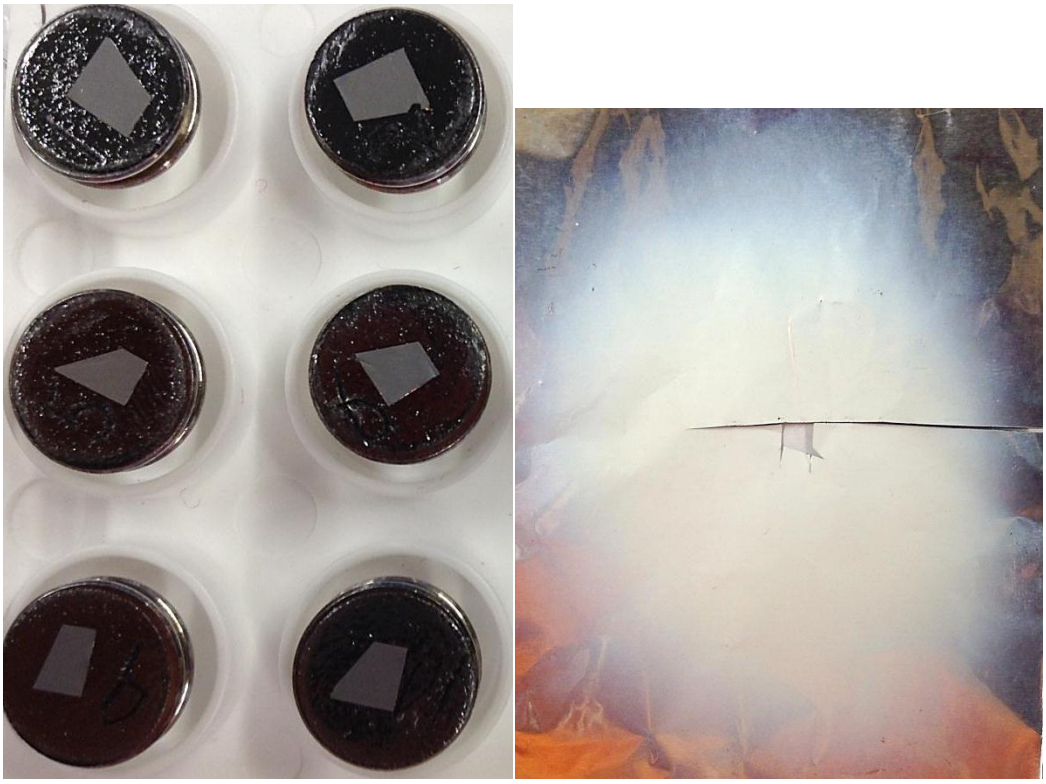

Figure 7. Gold-coated SEM samples cut from fiber mats.

2.3 Viscosity measurements

Shown in Figure 8 is the programmable rheometer which was used for the viscosity measurements (model RVDV-III Ultra, by Brookfield Engineering Laboratories Inc., Middleboro, Massachusetts, USA). A rotating spindle was placed into the solution to determine the viscosities at different rotating speeds and shear rates. The rotational speed limits for the rheometer were 0rpm and 250rpm. The testing temperature was set to 20.3ºC. For the given conditions, a proper spindle needs to be chosen in order to measure the viscosity accurately. A spindle type SC4-21 (Brookfield Engineering Laboratories Inc., Middleboro, Massachusetts, USA) was chosen to measure the viscosity of the given solutions. The measureable range of SC4-21 spindle is shown in Figure 9. From this figure, it can be observed that the viscosity measurement range for the spindle is from 10cp to more than 10^6cp. This test range covers the viscosity of commonly used polymer solutions.

Figure 8. BROOKFIELD RVDV-III Ultra programmable rheometer.

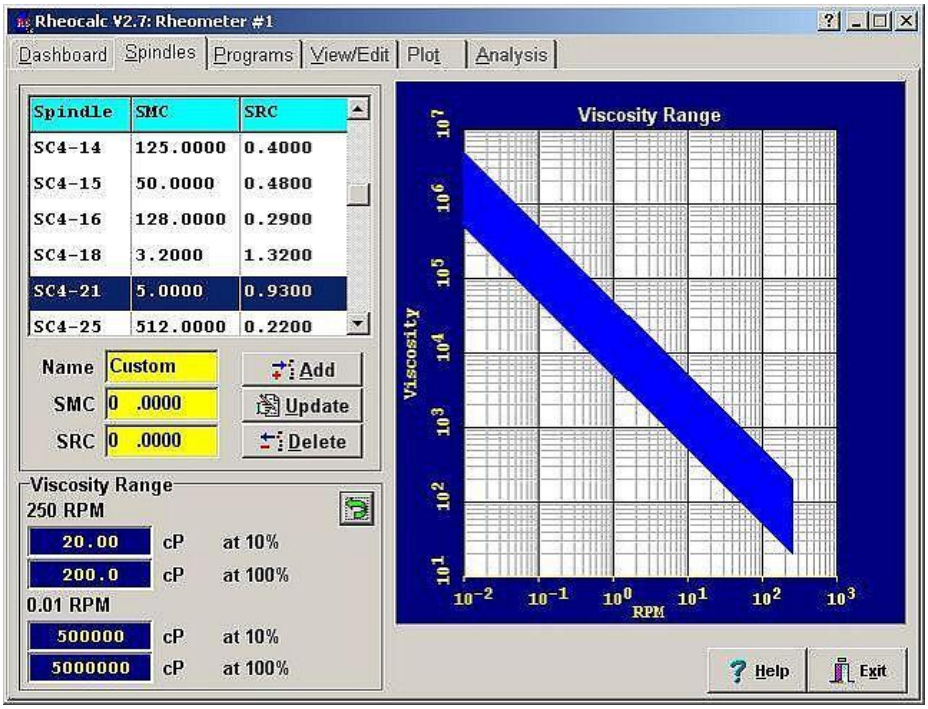

Figure 9. Measureable range of the SC4-21spindle.

2.4 Mechanical properties characterization of electrospun Nylon 6 nanofibers

Mechanical properties were characterized for each solution concentration (15wt%, 17.5wt% and 20wt%) using electrospun nanofiber samples with the smallest standard deviation with respect to the fiber diameter. Note that for solution concentrations of 10wt% and 25wt%, the nanofiber morphology was found to be poor. Results from the SEM image analysis for these concentrations are shown in Chapter 4.2.1 and 4.2.2. The statistical analysis results of the DOE method given in Chapter 4.3 provide a guideline on how to choose mechanical properties testing samples with the smallest standard deviation of fiber diameter.

For the tensile test sample preparation, electrospun Nylon 6 nanofiber mats were first carefully removed from the aluminum foil. Then, the nanofiber mats were cut using a pair of scissors to make a strip. Five test strips with 10mm width and 50mm length were cut from each electrospun fiber mat. For each strip, the width was measured at 10 locations using a digital caliper gauge with a precision of 0.01 mm. The average value of the width was used for calculating stress. The thickness of a representative fiber mat was measured at 10 locations using a digital micrometer with a precision of 0.001mm (ABSOLUTE, by Mitutoyo, Aurora, Illinois, USA). The average thickness was used to calculate the sample cross sectional area.

The shape of the tensile test fiber mat strip is chosen as rectangular. The reason is that it is very reliable to cut the rectangular shape fiber mat strip without causing any damage to the strip during the cutting process and it is easy to determine the cross section area for the rectangular fiber mat strip. Dumbbell shape could promote more reliable failure in the specimen gauge section center. But, there are mainly two issues to prepare the dumbbell shape tensile testing fiber strips and use it for tensile testing. It is challenging to make the desired dumbbell shape specimen without causing any damage to the fiber strips and the cross section area of the dumbbell shape tensile testing fiber strip is difficult to determine.

Nanofiber test strips could not directly be mounted into the grips of the tensile test machine as fiber strips are thus easily damaged. Hence, as shown in Figure 10, both extremities of a nanofiber strip were covered by Parafilm (Pechiney Plastic Packaging Company, Chicago, Illinois, USA).

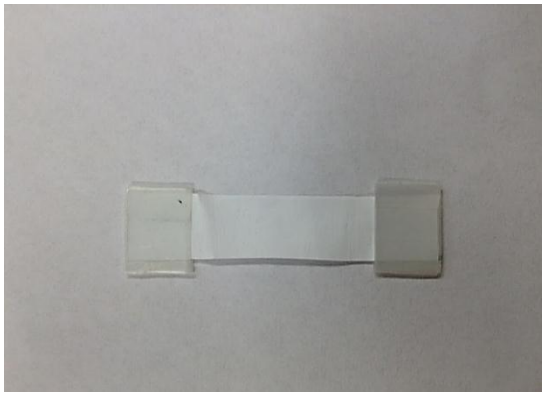

Figure 10. Nylon 6 fiber strip for tensile testing with Parafilm cover at both extremities.

Specimens were tested using an ES Series III ElectroForce tensile testing machine (BOSE, Framingham, Massachusetts, USA), which is shown in Figure 11. The testing machine was equipped with a load cell with maximum capacity of 450 N. During tensile testing, the strips were loaded at a rate of 2mm/min until failure occurred. Only specimens that exhibited necking during the tensile test and failed due to crack propagation from the gauge section center were analyzed for maximum elongation and tensile strength. Specimens that broke from the edge of the grips were omitted for the analysis of elongation and tensile strength since data obtained in such a case is considered erroneous due to the presence of stress concentration at the grips. A test specimen that failed in the gauge section center is shown in Figure 12. For the elastic modulus,

the elastic moduli of specimens that failed in the gauge section center and the elastic moduli of all specimens including the ones that failed at the edge of gripping system were both analyzed. For all the tensile tests, the original length of the strip was measured after adding a preload of 0.1N for the strain calculation.

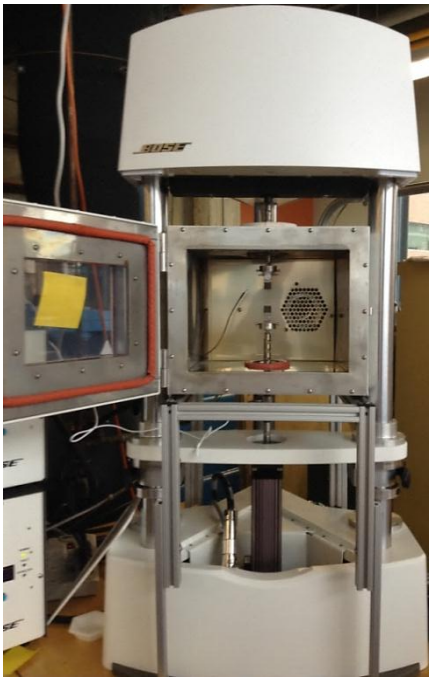

Figure 11. BOSE ES Series III ElectroForce test instrument.

Figure 12. Tensile test specimen that broke in the gauge section center during tensile testing.

The fiber mats are highly porous, and hence, a stress calculation of simply dividing force by the cross-section area is not appropriate. Instead, a representative fiber mat was weighed prior to testing in order to determine the actual density of the fiber mat, which was used to calculate the actual stress. The total volume of fiber mats was calculated by the measured thickness and area. Squares with areas of 1600mm^2 were cut from the electrospun Nylon 6 fiber mat for each sample, and the fiber mats were weighted by a scale with precision of 0.1 mg (Denver Instrument, Bohemia, New York, USA). The density of each sample was calculated based on the measured mass, area and thickness. The electrospun Nylon 6 fiber mat porosity was then calculated by:

$$\emptyset_{mat} = 1 - \frac{\rho_{mat}}{\rho_{Nylon\ 6}} \tag{2-1}$$

where ρ_{mat} is the actual density of the fiber mat, and $\rho_{Nylon\ 6}$ =1.084g/cm^3 (as specified by the manufacturer). The thickness, width, actual mat density, weight of the fiber mat per area and porosity of electrospun Nylon 6 nanofibers mats are summarized in Table 4.

Table 4. Properties of electrospun Nylon 6 fiber mats with concentrations of 15wt%, 17.5wt% and 20wt%.

Nylon 6 concentration	**15wt%**	**17.5wt%**	**20wt%**
Thickness (μm)	59.30±14.24	63.20±6.44	80.05±12.38
Width (mm)	10.05±0.16	9.88±0.28	9.87±0.15
Mat density, ρ_{mat} (g/cm^3)	0.189	0.191	0.193
Weight of mat per area (mg/cm^2)	1.12	1.20	1.54
Mat porosity, $ø_{mat}$ (%)	82.53	82.42	82.20

Chapter 3 - Design of Experiment for Electrospinning Nylon 6 Nanofibers

The Design of Experiment method is a powerful tool to assess the effects of multiple factors on responding variables. There are several important steps associated with the DOE method. The first step is to determine the purpose and objective. The second one is to select the responding variables, which are usually the average values or standard deviation values of measured characteristics. The third step is to determine the choice of factors, test range of the factors and levels. The factors include design factors and factors that are to be held constant. The test range is very important for determining the choice of DOE levels. After completion of the third step, the appropriate choice for a DOE method needs to be made. There are many useful DOE

methods such as screening test design, full factorial design, fractional factorial design and surface response design. After deciding upon the DOE method, experiments will be performed according to the chosen design. Then, the experimental data will be statistically analyzed [51]. Some of the useful statistical analysis methods included the mean plots analysis, ANOVA analysis, effect estimate analysis, regression model analysis and surface response analysis.

DOE and statistical analysis methods have not commonly been used in the field of electrospinning [52]. Anandhan [53] designed a mixed two- and three-level full factorial design to investigate the effects of electrospinning voltage and solution concentration on the electrospun polybenzimidazole (PBI) nanofiber diameter. Three levels were chosen for voltage and two levels were chosen for concentration. Using a two-way ANOVA analysis method, they found that the voltage and the interaction between voltage and concentration had significant effects on the electrospun PBI fiber diameter. Desai [54] designed a two-level full factorial design to investigate the effect of electrospinning voltage, solution concentration, flow rate and tip to collector distance on electrospun PANI/PMMA fiber thickness or diameter. Using the Pareto chart analysis, they found that the solution concentration had the most significant effect on fiber thickness. Coles [52] designed a 2^3 full factorial experiment, and used the main effect plot and interaction plot analysis to investigate the effects of solution concentration, electrospinning voltage and tip to collector distance on the electrospun poly(vinyl alcohol) (PVOH) fiber diameter and deposition rate. They ascertained that the electrospun PVOH fiber diameter increased with the increase of concentration and voltage and the decrease of distance. The deposition rate increased with the increase of voltage and concentration and the decrease of distance. Cui [55] applied the orthogonal experiments design method to investigate the effects of electrospinning voltage, solution concentration, flow rate, molecular weight, nozzle size and type of solvents on the electrospun poly(D,L-lactide) (PDLLA) nanofiber diameter. Using the ANOVA analysis and linear regression model analysis, it was found that the solution concentration and molecular weight had the most significant effects on electrospun PDLLA nanofiber diameter.

The above DOE related publications on electrospun nanofibers indicate that DOE and statistical analysis methods are suitable tools to investigate the effects of electrospinning parameters on the electrospun fiber diameter. In these publications, it was found that the solution concentration has

significant effect on the fiber diameter. The DOE and statistical analysis methods in these publications could be expanded further. Firstly, most of the publications designed a two-level DOE. Consequently, it was impossible to investigate whether the effects are linear or nonlinear. Secondly, the above publications only applied one or two kinds of statistical methods to analyze the data. None of the above publications applied the surface response analysis method. Thirdly, only one-time DOE approaches were used, e.g. small screening tests were not employed to investigate dominant factors. A screening test could make the use of DOE more efficient.

In the present study, the effects of solution concentration of Nylon 6, electrospinning voltage, and flow rate on the average nanofiber diameter and nanofiber uniformity were investigated using the DOE method and statistical analysis method. Nanofiber uniformity was represented by the standard deviation of the nanofiber diameters. In the second step of the DOE study, the mixed two- and three-level DOE was applied herein to determine whether the effects of the electrospinning parameters were linear or nonlinear and whether the effects of interactions among these factors on fiber diameter and standard deviation of fiber diameter were significant or not. Multiple statistical analysis methods, including Pareto chart, effect estimates analysis, mean plot analysis, regression model analysis and surface response analysis methods, were applied to analyze the experimental data. In addition, a two-step DOE approach was used in this study, that is, a screening test followed by a second DOE step.

Independent variable is the variable which is manipulated during the experiment. The three independent variables in this study were electrospinning voltage, flow rate and solution concentration of Nylon 6. The DOE test range for the electrospinning voltage, flow rate and solution concentration were set between 12kV and 24kV, 2µl/min and 5µl/min, and 15wt% and 20wt%, respectively. The limits for the electrospinning voltage were set in order to obtain a stable ejection jet and collect a sufficient amount of fibers. Below the lower bound of the flow rate test range, the Taylor cone was very small or disappeared. Beyond the upper bound, the ejection jet became unstable and a lot of the jet sprayed out during the electrospinning process. For the solution concentration test range, the lower and upper concentration limitations were investigated. When the solution concentration of Nylon 6 was 10wt%, it was found that very few fibers were collected during the electrospinning process while multiple beads in the nanofiber mats were noted for the various different parameters (this is described in conjunction with the

SEM images in Chapter 4.2.1). Therefore, Nylon 6 concentration equal or lower than 10wt% was not included in the DOE study and the Nylon 6 concentration of 15wt% was set as the lower limit of the DOE study. When the concentration of Nylon 6 was 25wt%, the electrospun Nylon 6 fibers were highly non-uniform, had a large amount of web-like structures between the nanofibers and the flat fiber morphology (this will be elucidated by the SEM images in Chapter 4.2.2). Hence, Nylon 6 concentration equal or higher than 25wt% was herein not included in the DOE study and the Nylon 6 concentration of 20wt% was set as the upper limit of the DOE study.

The responding variable is a variable that changes as a result of the change of the independent variables. The responding variables in this study were the average nanofiber diameter and the standard deviation of fiber diameters. The standard deviation of fiber diameter can indicate whether the fiber diameter distribution is uniform or not. The controlled variables, which were set at the constant values during the experiment, were temperature (27ºC), humidity (34%) and needle tip to collector distance (10cm).

Two DOE steps were considered in this study. In the first step, a screening test was performed to investigate the effects of the independent variables on the responding variables. In the screening test, two levels were chosen for electrospinning voltage, solution concentration and flow rate. The coded levels along with the real level values of the three variables are shown in Table 5. The coded levels were chosen as -1 and 1 for the two-level DOE, for input of the data into the employed STATISTICA® software. The screening test was a 2^3 full factorial design. The screening test was performed once (without replication), with the purpose of determining the most important factors. For factors that exhibited significant effects on fiber diameter and its standard deviation, more levels, especially middle levels were added in the second step of the DOE study to investigate whether associated effects were linear or nonlinear. In other words, the screening test constitutes a guideline for the second step of the DOE study and it could make the whole DOE study more efficient. The results of these analyses and a discussion thereof are presented in Chapter 4.3.1.

Table 5. Coded levels and real level values of variables for the screening test.

Electrospinning voltage (kV)	**Solution concentration (wt%)**	**Flow rate (μL/min)**	**Coded levels**
12	15	2	-1
24	20	5	1

Following the screening test, the second step of the DOE study was designed according to the conclusions from screening test (given in Chapter 4.3.1). Three levels were chosen for the electrospinning voltage (16kV, 20kV, 24kV) and, the Nylon 6 concentration (15wt%, 17.5wt%, 20wt%) while two levels were used for the flow rate (2µl/min, 5µl/min). The second step of the DOE study was a mixed two- and three-level full factorial design. The coded levels and real level values for the three variables in the second DOE step are presented in Table 6. The coded levels were set to -1, 0 and 1 for the three-level DOE. Again, data was analyzed using the STATISTICA® software. In this second DOE step, there were totally two groups: one original group and one replication group. For the replication group, new solutions were made and the electrospinning experiments using the same parameters as in the original group were again performed at a different time. For this full factorial design, the total number of runs including the one replication group was: 3*3*2*2=36.

Table 6. Coded levels and real level values of variables for the mixed two- and three-level design in the second DOE step.

Electrospinning voltage (kV)	**Solution concentration (wt%)**	**Flow rate (µL/min)**	**Coded levels**
16	15	2	-1
20	17.5	N/A	0
24	20	5	1

Note that there is one limitation of the DOE study. The experimental tests were run in a standard order not random order for both the screening test and the second step of the DOE study. Due to complications of switching between different solution concentration levels during the experiment, each block was run in a standard order as shown in Table 7 and Table 8.

As mentioned above, the STATISTICA® software, a professional statistical analysis software, was employed to conduct the statistical analysis for all the data of electrospun Nylon 6 nanofiber diameters. Pareto chart, effect estimates analysis, mean plot analysis, regression model analysis and surface response analysis were generated by STATISTICA® software to determine the effects of the three electrospinning parameters on the nanofiber diameter and its standard deviation.

A Pareto chart, herein generated by the STATISTICA® software, shows the importance of the effects of the independent variables on the responding variables [54]. From the Pareto chart, it

can easily be assessed which factors have the most significant effects and which factors do not have significant effect. The mean plot is a plot of mean values of responding variable with the standard deviation values versus each level of the independent variable. Mean plot can also be generated by the STATISTICA® software based on the experimental data. The effect estimate analysis results generated by the software provided P-values and the effect coefficients for each factor and interaction. P-values are used to judge whether a factor or interaction has a significant effect or not. If the P-value of one factor or interaction is smaller than the critical P-value, it can be concluded that this factor has a significant effect on the responding variable. The effect coefficients indicate the effect of each factor or interaction on the responding variable in the DOE. The regression model is a mathematical model which characterizes the relationship between the responding variables and the independent variables [51]. The regression model provides the model predicted values of responding variable after knowing the level values of each independent variable. The surface response analysis is a collection of mathematical and statistical techniques [51]. In this study, the surface response analysis was utilized to explore the relationships among the independent variables and the responding variables. The surface response method is a very useful analysis tool to determine how the responding variable changes with the independent variables especially when the interactions between the factors are significant.

Chapter 4 - Results and Discussions

The present chapter provides the results and discussions related to the experiments with electrospun Nylon 6, i.e., viscosity measurements, analyses of SEM images of nanofibers with 10wt% and 25wt% concentrations, and DOE screening tests and the second step of the DOE study including the associated SEM image analyses and statistical analyses.

4.1 Viscosity measurements

Shear rate (unit: s^{-1}) is the central parameter in measuring viscosity. Using an aforementioned rheometer, shear rate versus viscosity plots for Nylon 6 concentrations of 10wt%, 15wt%, 17.5wt% and 20wt% were produced as shown in Figure 13. Based on the viscosity test range and the

rotating speed limitation of the given rheometer, shear rate ranged from 18.6 s^{-1} to 55.8 s^{-1} for the investigated solutions.

Shown in Figure 13 is an increase in viscosity for the Nylon 6 solutions with an increasing shear rate. In other words, the Nylon 6 solutions exhibited shear thickening behavior for the applied test range. It can further be concluded that the viscosity of Nylon 6 solution increases with an increase in solution concentration.

For the electrospinning solution concentration of 25wt%, the solution was found to be comparatively viscous. Viscosity data were collected for shear rates between 18.6 s^{-1} and 27.9 s^{-1}, and the viscosities were 1125.25cp and 1190cp respectively. For comparison, the viscosity for the electrospinning solution concentration of 10wt% was less than 100cp. Referring to the results from SEM image analysis (see subsequent Chapter 4.2.1 and 4.2.2), the morphology of electrospun nanofibers with both 10wt% and 25wt% was found to be poor. It can therefore be concluded that the viscosity of Nylon 6 electrospinning solution should be in the range between 100cp and 1100cp in order to fabricate nanofibers that are easily spinnable and have well-formed morphology.

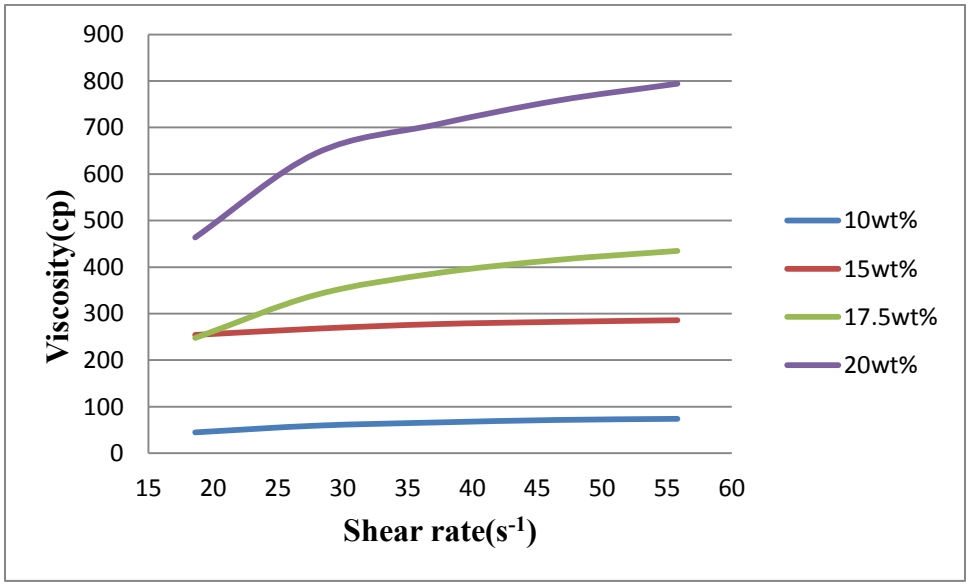

Figure 13. Viscosity of Nylon 6 solution versus shear rate for solution concentrations ranging from 10wt% to 20wt%.

4.2 SEM analysis results

4.2.1 SEM analysis of electrospun Nylon 6 nanofibers with 10wt% solution concentration

Prior to the screening test, an electrospinning experiment using a 10wt% Nylon 6 concentration was performed according to the design of the screening test to investigate whether the DOE test range could be expanded. During this experiment, it was observed that very few fibers were collected on the collector even for an extended process time. Subsequently, SEM images were taken and analyzed. Shown in Figure 14 are SEM images of electrospun Nylon 6 fibers with 10wt% concentration for different electrospinning voltages and flow rates. The magnification for these images was set at 5,000. In the SEM images, multiple beads can be observed for all electrospinning voltage and flow rate levels. In Figure 14 (a) and (c), since the beads were smaller than Figure 14 (b) and (d), larger magnification SEM images were needed to reveal the fiber morphology. SEM images with higher magnification of 10,000 are provided in Figure 15 and Figure 16, which exhibit numerous beads and a non-uniform fiber distribution. Due to the presence of multiple beads in the fiber mats and the very low amount of collected electrospun fibers, the 10wt% solution concentration was not included in the screening test and the second step of the DOE study.

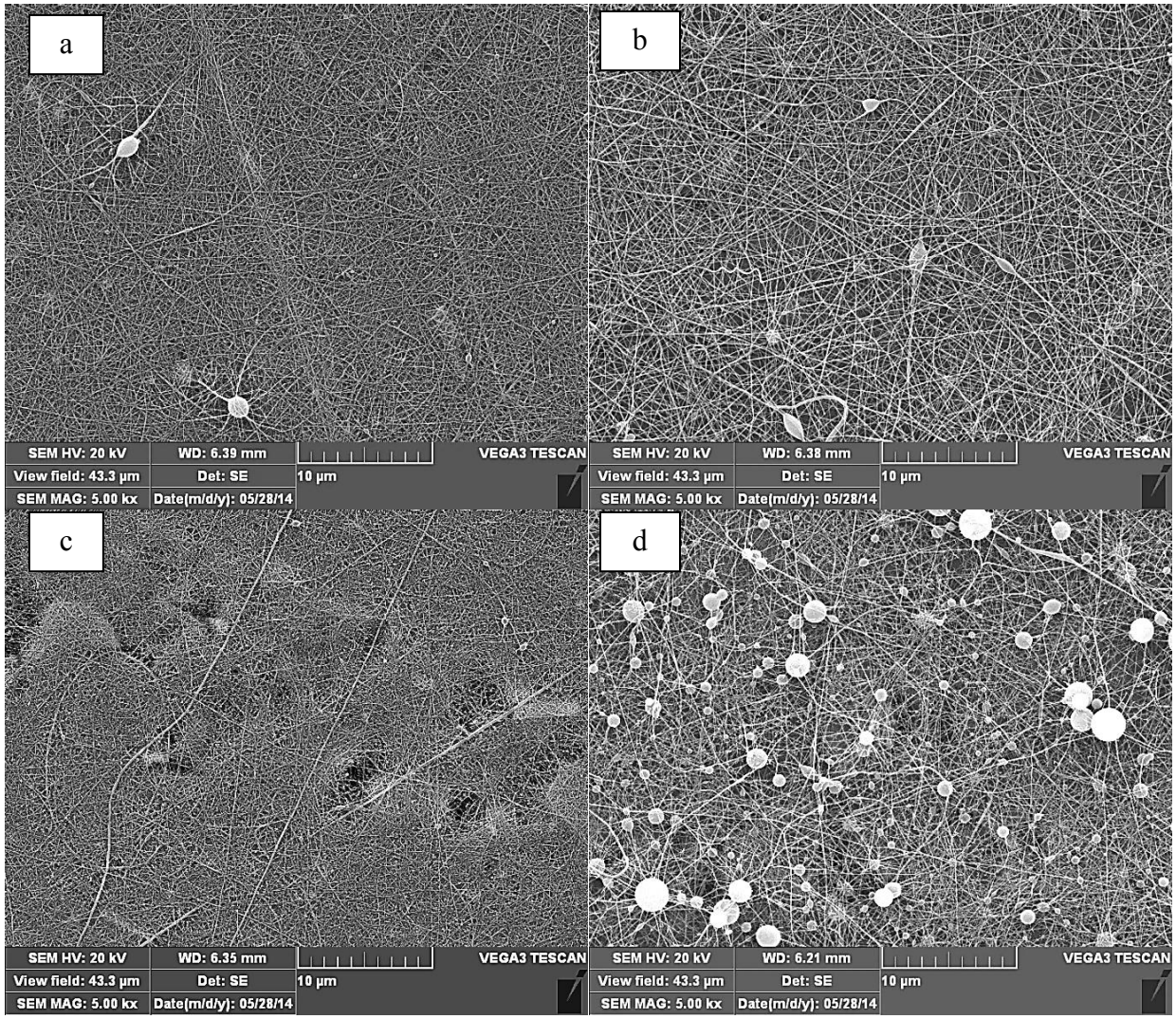

Figure 14. SEM images of electrospun Nylon 6 fibers with 10wt% solution concentration for different electrospinning voltages and flow rates: (a) 12kV, 2µl/min; (b) 20kV, 2µl/min; (c) 12kV, 5µl/min; and (d) 20kV, 5µl/min.

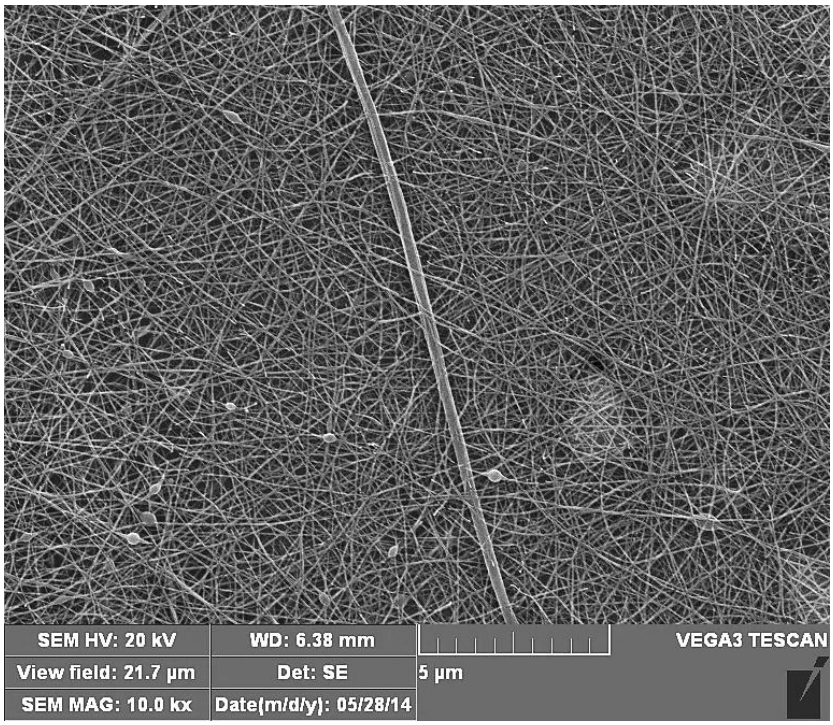

Figure 15. SEM image of electrospun Nylon 6 fibers with solution concentration of 10wt%, electrospinning voltage of 12kV and flow rate of 2µl/min.

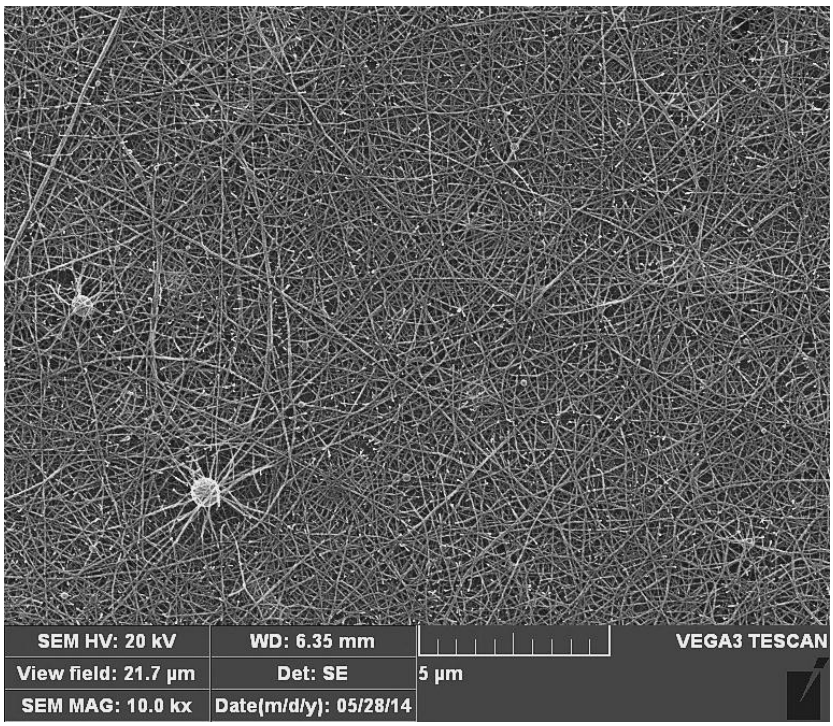

Figure 16. SEM image of electrospun Nylon 6 fibers with solution concentration of 10wt%, electrospinning voltage of 12kV and flow rate of 5µl/min.

4.2.2 SEM analysis of electrospun Nylon 6 nanofibers with 25wt% solution concentration

During the preparation of Nylon 6 solutions with 25wt% concentration, it is found that the dissolution of polymer in solvent was poor as even after 24 hours not all polymer could be dissolved. Following the DOE screening tests, it was again attempted to prepare a 25wt% Nylon 6 solution prior to commencing the second step of the DOE study. It was determined that a 25wt% Nylon 6 solution could be accomplished after a 48 hours dissolution period. As mentioned earlier, the solution was comparatively viscous (1190cp at room temperature). Electrospinning experiments with a 25wt% concentration were then performed prior to the second step of the DOE study in order to investigate whether the DOE test range could be expanded. SEM images of resulting fibers were taken and analyzed. Figure 17 shows these SEM images with a magnification of 10,000 for different electrospinning voltages and flow rates. The SEM images in Figure 17 exhibit web-like structures for all the samples. It should be noted that some small amount of web-like structures was observed for a Nylon 6 concentration of 20wt%. For the higher solution concentration of 25wt%, however, the amount of web-like structures in the fiber mats increased substantially. In addition, numerous flat fibers were observed (indicated by red arrows in Figure 17), and fibers were generally non-uniform. Based on these observations, the 25wt% solution concentration was not included in the screening test and second step of the DOE study.

Voltage (kV)	Flow rate(µl/min)	
	2	5
16	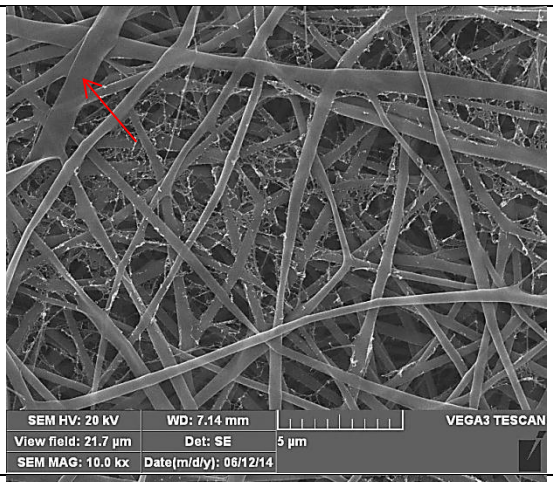	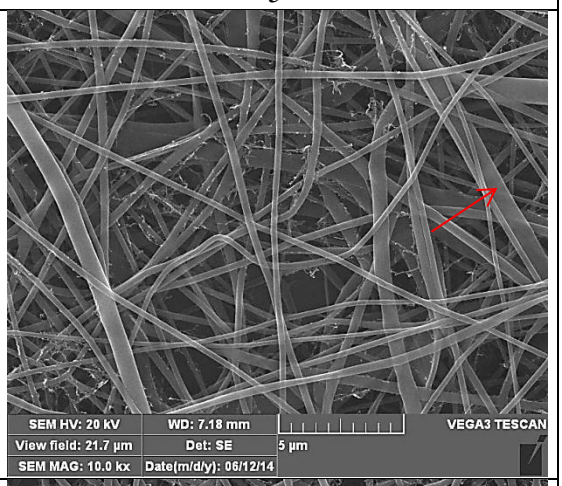
20	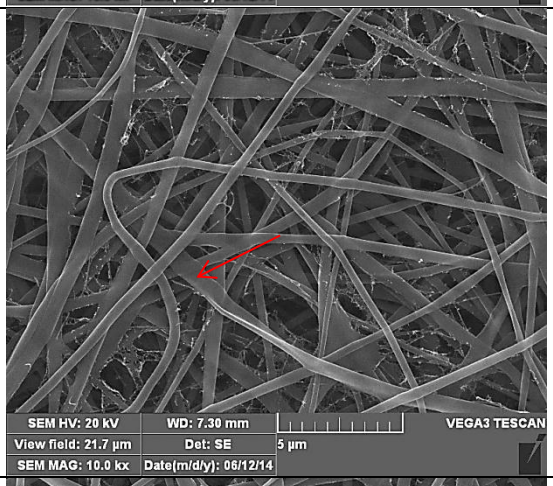	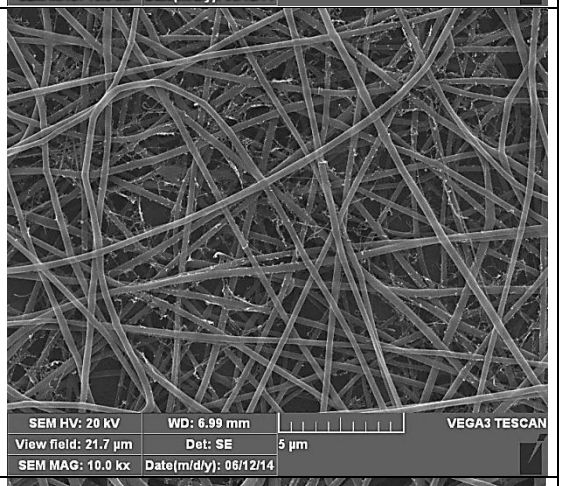
24	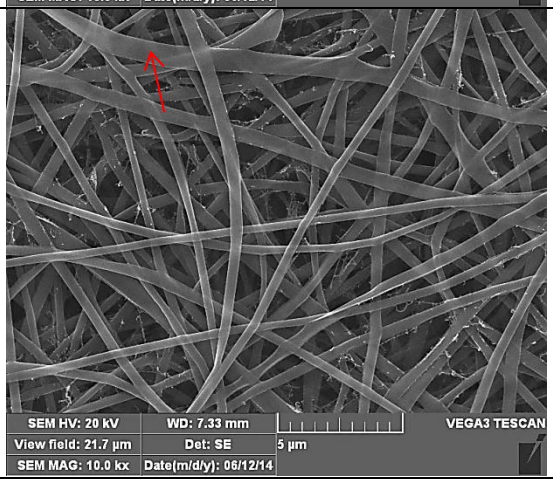	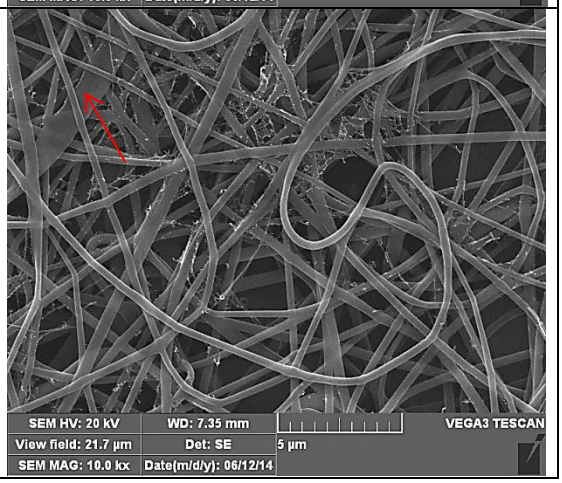

Figure 17. SEM images of electrospun Nylon 6 fibers with 25wt% solution concentration at electrospinning voltages of 16, 20, 24kV and flow rates of 2 and 5 µl/min.

4.2.3 SEM images analysis for DOE screening test

For the screening test as part of the DOE study, SEM images of Nylon 6 electrospun nanofibers with 20,000 magnification were produced as shown in Figure 18. From analyzing these SEM images, it was concluded that the fiber diameter increased significantly with the increase of solution concentration. Conversely, the fiber diameter decreased with the increase of electrospinning voltage. It was also observed that the uniformity of nanofibers distribution was poor when the electrospinning voltage was 12kV no matter which levels of solution concentration and flow rate were chosen. In fact, for the solution concentration increasing from 15wt% to 20wt%, the uniformity of Nylon 6 nanofiber distribution became worse. Note that these results are also reflected by the statistical analysis results using STATISTICA® software in as explained in Chapter 4.3.1. In addition, the nanofiber diameter distribution analysis for the screening test was done.

In addition to the average fiber diameter, the nanofiber diameter distribution was analyzed by the fiber diameter distribution plots. Fiber diameter distribution plots were created where the abscissa shows the fiber diameter range and ordinate shows the number of fibers in each diameter range. For each sample, a total of 60 nanofibers were chosen for fiber diameter measurements, and the fiber diameter distribution plot was composed from these data for each sample. The fiber diameter distribution plots of the screening test are shown in Appendix A. Figure 19 shows the fiber diameter distribution plots for two electrospinning voltages, i.e., 12kV and 24kV, for a solution concentration of 20wt% and a flow rate of 5µl/min. It can be inferred from these graphs that the fiber diameter distribution was more uniform for the 24kV electrospinning voltage than for 12kV. Note that the conclusion derived from fiber diameter distribution plots is congruent to the one deduced from preceding SEM images analyses.

Concentration (wt%)	Flow rate (µl/min)	Electrospinning voltage(kV)	
		12	24
15	2	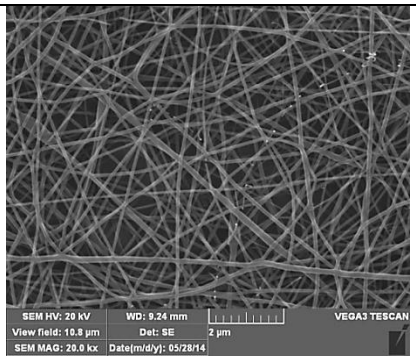 **Average diameter: 106.67nm**	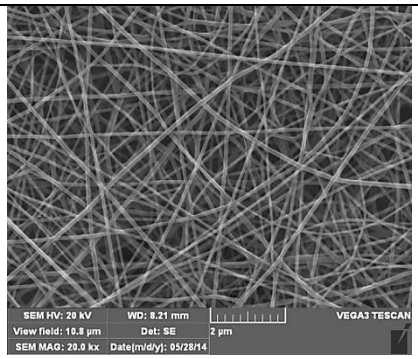 **Average diameter:101.30nm**
20	2	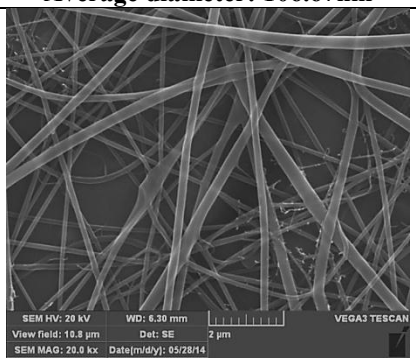 **Average diameter:200.12nm**	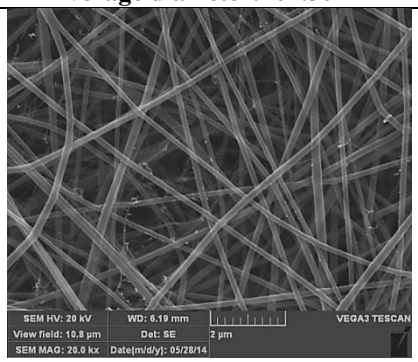 **Average diameter:156.00nm**
15	5	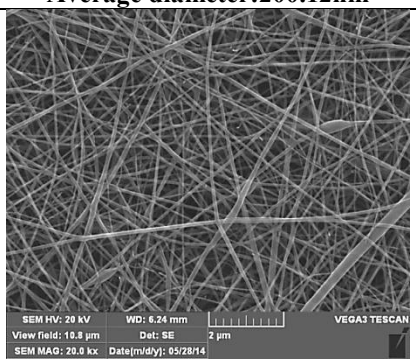 **Average diameter:105.54nm**	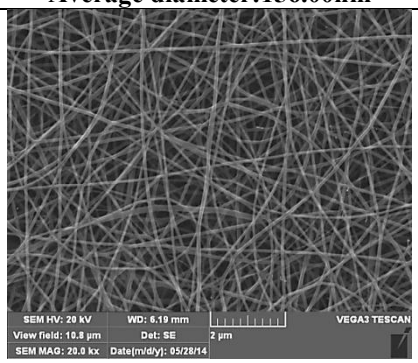 **Average diameter:101.74nm**
20	5	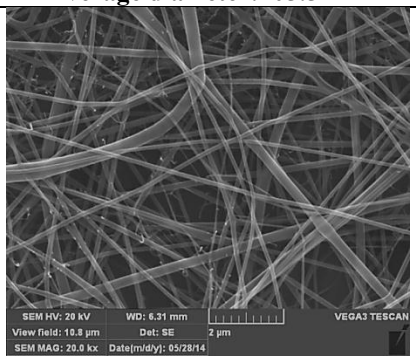 **Average diameter:194.13nm**	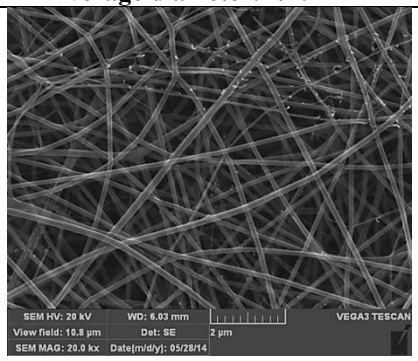 **Average diameter:149.60nm**

Figure 18. SEM images with average fiber diameters for the screening test of DOE study at different levels of solution concentration, flow rate and electrospinning voltage.

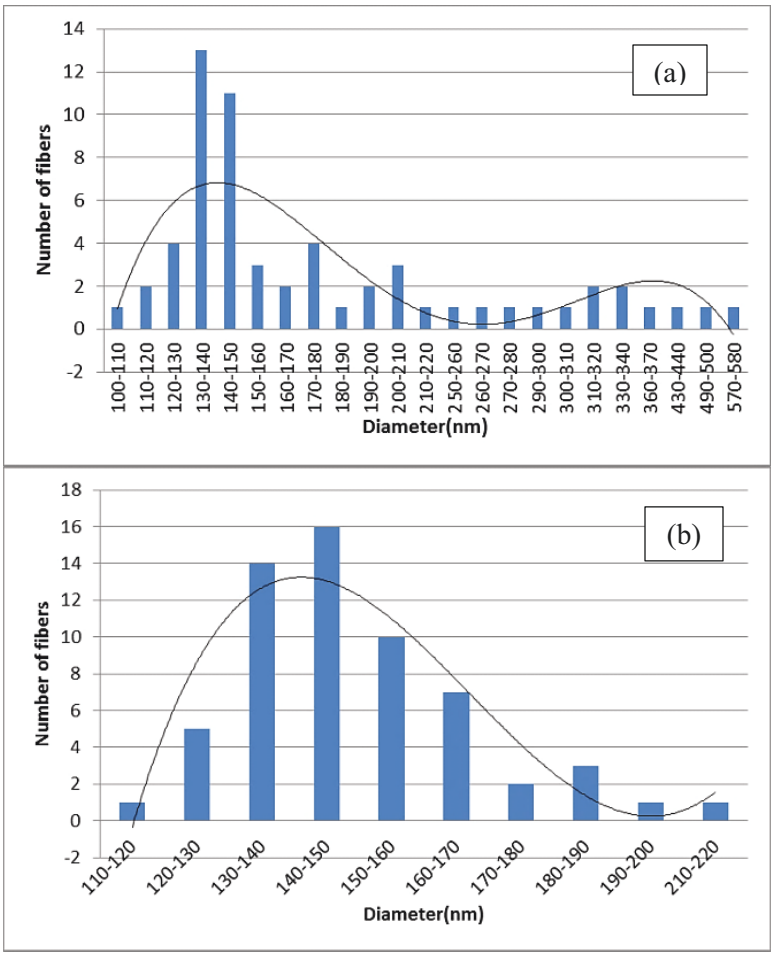

Figure 19. Nylon 6 fiber diameter distribution plots for samples prepared with 20wt% solution concentration, flow rate of 5µl/min and electrospinning voltage of (a) 12kV and (b) 24kV.

4.2.4 SEM images analysis for the second step of the DOE study (original group)

For the second step of the DOE study (referring to the original group), SEM images of electrospun Nylon 6 nanofibers were obtained as shown in Figure 20 and Figure 21. Fiber samples were produced with solution concentrations ranging from 15wt% to 20wt%, electrospinning voltages ranging from 16kV to 24kV, and flow rates ranging from 2µl/min to 5µl/min respectively. The set image magnification of was 20,000. SEM images in Figure 20 and Figure 21 reveal that fiber diameters increased significantly with the increase of solution concentration from 15wt% to 20wt%. Based on all the SEM images in Figure 20 and Figure 21, it can further be observed that the nanofibers in all images were fine and uniform. Compared to the SEM images in Figure 18 of electrospun Nylon 6 nanofibers fabricated using an electrospinning voltage of 12kV (screening test), fibers were more uniform for the higher

electrospinning voltages of 16kV, 20kV and 24kV. Note that corresponding fiber diameter distribution plots for the second step of the DOE study (original group) are shown in Appendix B.

Concentration (wt%)	**Electrospinning voltage(kV)**		
	16	20	24
15	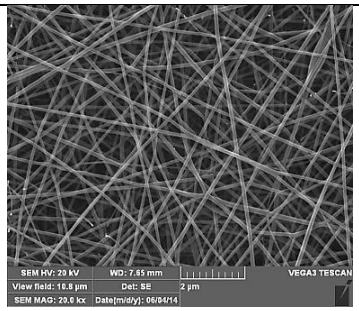 **Average diameter: 105.78nm**	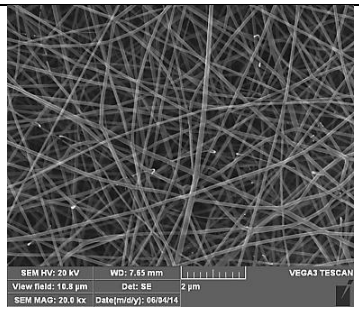 **Average diameter:101.87nm**	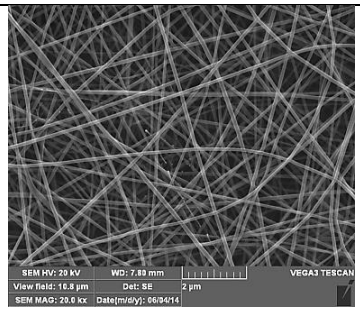 **Average diameter:105.83nm**
17.5	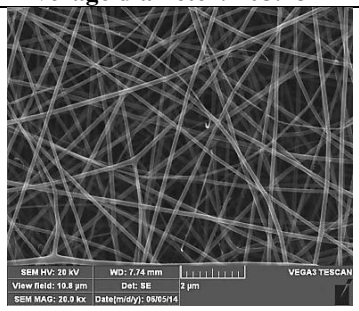 **Average diameter:126.77nm**	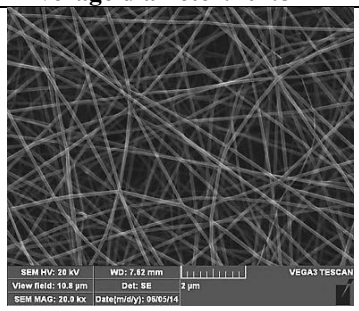 **Average diameter:114.78nm**	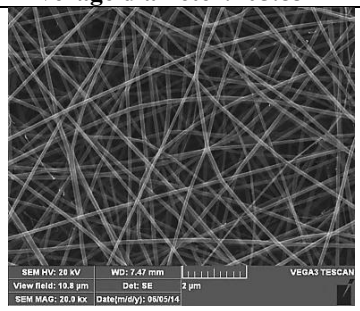 **Average diameter: 119.89nm**
20	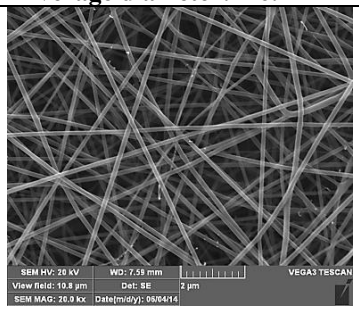 **Average diameter:148.44nm**	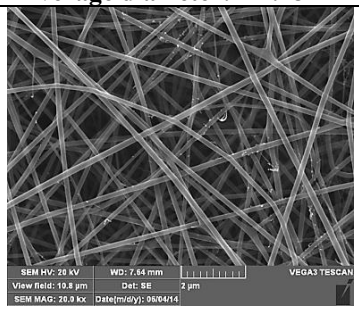 **Average diameter:158.47nm**	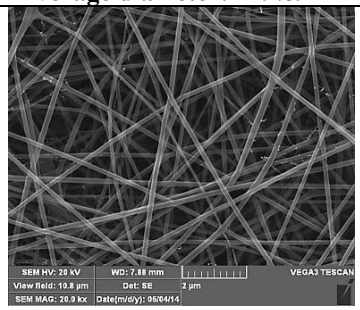 **Average diameter:147.79nm**

Figure 20. SEM images with average fiber diameters for electrospun Nylon 6 nanofibers made with different solution concentrations and electrospinning voltages and a fixed flow rate of 2µl/min.

Concentration (wt%)	Electrospinning voltage(kV)		
	16	20	24
15	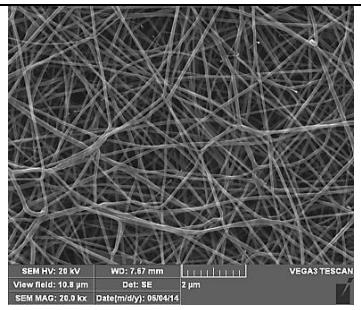 **Average diameter:104.17nm**	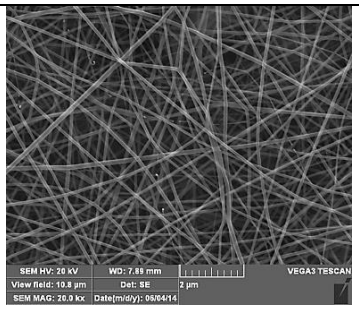 **Average diameter:102.16nm**	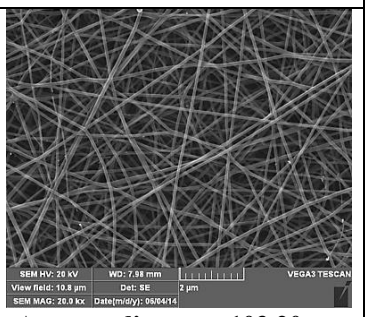 **Average diameter:103.20nm**
17.5	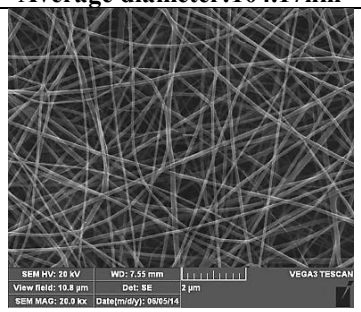 **Average diameter:116.05nm**	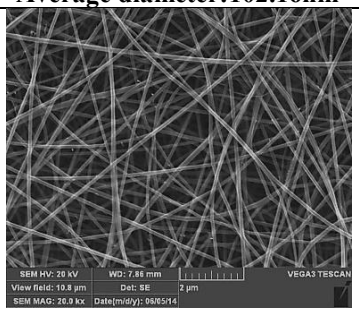 **Average diameter:119.17nm**	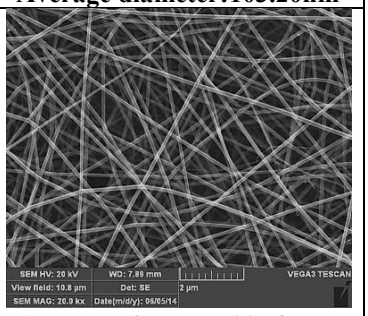 **Average diameter:115.25nm**
20	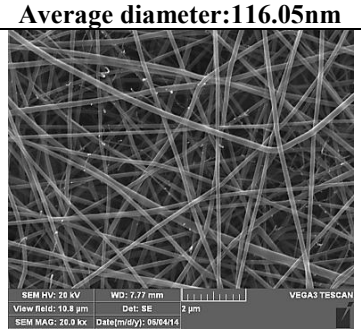 **Average diameter:154.34nm**	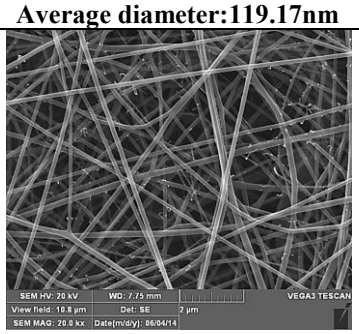 **Average diameter:147.62nm**	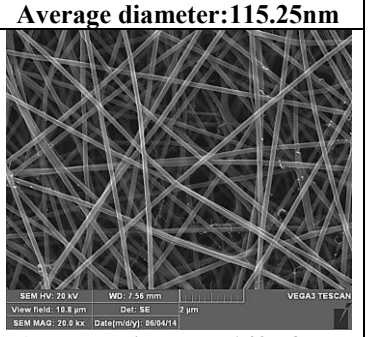 **Average diameter:149.53nm**

Figure 21. SEM images with average fiber diameters for electrospun Nylon nanofibers made with different solution concentrations and electrospinning voltages and a fixed flow rate of 5µl/min.

4.3 Statistical analysis results

4.3.1 Statistical analysis for the screening test of the DOE study

The screening test in this DOE study is a 2^3 full factorial design. Table 7 is the 2^3 corresponding design table with the results of the screening test. Note that information on code levels and real levels was already given in Table 5 in Chapter 3, and SEM images for screening test were presented in Chapter 4.2.3. From Table 7 it can be found that the fiber diameter increases significantly with the increase of solution concentration level from -1 to 1. The fiber diameter decreases with the increase of electrospinning voltage level from -1 to 1. The standard deviations

were found to be much larger when the electrospinning voltage was chosen at the lowest level (-1), which is 12kV.

Table 7. 2^3 full factorial design table with the results from the screening test of DOE study.

Solution concentration	Electrospinning voltage	Flow rate	Average fiber diameter(nm)	Standard deviation of fiber diameter(nm)
-1	-1	-1	106.666	25.552
-1	1	-1	101.298	11.950
-1	-1	1	105.538	34.722
-1	1	1	101.744	20.234
1	-1	-1	200.119	89.959
1	1	-1	156.002	21.057
1	-1	1	194.127	95.558
1	1	1	149.595	19.022

4.3.1.1 Statistical analysis for fiber diameters

The effect estimate analysis was done using the STATISTICA® software for the data of the screening test. The effect estimate table is shown in Appendix C. P-value was used to assess the significance of the effects of factors, where the critical P-value was 0.1. If the P-value is smaller than 0.1, the effect of the factor is judged significant; if not, the effect of the factor is insignificant. Based on the effect estimate analysis results for the fiber diameter, the P-values for the solution concentration, electrospinning voltage and flow rate were found to be 0.0045, 0.013 and 0.096, respectively. The effect coefficients for the solution concentration, electrospinning voltage and flow rate were found as 35.57, -12.23 and -1.64, respectively. The absolute value of the effect coefficient of solution concentration is the largest. Consequently, the solution concentration has the most significant effect on the nanofiber diameter. Moreover, the electrospinning voltage also has significant effect on nanofiber diameter. For the flow rate, P-value is 0.096, which is close to the critical value of 0.1. The effect of flow rate therefore needed to be investigated further in the second step of the DOE study.

The effects of interactions between the three parameters on the fiber diameter were also investigated. The P-value for the interaction between solution concentration and electrospinning voltage was determined as 0.016, which indicates a significant effect on fiber diameter. The P-value for the interaction between electrospinning voltage and flow rate was 0.66, indicating an insignificant effect on fiber diameter. Finally, the P-value for the interaction between the solution

concentration and flow rate was 0.107, which is close to the critical value 0.1. Hence, it was necessary to further investigate the effect of the interaction between the solution concentration and flow rate on fiber diameter in the second step of the DOE study.

Means plots as shown in Figure 22 were generated by the STATISTICA® software. From the mean plots of the fiber diameter versus correspondingly solution concentration, electrospinning voltage and flow rate, it was found that the solution concentration had a positive effect on fiber diameter, whereas the electrospinning voltage had a negative effect on fiber diameter. Flow rate did not have an appreciable effect on fiber diameter. However, since the interaction between solution concentration and electrospinning voltage also had a significant effect on the fiber diameter and the mean plot of single factor did not consider the interaction, the mean plot analysis of single factor was not enough to gain a final conclusion. So, a regression model analysis was performed by the STATISTICA® software. The regression model equation generated from the software for the fiber diameter was simplified to $D = 139.39 + 35.57\,C - 12.23\,V - 9.94\,CV$, where D, C and V are the fiber diameter, solution concentration, and electrospinning voltage, respectively. Based on this regression model equation, since the effect coefficient of solution concentration is positive, the effect coefficient of electrospinning voltage is negative and the absolute values of the effect coefficients of electrospinning voltage and solution concentration are larger than the absolute value of the coefficient of the interaction between electrospinning voltage and solution concentration, it can be concluded that the fiber diameter increases with the increase of solution concentration and decrease of electrospinning voltage.

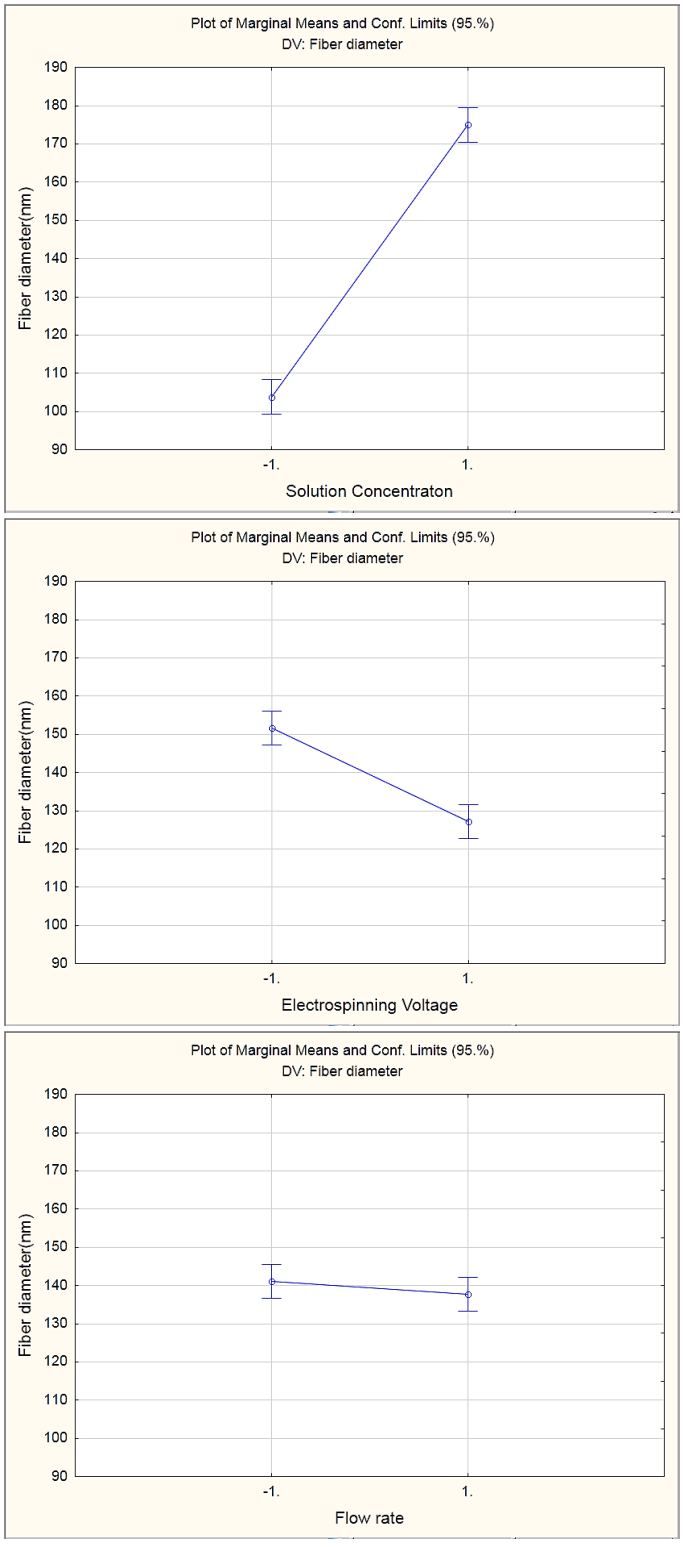

Figure 22. Mean plots of fiber diameter versus, correspondingly, solution concentration, electrospinning voltage and flow rate for the screening test.

4.3.1.2 Statistical analysis of the standard deviation of fiber diameter

Based on the effect estimate analysis results generated by the STATISTICA® software for the standard deviation of the fiber diameter, the P-values for the solution concentration, electrospinning voltage and flow rate were determined as 0.032, 0.025 and 0.198, respectively. Note that the effect estimate table is shown in Appendix C. Since both the P-values for the solution concentration and electrospinning voltage were considerably smaller than the critical P-value of 0.1, both parameters were deemed to have significant effects on the standard deviation of fiber diameter. The flow rate does not have a significant effect on the standard deviation. The P-value for the interaction between the solution concentration and electrospinning voltage was found as 0.037, which indicates a significant effect on the standard deviation of fiber diameter. The effect coefficients for the electrospinning voltage and solution concentration were found to be correspondingly -21.69 and 16.64, while the effect coefficient for the interaction between the electrospinning voltage and solution concentration was -14.67. P-values for the interaction between the solution concentration and flow rate, and the interaction between electrospinning voltage and flow rate were found as 0.29 and 0.43, respectively, which indicates that the effects of these two interactions on the standard deviation of fiber diameter were insignificant.

Means plots for the standard deviation of fiber diameter versus solution concentration, electrospinning voltage and flow rate were generated by the STATISTICA® software. These mean plots shown in Figure 23 indicate that the solution concentration had a positive effect on the standard deviation, while the electrospinning voltage had a negative effect, and flow rate did not have any significant effect. Nevertheless, since the interaction between the solution concentration and electrospinning voltage had significant effect on the standard deviation of fiber diameter and the single factor mean plot does not consider the interaction, the single factor mean plot analysis is not sufficient to derive a final conclusion. Therefore, a regression model analysis was again applied. The regression model equation generated from the STATISTICA® software for the standard deviation of fiber diameter was simplified to $S = 39.76 + 16.64\ C - 21.69\ V - 14.67\ CV$ (S: standard deviation of fiber diameter, C: solution concentration, V: electrospinning voltage). Based on this regression model equation, since the absolute value of the effect coefficients of both electrospinning voltage and solution concentration were larger than the absolute value of the effect coefficient of the interaction

between solution concentration and electrospinning voltage, the effects of both electrospinning voltage and solution concentration were more significant than the effect of the interaction between voltage and concentration on the standard deviation. Therefore, it was concluded that the standard deviation of fiber diameter is lowest when the solution concentration is at its lowest level (-1) and the electrospinning voltage is at its highest level (+1).

Referring to the results of the standard deviation of fiber diameter for the screening test shown in the Table 7, the standard deviation values were all very large when the electrospinning voltage was chosen at the lowest level, i.e., -1 (12kV). In other words, nanofiber uniformity was poor at the lowest voltage level, which corroborates the deductions from the SEM image analysis of the screening test shown in Figure 18 in Chapter 4.2.3. Therefore, for the second step of the DOE study, the lowest voltage level of 12kV was omitted, and three additional levels of voltage (16kV, 20kV, 24kV) were included to investigate the effect of electrospinning voltage on nanofiber diameter and its standard deviation. As discussed above, solution concentration is the most important factor. In order to investigate whether the effects of solution concentration on fiber diameter and its standard deviation are linear or nonlinear, a middle level value of 17.5wt% was added between 15wt% and 20wt% for the second step of the DOE study. For flow rate, since the screening test results revealed a P-value for its effect on fiber diameter that was quite close to the critical P-value of 0.1, the existing two level values of 2 μl/min and 5 μl/min were maintained to investigate the effects of flow rate on the fiber diameter and its standard deviation in the second step of the DOE study. Consequently, the second step of the DOE study is a mixed two- and three- level full factorial design.

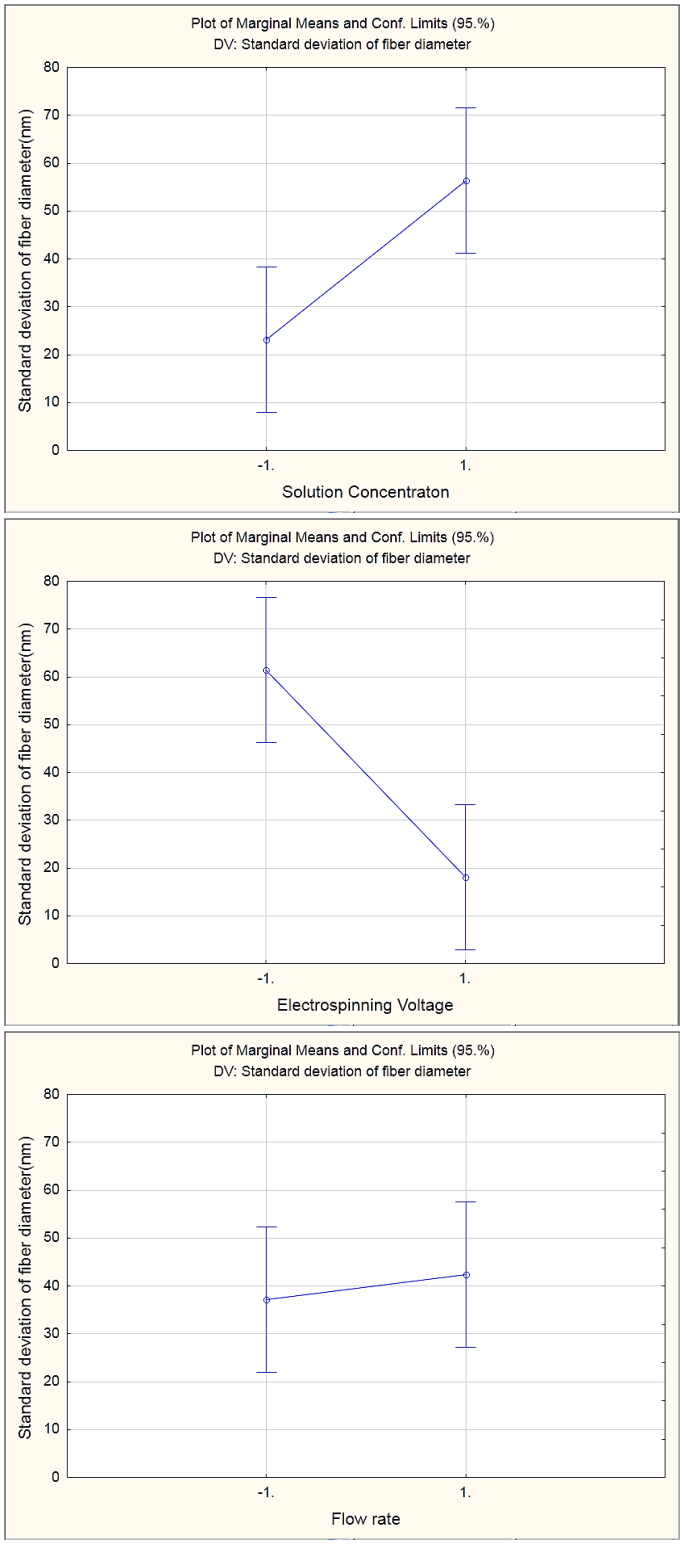

Figure 23. Mean plots of standard deviation of fiber diameter versus solution concentration, electrospinning voltage and flow rate for the screening test.

4.3.2 Statistical analysis for the second step of the DOE study

The second step of the DOE study was executed using the code levels and real level values given in Table 6 in Chapter 3. The second step of the DOE study included one original group and one replication group. The total experiment runs were 36. Table 8 provides the mixed two- and three-level full factorial design table with results. The run number in Table 8 indicates the test order for the electrospinning experiments for different parameters. Run number 1-18 is the original group and run number 19-36 is the replication group. Data in Table 8 shows that the fiber diameter increases significantly with the solution concentration increasing from level -1 to 1. Note that SEM images for the original group were already shown in Chapter 4.2.4.

Table 8. Mixed two- and three-level full factorial design table with all results for the second step of the DOE study.

Run number	Solution concentration	Electrospinning voltage	Flow rate	Average fiber diameter (nm)	Standard deviation of fiber diameter (nm)
1	-1	-1	-1	105.784	12.135
2	-1	0	-1	101.870	11.818
3	-1	1	-1	105.828	13.324
4	-1	-1	1	104.170	15.748
5	-1	0	1	102.165	14.900
6	-1	1	1	103.204	11.763
7	1	-1	-1	148.445	15.139
8	1	0	-1	158.474	15.878
9	1	1	-1	147.787	17.746
10	1	-1	1	154.342	34.706
11	1	0	1	147.616	13.792
12	1	1	1	149.527	10.460
13	0	-1	-1	126.774	11.678
14	0	0	-1	114.776	10.185
15	0	1	-1	119.886	12.371
16	0	-1	1	116.047	19.615
17	0	0	1	119.171	15.462
18	0	1	1	115.248	10.334
19	-1	-1	-1	106.449	10.151
20	-1	0	-1	100.726	11.620
21	-1	1	-1	105.217	12.972
22	-1	-1	1	105.528	12.770
23	-1	0	1	101.729	10.633
24	-1	1	1	101.152	10.190
25	1	-1	-1	151.287	14.318
26	1	0	-1	152.075	13.845
27	1	1	-1	144.983	16.448
28	1	-1	1	152.948	31.480
29	1	0	1	144.475	12.590
30	1	1	1	148.822	11.789
31	0	-1	-1	126.412	12.343
32	0	0	-1	117.568	13.367
33	0	1	-1	119.190	12.609
34	0	-1	1	117.566	17.832
35	0	0	1	114.113	15.205
36	0	1	1	113.826	10.540

4.3.2.1 Statistical analysis for fiber diameter

Using the STATISTICA® software to analyze the data, the effect estimate results for the effects of electrospinning voltage, solution concentration, flow rate, and the interactions between these factors on the fiber diameter were obtained. The effect estimate table is shown in Appendix C. Based on the effect estimate analysis results for fiber diameter, the P-values for the electrospinning voltage, flow rate and solution concentration were found to be 0.015, 0.040 and smaller than 0.000001, respectively. Correspondingly, the effect coefficients of the electrospinning voltage, flow rate and solution concentration were -1.7116, -1.1634 and 23.2066, respectively. Since the absolute effect coefficient value of solution concentration is the largest and P-value of solution concentration is smaller than 0.000001, solution concentration has the most significant effect on the nanofiber diameter. As mentioned earlier, the critical P-value is 0.1. P-values for both the electrospinning voltage and flow rate are smaller than 0.1, and hence, both electrospinning voltage and flow rate have significant effects on the fiber diameter. P-values for the interactions between the three parameters were found to be all much higher than 0.1. Therefore, the interactions do not have significant effect on the fiber diameter. Furthermore, the P-value for the effect of solution concentration (quadratic) was found to be smaller than 0.000001, which means that the effect of solution concentration on fiber diameter is nonlinear. These conclusions can also be derived from the Pareto Chart shown in Figure 24. This Pareto Chart shows that solution concentration, solution concentration (quadratic), electrospinning voltage and flow rate all have significant effects on the fiber diameter.

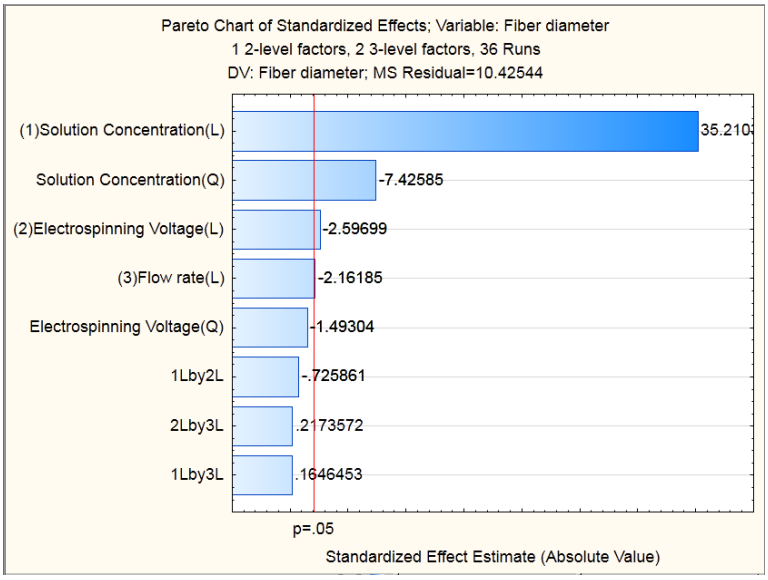

Figure 24. Pareto Chart for the effect of electrospinning parameters on fiber diameter in the second step of the DOE study.

The mean plots given in Figure 25 and generated by the STATISTICA® software, indicate that the solution concentration has a positive effect on fiber diameter, while both electrospinning voltage and flow rate have negative effects. In addition, it is found that the effect of solution concentration on nanofiber diameter is nonlinear, which concurs with the conclusion derived from the effect estimate analysis. Based on the mean plots for the two factors (see Figure 26 and Figure 27), which were generated by the STATISTICA® software, it is confirmed that the fiber diameter increases with the increase of solution concentration and the decrease of electrospinning voltage. It can further be observed that the curves in the mean plots do not cross each other, which verifies that the effect of interaction between electrospinning voltage and solution concentration on the fiber diameter was not significant. Note that the result of an increasing fiber diameter with the increase of solution concentration and the decrease of electrospinning voltage is congruent with findings from other researchers as described in Chapter 1.3. In addition, it is found that the Nylon 6 fiber diameter decreases with the increasing flow rate.

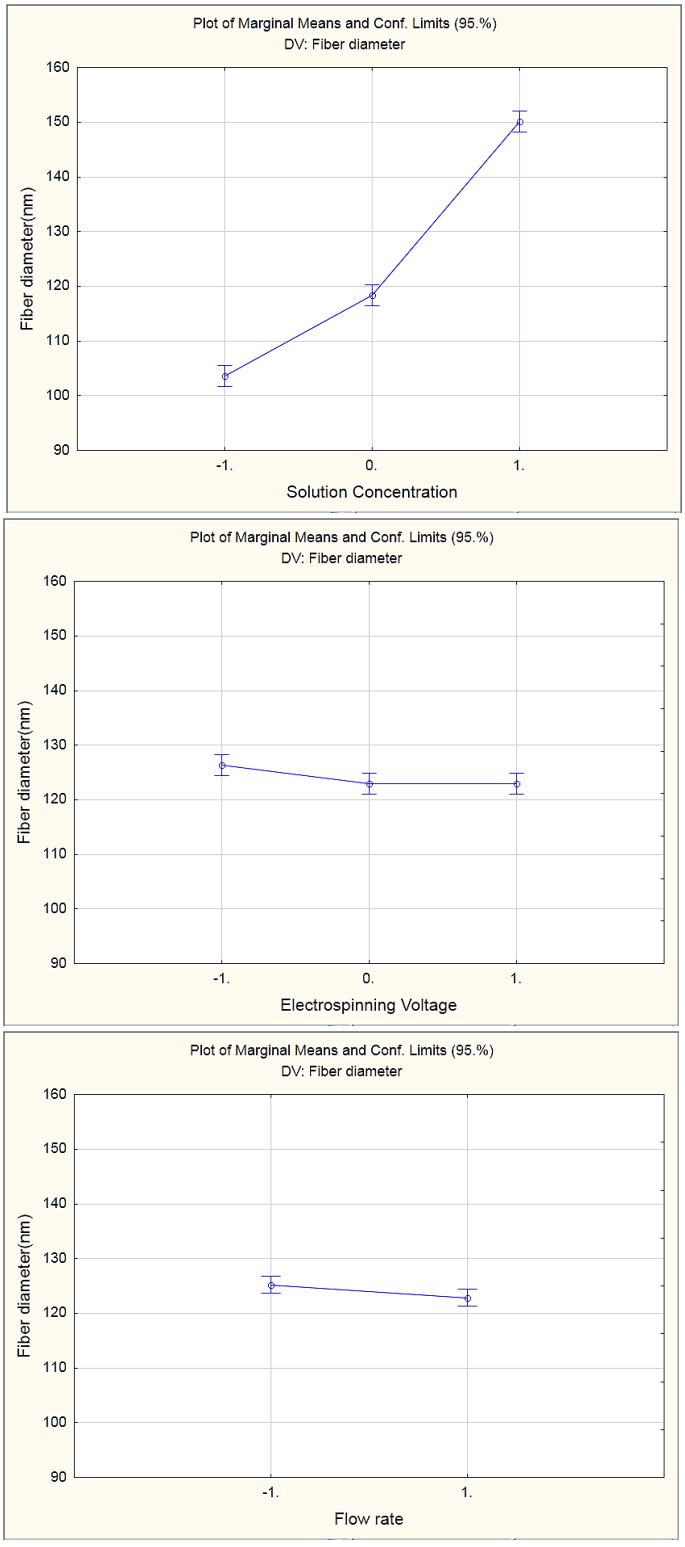

Figure 25. Mean plots of fiber diameter versus, correspondingly, solution concentration, electrospinning voltage and flow rate for the second step of the DOE study.

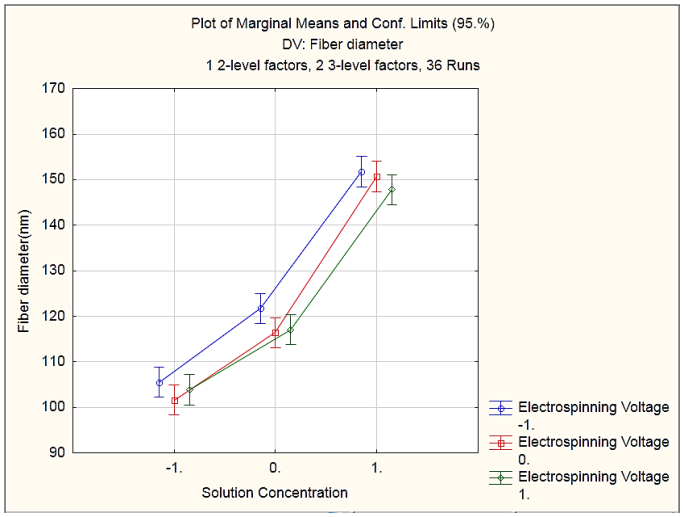

Figure 26. Relationship between fiber diameter and solution concentration for electrospinning voltage levels of -1, 0 and 1.

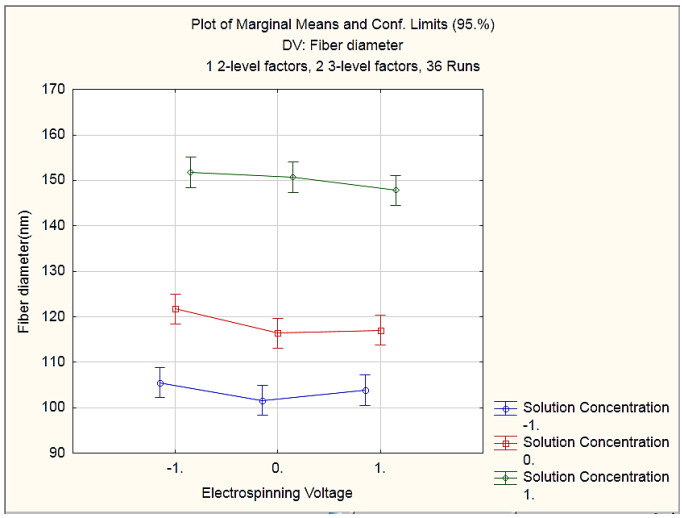

Figure 27. Relationship between fiber diameter and electrospinning voltage for solution concentration levels of -1, 0 and 1.

Comparing average fiber diameter values between the original group (run number 1-18) and the replication group (run number 19-36), a difference of less than 5% can be ascertained. Hence, no significant difference exists between the original group and the replication group.

A regression model analysis was completed next. Based on the coefficients values of effect estimate analysis, the regression model equation generated by the STATISTICA® software for the fiber diameter was simplified to $D = 124.0328 + 23.2066\ C - 4.2386\ C^2 - 1.7116\ V - 1.1634\ F$ (D: fiber diameter, C: solution concentration, V: electrospinning voltage, F: flow rate). To

calculate the regression model predicted values for the fiber diameter for each run (number 1 to 36), the level values of solution concentration, electrospinning voltage and flow rate of each run were applied to the above regression model. The level values for each run are already shown in Table 8. In this manner, the absolute differences between the regression model predicted fiber diameters and the experimental data for all the 36 runs were calculated and are shown in Table 9. The percent differences between the experimental average fiber diameters and model predicted values are also displayed in the Table 9. The average of the experimental average fiber diameter values is 124.033nm and the average of the absolute difference between regression model predicted values and experimental values is 6.593nm. The error percentage is thus 5.3%, which was calculated by 6.593/124.033. Therefore, this regression model can accurately predict the fiber diameter after knowing the values for the solution concentration, electrospinning voltage and flow rate. In addition, based on the regression model, since the coefficient of the solution concentration is positive and the coefficients of the electrospinning voltage and flow rate are negative, it can also be concluded that the fiber diameter increases with the increase of solution concentration and the decrease of both electrospinning voltage and flow rate.

Based on Figure 28 shown below, it can be observed that nearly all the data falls close to the 45º straight line, which means the regression model predicted fiber diameter values are close to the experimental fiber diameter.

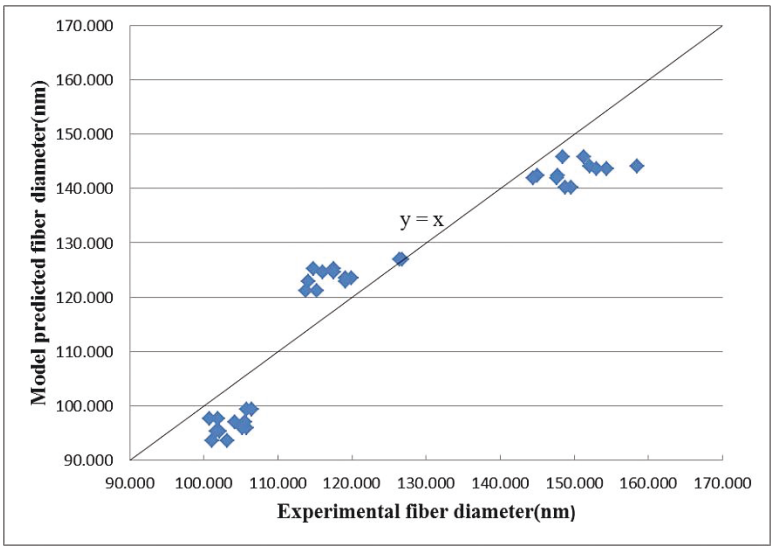

Figure 28. Regression model predicted fiber diameters versus experimental fiber diameters.

Table 9. Regression model predicted fiber diameter values and absolute difference between experimental fiber diameter and regression model predicted values for all 36 test runs.

Run number	Experimental average fiber diameter (nm)	Regression model predicted values (nm)	Absolute difference between experimental and model predicted values (nm)	Percent difference
1	105.784	99.463	6.321	6.0%
2	101.870	97.751	4.119	4.0%
3	105.828	96.039	9.789	9.2%
4	104.170	97.136	7.034	6.8%
5	102.165	95.424	6.740	6.6%
6	103.204	93.713	9.492	9.2%
7	148.445	145.876	2.569	1.7%
8	158.474	144.164	14.310	9.0%
9	147.787	142.453	5.334	3.6%
10	154.342	143.549	10.793	7.0%
11	147.616	141.837	5.778	3.9%
12	149.527	140.126	9.401	6.3%
13	126.774	126.908	0.134	0.1%
14	114.776	125.196	10.421	9.1%
15	119.886	123.485	3.598	3.0%
16	116.047	124.581	8.534	7.4%
17	119.171	122.869	3.699	3.1%
18	115.248	121.158	5.910	5.1%
19	106.449	99.463	6.986	6.6%
20	100.726	97.751	2.975	3.0%
21	105.217	96.039	9.177	8.7%
22	105.528	97.136	8.392	8.0%
23	101.729	95.424	6.305	6.2%
24	101.152	93.713	7.440	7.4%
25	151.287	145.876	5.412	3.6%
26	152.075	144.164	7.911	5.2%
27	144.983	142.453	2.530	1.7%
28	152.948	143.549	9.399	6.1%
29	144.475	141.837	2.638	1.8%
30	148.822	140.126	8.696	5.8%
31	126.412	126.908	0.496	0.4%
32	117.568	125.196	7.628	6.5%
33	119.190	123.485	4.294	3.6%
34	117.566	124.581	7.015	6.0%
35	114.113	122.869	8.757	7.7%
36	113.826	121.158	7.332	6.4%
Average	124.033		6.593	

Surface response analysis is very useful for investigating the relationship between the fiber diameter and two electrospinning parameters. Such plots are shown in Figure 29, where blue dots represent experimental data of fiber diameter. The colors scale in these plots corresponds to the fiber diameter range. Each surface plot indicates the change in nanofiber diameter as a function of two parameters with the third one fixed. For example, the surface response plots in Figure 29(a) and (b) show that nanofiber diameter is increasing with the increase of Nylon 6 concentration, while only a minor effect of electrospinning voltage and flow rate can be observed. This behavior is easily explained by the regression model, in which both coefficients of electrospinning voltage and flow rate are much smaller than the coefficient of solution concentration.

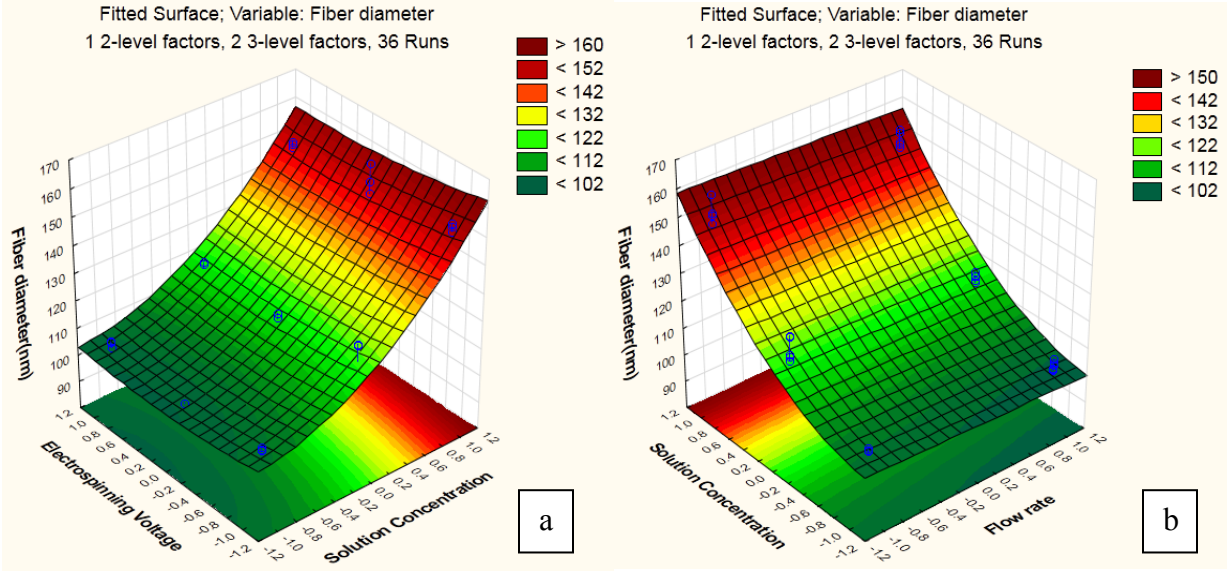

Figure 29. Fitted surface response plots showing the nanofiber diameter as a function of (a) electrospinning voltage and solution concentration for a fixed flow rate, and (b) flow rate and solution concentration for a fixed electrospinning voltage.

The final aspect discussed in this section is a residual analysis, which was also performed by the STATISTICA® software. A residual is the difference between an observed value and a predicted value. The residual analysis was used herein to examine whether the regression model is an adequate model. Three residual plots are shown in Figure 30. A normal probability plot was used to examine if the experimental data approximately follows a normal distribution. In the normal probability plot of residuals in Figure 30(a), all points fall onto a straight line. In the plot of residual values versus predicted values in Figure 30(b), no unique and discernible pattern can be

observed. These observations lead to the conclusion that the experimental data is indeed normally distributed. In the plot of predicted values versus observed values given by Figure 30(c), nearly all points fall onto a straight line, which confirm that the regression model fits the experimental data very well. Moreover, the residual analysis results of the regression model from the STATISTICA® software indicate that there is no outlier for the entire data set. Therefore, the regression model can thus be considered as an adequate and valid prediction model.

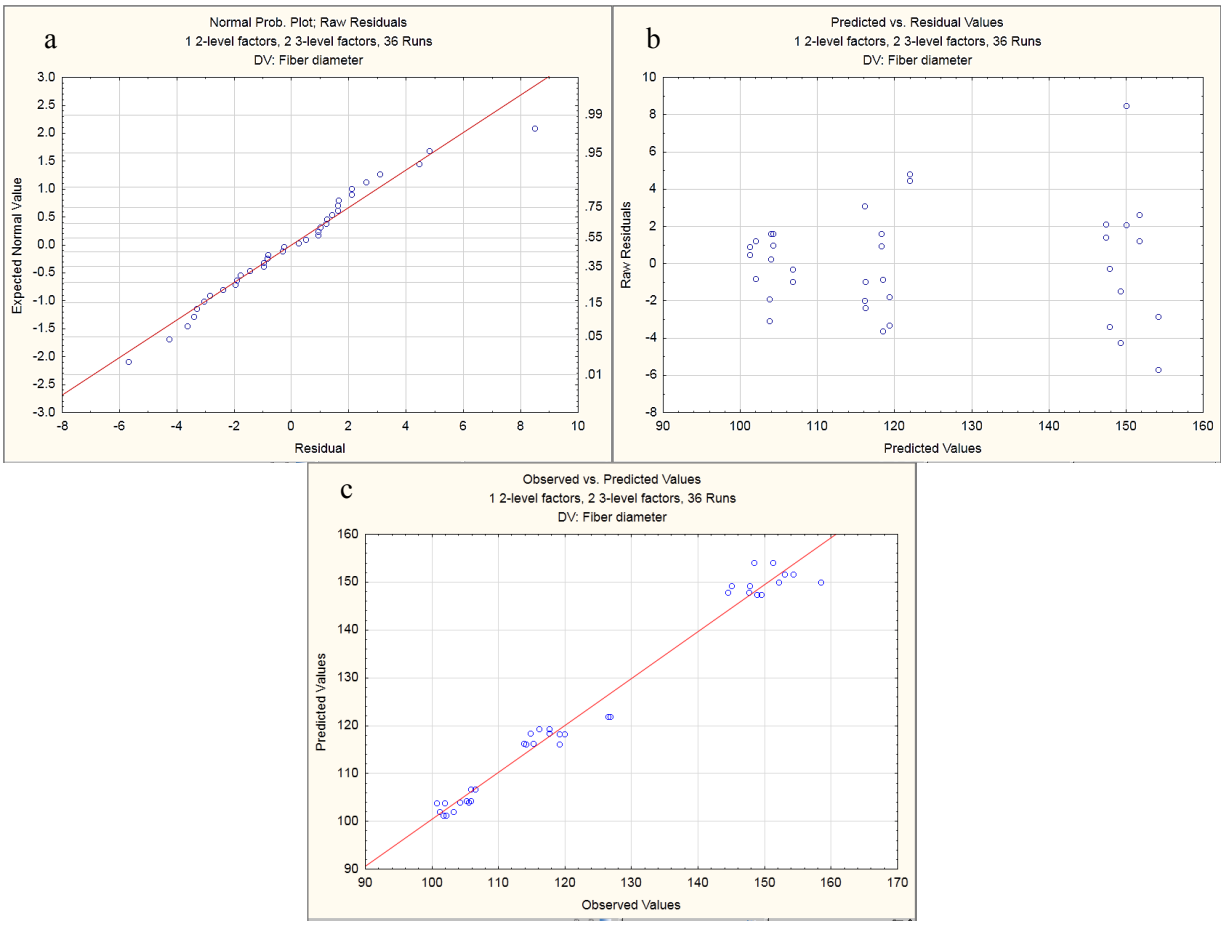

Figure 30. (a) Normal probability plot of residuals, (b) plot of residual values versus predicted values and (c) plot of predicted values versus the observed values for the fiber diameter.

4.3.2.2 Statistical analysis of the standard deviation of fiber diameter

Again using the STATISTICA® software to analyze all the data, the effect estimate results for the electrospinning voltage, solution concentration and flow rate on the standard deviation of fiber diameter were obtained. The effect estimate table is shown in Appendix C. The P-values for solution concentration, electrospinning voltage and flow rate were determined as 0.000234, 0.000396 and 0.0231, respectively. The critical P-value is again 0.1. Obtained P-values for the

above parameters are all smaller than the critical P-value, and hence, all these parameters have significant effects on the standard deviation of fiber diameter. Furthermore, P-values for the interactions between (i) solution concentration and electrospinning voltage and (ii) electrospinning voltage and flow rate were found as 0.00385 and 0.00001, respectively. Consequently these two interactions have significant effects on the standard deviation of fiber diameter. Conversely, the P-value for the interaction between solution concentration and flow rate was 0.229, which is much larger than the critical P-value. The effect of this interaction is therefore insignificant. The coefficient for the interaction between electrospinning voltage and flow rate was -3.1992. The absolute value of this coefficient is the largest and P-value is the smallest, indicating that the effect of this interaction is the most significant. This conclusion can also be derived from the Pareto Chart in Figure 31. In the Pareto Chart, it can be found that the 2L by 3L, which represents the interaction between electrospinning voltage and flow rate, has the most significant effect on the standard deviation of fiber diameter. In addition, the P-value for the solution concentration (quadratic) was 0.189, which is larger than the critical P-value; therefore the effect of solution concentration (quadratic) is insignificant. The P-value of electrospinning voltage (quadratic) was found to be 0.116, which is a little larger than the critical P-value, indicating the effect is also not significant. In other words, the effects of solution concentration and electrospinning voltage on the standard deviation of fiber diameter can be considered as linear. From the analysis results of mean plots shown in Figure 32, the same conclusion can be gained. In the mean plots, the variances at each level of solution concentration and electrospinning voltage are all very large. Therefore, the effects of solution concentration and electrospinning voltage can be considered as linear.

In addition, based on the mean plots (Figure 32) which were again generated by the STATISTICA® software, it can be found that the solution concentration and flow rate have positive effects on the standard deviation, while electrospinning voltage has a negative effect on the fiber diameter standard deviation. However, this conclusion is not quite reliable. The single factor mean plot is only useful when the effects of the interactions are not significant. Single factor mean plot does not consider the interactions between the different parameters. Since the interaction between solution concentration and electrospinning voltage and the interaction between electrospinning voltage and flow rate also have significant effects on the standard deviation of fiber diameter, the two interactions should be considered. In the mean plots for two

factors shown in Figure 33 and Figure 34, which were generated by STATISTICA® software, the curves in the mean plots cross each other indicating that both effects of the interaction between solution concentration and electrospinning voltage and the interaction between electrospinning voltage and flow rate have significant effects on the standard deviation of fiber diameter. In the mean plot of solution concentration and flow rate (Figure 35), the curves in the mean plots do not cross each other indicating that the effect of the interaction between flow rate and solution concentration on the standard deviation of fiber diameter is not significant. These conclusions also corroborate the results of the effect estimate analysis given above. In the below sections, the regression model and surface response analysis were applied to analyze the effects of each factor and interaction on the standard deviation of fiber diameter.

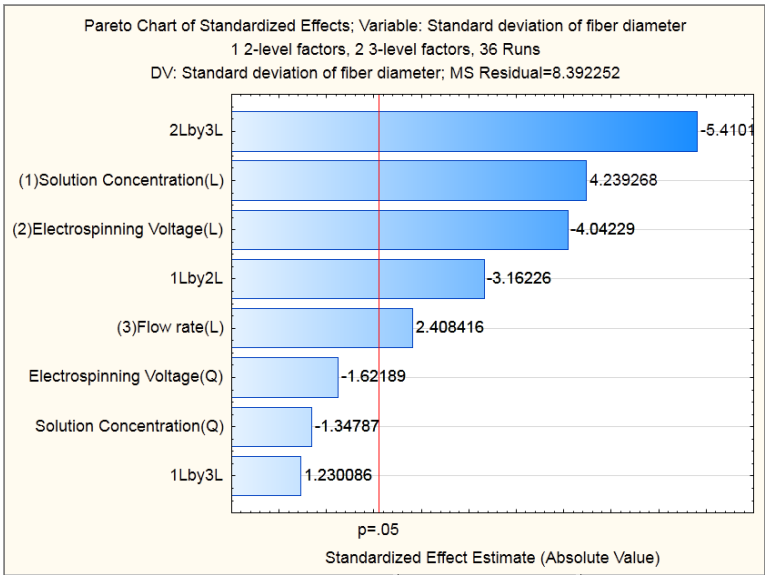

Figure 31. Pareto Chart for the effect of the electrospinning parameters on the standard deviation of fiber diameter in the second step of the DOE study.

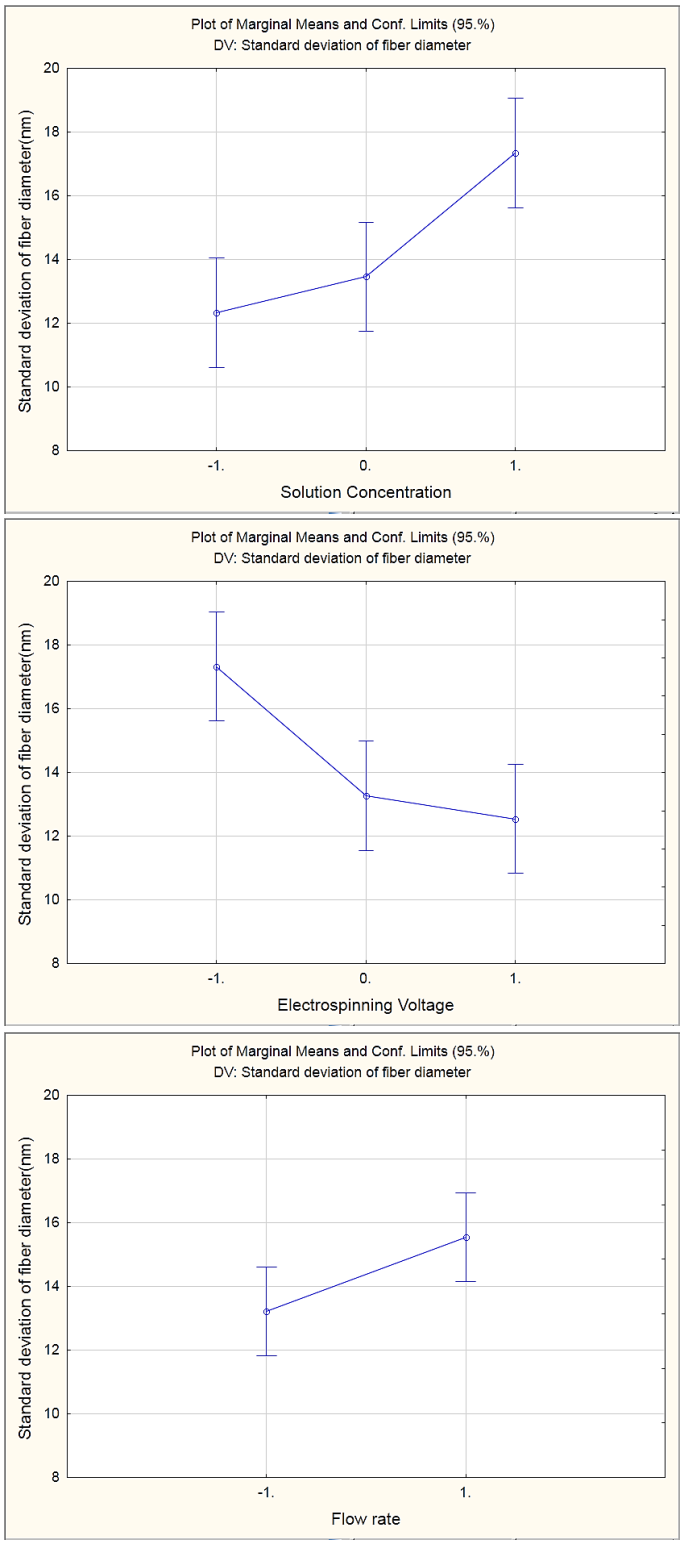

Figure 32. Mean plots of standard deviation of fiber diameter versus solution concentration, electrospinning voltage and flow rate for the second step of the DOE study.

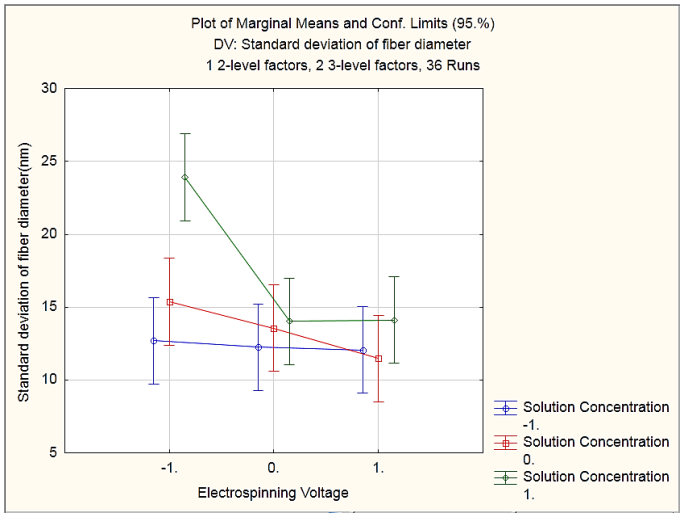

Figure 33. Relationship between the standard deviation of fiber diameter and electrospinning voltage for solution concentration levels of -1, 0 and 1.

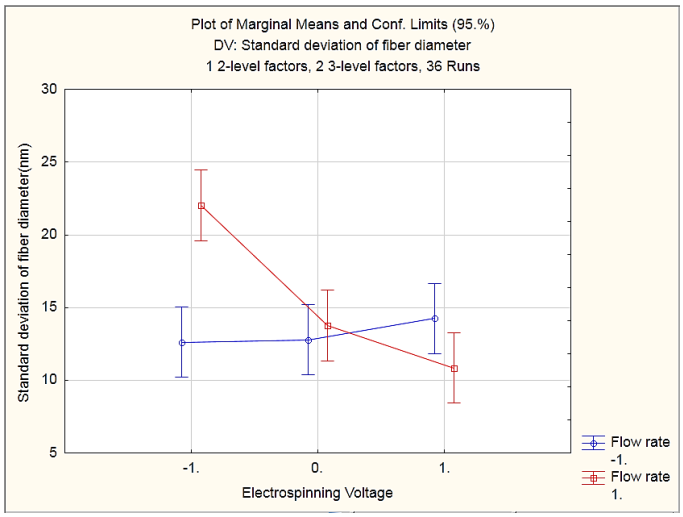

Figure 34. Relationship between the standard deviation of fiber diameter and electrospinning volate for flow rate levels of -1 and 1.

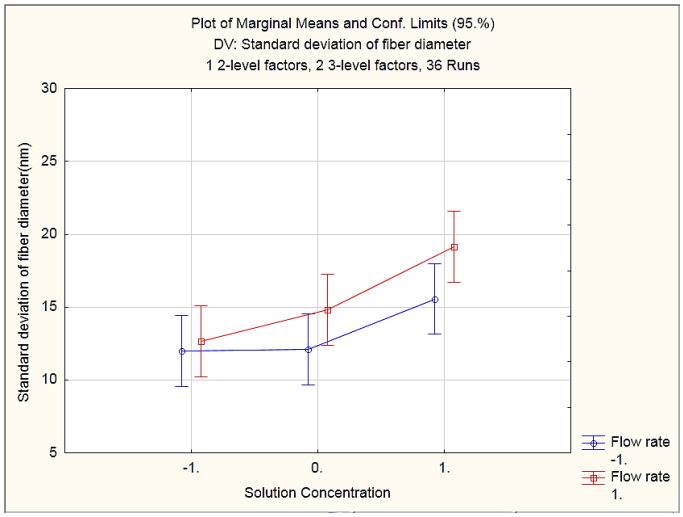

Figure 35. Relationship between the standard deviation of fiber diameter and solution concentration for flow rate levels of -1 and 1.

Based on the coefficients values of effect estimate analysis, the regression model equation generated by the STATISTICA® software for fiber diameter standard deviation was simplified to $S = 14.382 + 2.507\,C - 2.390\,V + 1.163\,F - 2.290\,CV - 3.199\,VF$ (S: standard deviation of fiber diameter, C: solution concentration, V: voltage, F: flow rate). To calculate the regression model predicted values for the standard deviation of fiber diameter of each run (number 1 to 36), the level values of solution concentration, electrospinning voltage and flow rate of each run were applied to the above the regression model. The level values for each run are already shown in Table 8. In this manner, the absolute differences between the regression model predicted standard deviation values and the experimental standard deviation values for all the 36 runs were calculated and are shown in Table 10. The percent differences between the experimental standard deviation values and model predicted standard deviation values based on the experimental standard deviation of fiber diameter are also displayed in the Table 10. The average of the experimental standard deviation values is 14.382nm and the average of the absolute difference between regression model predicted standard deviation values and experimental standard deviation values is 2.034nm. The error percentage is thus 14.1%, which was calculated by 2.034/14.382. For some runs, the differences between experimental standard deviation value and regression model predicted standard deviation value are big. These big differences make the final model prediction error percentage relatively large. Since the prediction error percentage of this regression model is relatively high, the analysis should not be only depended on the regression model. Therefore, the analysis of the real experimental data is also very necessary.

Table 10. Regression model predicted standard deviation values and absolute difference between experimental values and regression model predicted standard deviation values for all the 36 runs.

Run number	Experimental standard deviation of fiber diameter(nm)	Regression model predicted values (nm)	Absolute difference between experimental and model predicted values (nm)	Percent difference
1	12.135	7.613	4.522	37.3%
2	11.818	10.712	1.105	9.4%
3	13.324	13.812	0.488	3.7%
4	15.748	16.337	0.589	3.7%
5	14.900	13.038	1.862	12.5%
6	11.763	9.739	2.025	17.2%
7	15.139	17.207	2.069	13.7%
8	15.878	15.726	0.152	1.0%
9	17.746	14.245	3.501	19.7%
10	34.706	25.932	8.774	25.3%
11	13.792	18.052	4.260	30.9%
12	10.460	10.172	0.288	2.8%
13	11.678	12.410	0.733	6.3%
14	10.185	13.219	3.034	29.8%
15	12.371	14.028	1.657	13.4%
16	19.615	21.134	1.520	7.7%
17	15.462	15.545	0.083	0.5%
18	10.334	9.955	0.379	3.7%
19	10.151	7.613	2.538	25.0%
20	11.620	10.712	0.908	7.8%
21	12.972	13.812	0.840	6.5%
22	12.770	16.337	3.567	27.9%
23	10.633	13.038	2.405	22.6%
24	10.190	9.739	0.451	4.4%
25	14.318	17.207	2.890	20.2%
26	13.845	15.726	1.881	13.6%
27	16.448	14.245	2.203	13.4%
28	31.480	25.932	5.549	17.6%
29	12.590	18.052	5.462	43.4%
30	11.789	10.172	1.617	13.7%
31	12.343	12.410	0.068	0.5%
32	13.367	13.219	0.148	1.1%
33	12.609	14.028	1.419	11.3%
34	17.832	21.134	3.303	18.5%
35	15.205	15.545	0.340	2.2%
36	10.540	9.955	0.584	5.5%
Average	14.382		2.034	

One of the purposes to investigate the standard deviation of fiber diameter is to find how more uniform electrospun Nylon 6 nanofibers can be obtained. Based on the regression model above, it can be concluded the standard deviation of fiber diameter is smallest when electrospinning voltage, solution concentration and flow rate are all chosen lowest level (-1). The regression model predicted value is 7.613, while the experimental standard deviation values are 12.135 in the original group and 10.151 in the replication group (run number 1 and 19 in Table 10). Although there is difference between the regression model predicted value and experimental value, the experimental standard deviation value of 10.151 is already the lowest value of all the 36 runs. Therefore, the regression model could provide the right direction to obtain the lowest standard deviation of fiber diameter.

The second purpose to analyze the standard deviation of fiber diameter is to provide the criterion for the mechanical properties characterization. For the mechanical properties characterization, three kinds of samples of the three solution concentrations (15wt%, 17.5wt%, 20wt%) were tested. For each concentration level, the electrospun Nylon 6 nanofiber with the smallest fiber diameter standard deviation will be chosen for the tensile test. Therefore, when the solution concentration is fixed, the law of the change of fiber diameter standard deviation with electrospinning voltage and flow rate is very important. When concentration is fixed at a certain positive level (0 or +1), from the regression model, it can be concluded that the standard deviation was smallest when both electrospinning voltage and flow rate are chosen the highest level (+1). In addition, this result can also be gained from the analysis of the surface response plots shown in Figure 37 (a) and (b). This conclusion based on the regression model analysis coincides with the analysis results of the experimental standard deviation data. The average experimental standard deviation values of the original group and replication group are shown in the Table 11 below and yellow ones are the smallest average experimental standard deviation values for each solution concentration level: -1, 0, +1.

Table 11. Experimental average standard deviation values of the two groups and the regression model predicted values.

Solution concentration	Electrospinning voltage	Flow rate	Average experimental standard deviation of original group and replication group (nm)	model predicted value (nm)
-1	-1	-1	11.143	7.613
-1	0	-1	11.719	10.712
-1	1	-1	13.148	13.812
-1	-1	1	14.259	16.337
-1	0	1	12.767	13.038
-1	1	1	10.977	9.739
1	-1	-1	14.728	17.207
1	0	-1	14.862	15.726
1	1	-1	17.097	14.245
1	-1	1	33.093	25.932
1	0	1	13.191	18.052
1	1	1	11.124	10.172
0	-1	-1	12.010	12.410
0	0	-1	11.776	13.219
0	1	-1	12.490	14.028
0	-1	1	18.723	21.134
0	0	1	15.334	15.545
0	1	1	10.437	9.955

When the solution concentration is fixed at the negative level of -1, it is found that the regression model predicted standard deviation value when both electrospinning voltage and flow rate are chosen the lowest levels (-1) is very close to the value when both electrospinning voltage and flow rate are chosen the highest level (+1). The difference between the two standard deviation values is only 2.126nm. This regression model analysis results can also be concluded from the analysis of the surface response plot shown in Figure 37(c). Therefore, when solution concentration is fixed at the -1 level, the better method is to analyze the actual experimental standard deviation data. Based on the experimental standard deviation data shown in the Table 11, when the solution concentration is fixed at the negative level of -1, it is found that the standard deviation of fiber diameter is smallest when both electrospinning voltage and flow rate are chosen the highest levels.

Therefore, when solution concentration is fixed at the level of -1 or 0 or 1, based on above regression model analysis and the experimental data analysis, it can be concluded that the

standard deviation of fiber diameter is smallest when both electrospinning voltage and flow rate are chosen the highest levels.

The surface response plots were generated by STATISTICA® software to indicate the change of standard deviation of fiber diameter as a function of two electrospinning parameters with the third one fixed. Such plots are shown in Figure 36 and Figure 37, where blue dots represent experimental data of fiber diameter standard deviation. The colors scale in these surface response plots corresponds to the range of fiber diameter standard deviation.

Here, the surface response analysis for standard deviation of fiber diameter is complicated. The reason is that both the interaction between the solution concentration and electrospinning voltage and the interaction between the electrospinning voltage and flow rate are significant. From the surface response plot in Figure 36(a), it can be concluded that under a certain flow rate, the standard deviation is lowest when solution concentration is chosen at the lowest level and electrospinning voltage is in the level range from -1 to 1. From the surface response plot in Figure 36(b), it could be concluded that under a certain electrospinning voltage, the standard deviation is lowest when both solution concentration and flow rate are chosen at the lowest levels. Furthermore, the surface response analysis was done when solution concentration is fixed at the each of the three levels: -1, 0, +1. Based on the surface response plots shown in Figure 37(a) and (b), when concentration is fixed at the level of 0 or 1, it is found that the standard deviation of fiber diameter is lowest when both electrospinning voltage and flow rate are chosen at the highest levels (+1). Based on the surface response plot shown in Figure 37(c), when solution concentration is fixed at the level of -1, it can be found that the standard deviation values are both relatively small when both electrospinning voltage and flow rate are chosen at the highest levels (+1) or the lowest levels(-1). The conclusion of this surface response analysis corroborates the conclusion of regression model analysis in the above section.

In addition, for all the surface response plots shown in Figure 36 and Figure 37, it is observed that several points do not fit the surface response plots well. The standard deviation values of these points are all very high; so they can not fit the surface response plot very well. For the run number of 10 and 28 given in Table 8, the standard deviation values are much higher than the other runs. Since both the original group and replication group give the similar results for the

standard deviation values of run number 10 and 28, the high standard deviations values can be considered reasonable and acceptable.

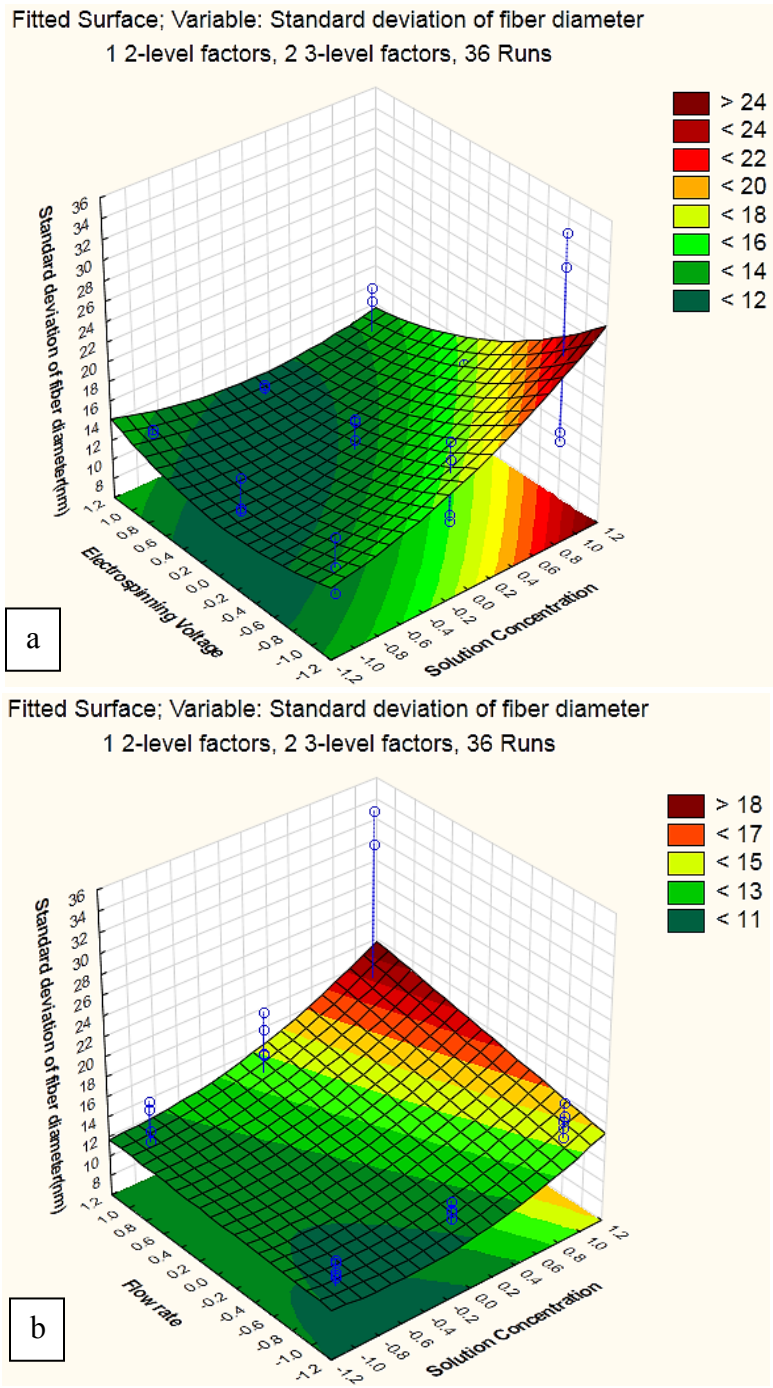

Figure 36. Fitted surface response plots showing the standard deviation of fiber diameter as a function of (a) electrospinning voltage and solution concentration for a fixed flow rate, and (b) flow rate and solution concentration for a fixed electrospinning voltage.

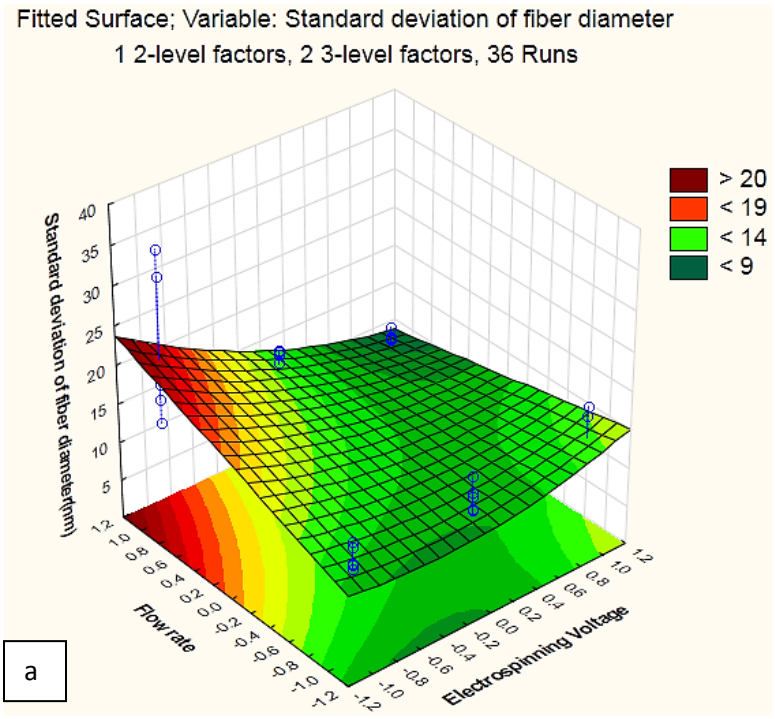
Fitted Surface; Variable: Standard deviation of fiber diameter
1 2-level factors, 2 3-level factors, 36 Runs
Standard deviation of fiber diameter(nm)
Flow rate
Electrospinning Voltage
> 20
< 19
< 14
< 9
a

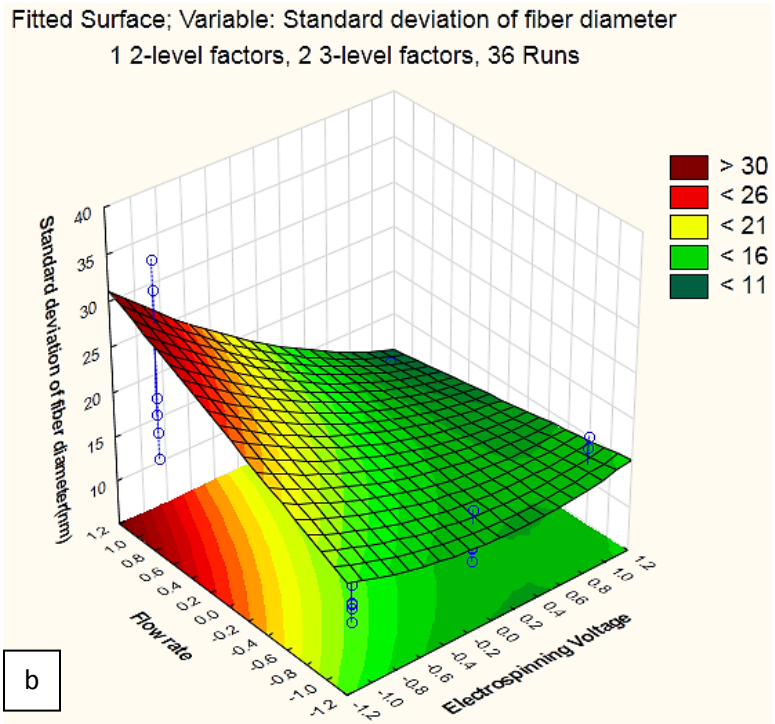
Fitted Surface; Variable: Standard deviation of fiber diameter
1 2-level factors, 2 3-level factors, 36 Runs
Standard deviation of fiber diameter(nm)
Flow rate
Electrospinning Voltage
> 30
< 26
< 21
< 16
< 11
b

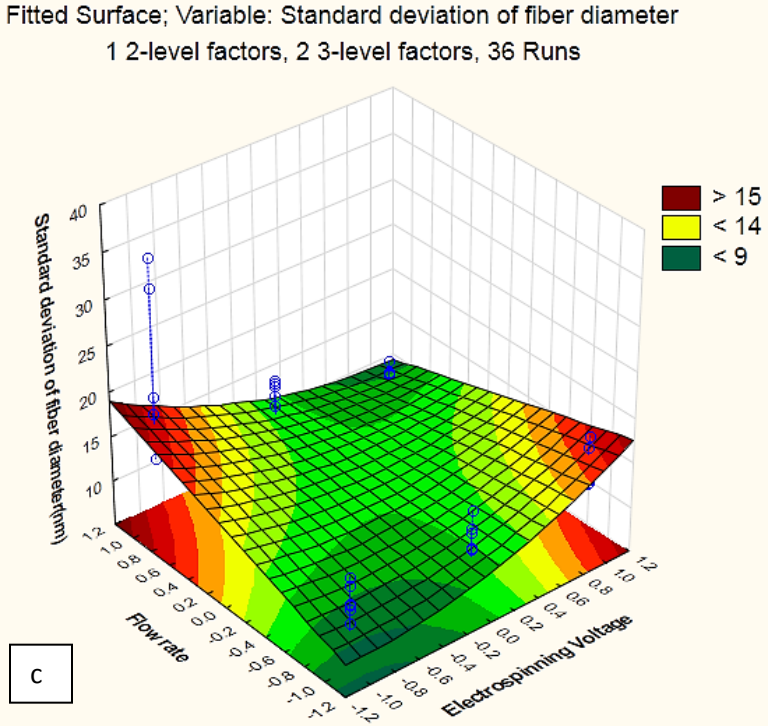

Figure 37. Surface response plots showing the standard deviation of fiber diameter as a function of (a) electrospinning voltage and flow rate for a fixed solution concentration at level: 0 (b) electrospinning voltage and flow rate for a fixed solution concentration at level: 1 (c) electrospinning voltage and flow rate for a fixed solution concentration at level:-1.

The final aspect discussed in this section is a residual analysis, which was also performed by the STATISTICA® software. In the normal probability plot of residuals in Figure 38(a), nearly all points fall onto a straight line. Therefore, the experimental data approximately distributed normally. In the plot of residual values versus predicted values in Figure 38(b), no unique and discernible pattern can be observed. But there are two points which are away from the other points. The reason is that the standard deviation values for the two runs (run number 10 and 28) are much higher than other runs. The two experimental data could be considered as the outliers.

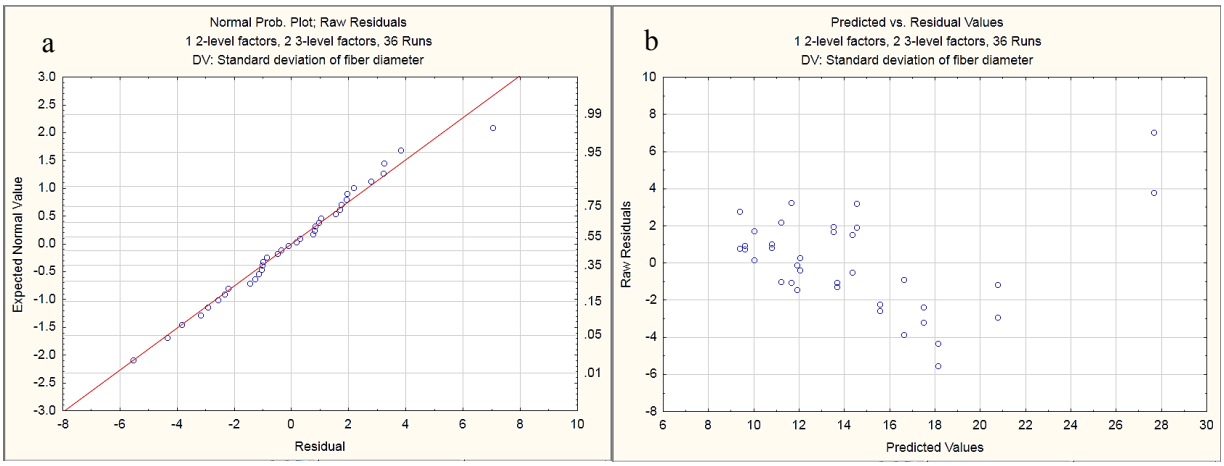

Figure 38. (a) Normal probability plot of residuals and (b) plot of residual values versus predicted values for fiber diameter standard deviation in the second step of the DOE study.

In sum, based on the analysis results of the regression model, experimental data and surface response plots, the mechanical properties test was done for each of the three concentrations (15wt%, 17.5wt%, 20wt%) when the electrospinning voltage is chosen at the highest level (24kV) and flow rate is also chosen at the highest level (5µl/min).

Chapter 5 - Mechanical Properties Characterization of electrospun Nylon 6 fibers

To prepare for the tensile testing samples, each electrospinning experiment for the three Nylon 6 solution concentrations was completed in a one-day period. As discussed in Chapter 4, for the electrospinning parameters, the electrospinning voltage was chosen at 24kV, and a flow rate of 5µl/min was selected for the three solution concentrations. The distance, temperature and humidity remained at 10cm, 27ºC and 34%, respectively. As mentioned in Chapter 2 about tensile testing procedures, only the specimens that failed in the gauge section center (i.e., not near or at the edge of the gripping system) were included for the determination of the tensile strength and elongation at break.

Considering fiber mat porosity, the stress within a specimen was calculated by

$$\sigma = \frac{T}{A * (1 - \emptyset_{mat})} \tag{5-1}$$

$$A = \delta * W \tag{5-2}$$

In the equation above, T is the tensile force, A is the cross sectional area, δ is the average fiber mat thickness and W is the average width of the test strip. Note that the method for calculating mat porosity and the mat porosities values for the three tested Nylon 6 solution concentrations are given in Chapter 2.4.

Shown in Figure 39 are characteristic stress-strain curves of electrospun Nylon 6 fiber mats that failed within the gauge section center for solution concentrations of 15wt%, 17.5wt% and 20wt%. It was observed that specimens broke immediately after the initiation of a crack. The data in Figure 39 indicates that the elongation at break and tensile strength increased with increasing solution concentration. The initial part of each stress/strain curve is clearly nonlinear. This behavior can be explained as follows. At the beginning of each tensile test, when tensile force was applied to the fiber mat specimen, the randomly distributed nanofibers realigned in the direction of the applied loading. After this realignment process, a linear stress/strain becomes apparent in the curves. The slope of this linear part in the stress/strain curves was used to calculate the elastic modulus. Note that the calculation method of elastic modulus is congruent with ASTM standard D2256/D2256M for tensile property determination of yarns. The stress/strain curves for all the tensile testing specimens are shown in Appendix D.

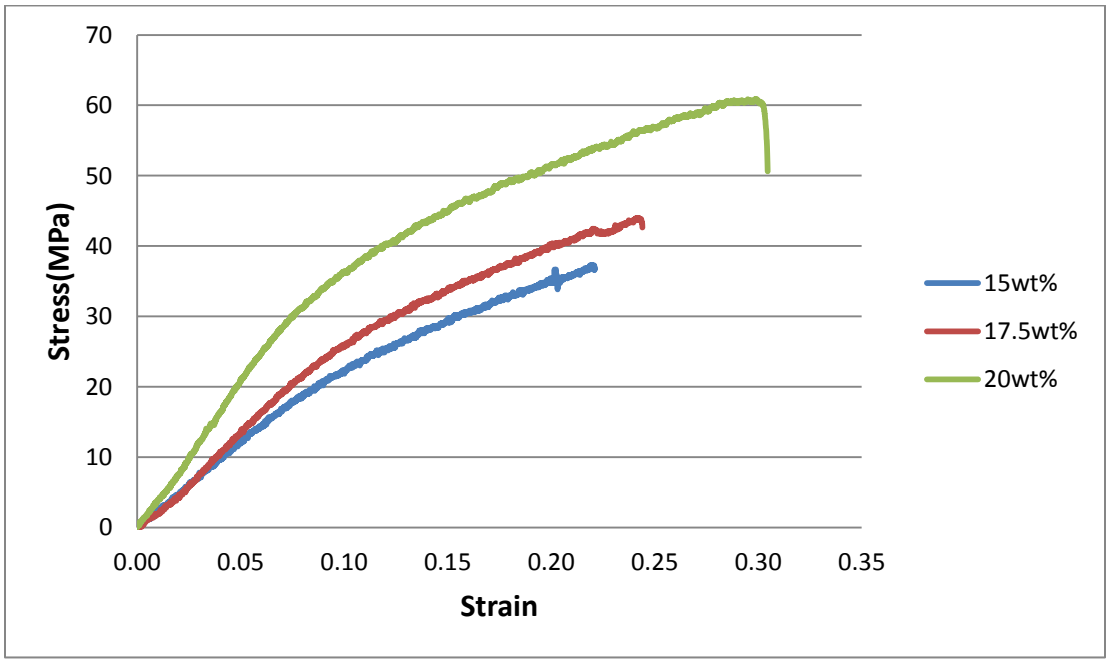

Figure 39.Tensile stress/strain curves of Nylon 6 nanofiber mats electrospun from solutions with concentrations of 15wt%, 17.5wt% and 20wt%.

Table 12 summarizes the tensile test results for maximum elongation at break, elongation at maximum stress, tensile strength, elastic modulus of the specimens that failed in the gauge section center and elastic modulus of all specimens along with their standard deviations for the three solution concentrations. Figures 40 to 43 show the change of elongation at break, tensile strength and elastic modulus with increasing Nylon 6 concentration from 15wt% to 20wt%. The error bars in these figures represent standard deviation values.

Table 12. Elongation at maximum stress and at break, tensile strength and elastic modulus of Nylon 6 fiber mat tensile specimens for different electrospinning solution concentrations.

Concentration of Nylon 6	**15wt%**	**17.50wt%**	**20wt%**
Elongation at maximum stress (%)	20.8±4.4	24.5±4.3	29.0±3.0
Elongation at break (%)	20.9±4.4	24.7±4.2	29.2±3.0
Tensile strength (MPa)	42.6±11.2	49.3±8.2	54.7±6.9
Elastic modulus of specimens that failed in the gauge section center (MPa)	302.9±78.3	362.9±50.8	383.5±57.3
Elastic modulus of all specimens (MPa)	325.2±74.1	373.1±51.6	349.1±58.0

As shown in Table 12 and Figure 40, the maximum elongation at break of Nylon 6 fiber strips increased from 20.9% to 29.2% with the increase in solution concentration from 15wt% to 20wt%. In addition, it was ascertained that the elongation at break was nearly the same as the elongation at maximum stress as fiber mat specimen broke nearly immediately after the applied stress reached its highest level. In terms of tensile strength, it can be observed in Table 12 and Figure 41 that average values increased from 42.6MPa to 54.7MPa with the solution concentration increasing from 15wt% to 20wt%.

A trend similar to tensile strength and elongation at break could also be observed for the average elastic modulus values of the specimens that failed in the gauge section center. For the 15wt% solution concentration, a total of six specimens failed in the gauge section center. For the 17.5wt% and 20wt% solution concentrations, eight and seven specimens failed in the gauge section center, respectively. As shown in Table 12 and Figure 42, the average elastic modulus increased from 302.9MPa to 383.5MPa with the Nylon 6 solution concentration increasing from 15wt% to 20wt%. This trend is also visible in Figure 39. Standard deviations associated with the elastic modulus are comparatively high for all of the employed solution concentrations (15wt%, 17.5wt%, 20wt%). In light of the high standard deviations, it appears that the increase in elastic modulus is not as significant as suggested by the average elastic modulus values, i.e., many data

points fall within the band given by the overall maximum and minimum values. The t-test is necessary to judge whether there is significant change of the elastic modulus with the increase of solution concentration from 15wt% to 20wt%. Three t-tests, including the t-test between 15wt% and 17.5wt%, the t-test between 17.5wt% and 20wt%, and the t-test between 15wt% and 20wt%, were performed for the elastic modulus values. For the t-test results, the three P-values are all larger than the critical P-value of 0.05. Therefore, it can be concluded that the there is no significant change of elastic modulus of the specimens that failed in the gauge section center with the increase of solution concentration from 15wt% to 20wt%.

On the other hand, the elastic modulus for all specimens, including the ones that failed at the edge of the grips, was analyzed. The total numbers of specimens were 15, 13 and 13 for the solution concentrations of 15wt%, 17.5wt% and 20wt%, respectively. Based on Table 12 and Figure 43, the standard deviations are all relatively high for the elastic modulus for all specimens. In light of the high standard deviations, it can be found that the elastic modulus values of the three solution concentrations are nearly at the same level. Again, t-tests were performed for the elastic modulus values for the three different solution concentrations. For the t-test results, the P-values are all larger than the critical P-value of 0.05. Therefore, it can be concluded that there is no significant change for the elastic modulus of all specimens with the increasing solution concentration from 15wt% to 20wt%.

Possible reasons for the high scatter of test data are as follows. As mentioned previously, most nanofibers in the fiber strip are not aligned to the applied loading direction leading to a realignment process upon load application. Since the nanofibers contact each other, the realignment process may cause a random amount of friction force to individual nanofibers. Moreover, the number of nanofibers inside each fiber strip, their length and alignment are not controlled and may vary from sample to sample, which also contribute to a high variability in mechanical properties. Note that based on the observed trends, increasing the Nylon 6 solution concentration beyond the tested range may promise even further enhancements in the mechanical properties. However, as pointed out in Chapters 4.2.1 and 4.2.2 using SEM images analysis, tested concentrations from 15wt% to 20wt% already represent the usable solution concentration range for the quality electrospun Nylon 6 nanofibers.

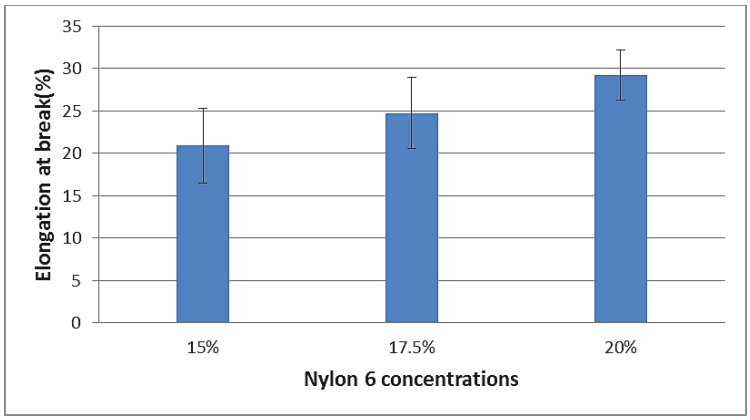

Figure 40. Elongation at break versus solution concentrations for electrospun nanofiber mat specimens.

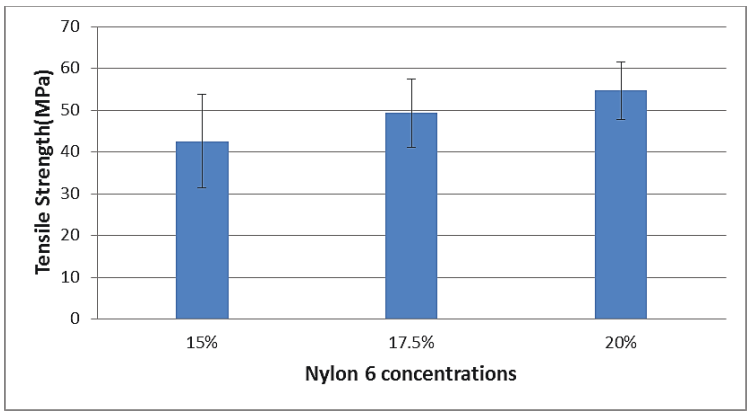

Figure 41. Tensile strength versus solution concentrations for electrospun nanofiber mat specimens.

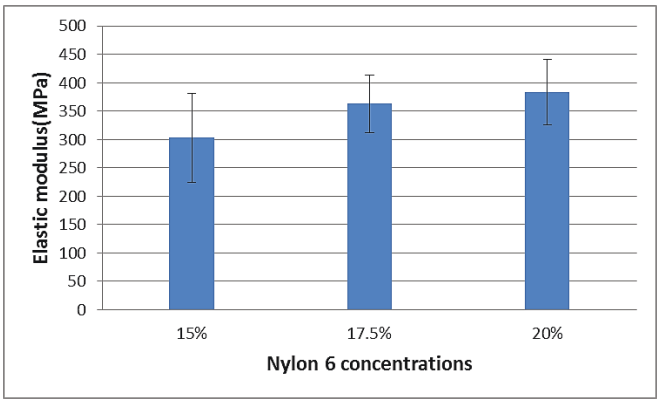

Figure 42. Elastic modulus versus solution concentrations for electrospun nanofiber mat specimens that failed in the gauge section center.

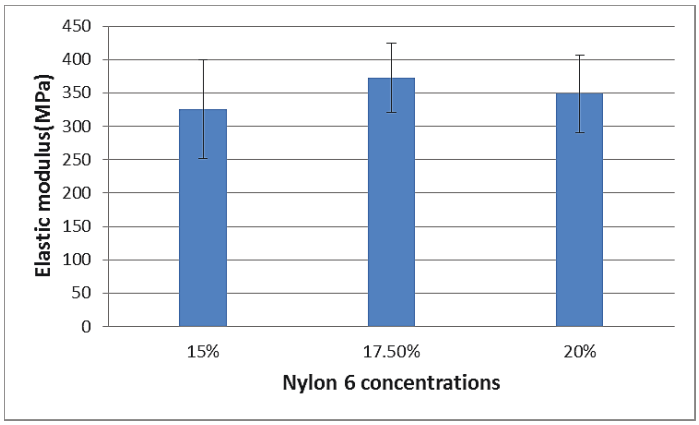

Figure 43. Elastic modulus versus solution concentrations for all electrospun nanofiber mat specimens.

Recall that results from the DOE study (Chapter 4.3.2.2) guided the selection of electrospinning parameters, i.e., solution concentrations of 15wt%, 17.5wt% and 20wt%, and highest level of electrospinning voltage (24kV) and flow rate (5µl/min) for the quality nanofiber production. These parameters produced average fiber diameters as summarized in Table 13, that is, the average fiber diameter increases from 103.2nm to 149.5nm with the increase of Nylon 6 solution concentration from 15wt% to 20wt%. Correlating results from Table 12 and Table 13, it could be inferred that an increase in fiber diameter is accompanied with an increase in mechanical properties for the range of tested electrospinning parameters.

Table 13. The average Nylon 6 fiber diameter and electrospinning parameters for the three different groups of tensile test samples.

Solution concentration (wt%)	Electrospinning voltage (kV)	Flow rate (µl/min)	Average fiber diameter (nm)
15	24	5	103.204
17.5	24	5	115.248
20	24	5	149.527

Chapter 6 - Conclusions and Future Work

6.1 Summary of the thesis

In this thesis research, Nylon 6 nanofibers were successfully fabricated by the electrospinning technique. Design of experiment and statistical analysis methods were applied to investigate which parameters and their interactions have significant effects on nanofiber diameter and its

standard deviation and whether these effects are linear or nonlinear. In this manner, a method providing valuable design guidance for effectively producing electrospun nanofibers was developed. In this thesis, electrospinning voltage, solution concentration and flow rate are the three investigated electrospinning parameters. Firstly, a 2^3 full factorial screening test was performed as part of the DOE study to evaluate the influence of the different parameters on nanofiber quality and fiber diameter. The maximum and minimum limits were selected for the screening test for electrospinning voltage (12kV, 24kV), solution concentration (15wt%, 20wt%) and flow rate(2 µl/min, 5 µl/min). Analysis results from the screening test indicated that both the solution concentration and the electrospinning voltage had significant effects on the fiber diameter and its standard deviation. The effect of flow rate on the fiber diameter was not very significant and the associated P-value of the effect of flow rate on the fiber diameter was found to be very close to the critical P-value of 0.1. In addition, it was found that the standard deviation of fiber diameter was considerable when the electrospinning voltage was chosen at the lowest level of 12kV. Hence, this voltage level was eliminated from the second step of the DOE study.

In the second step of the DOE study, additional levels were added for electrospinning parameters based on their influence concluded from the screening test. Three levels were chosen for the electrospinning voltage (16kV, 20kV, 24kV), one intermediate level was added for the solution concentration (15wt%, 17.5wt%, 20wt%) and two levels were maintained for the flow rate (2µl/min, 5µl/min). In this second step of the DOE study, the investigation of electrospinning parameters was expanded beyond evaluating merely the influence on fiber diameter and its standard deviation, that is, it was studied whether the effects are linear or nonlinear. From the statistical analysis results, it was concluded that the solution concentration, electrospinning voltage and flow rate all had significant effects on the Nylon 6 nanofiber diameter. Solution concentration had the most significant effect on nanofiber diameter, and the effect was nonlinear. The second step of the DOE study showed that the average nanofiber diameter increased with increasing solution concentration, whereas nanofiber diameter decreased with the increase of electrospinning voltage and flow rate. The collected data allowed for a regression model equation to be generated to accurately predict fiber diameters based level values for solution concentration, electrospinning voltage and flow rate. The average prediction error percentage for this regression model was 5.3%.

On the other hand, statistical analyses as part of the second step of the DOE study indicated that the solution concentration, electrospinning voltage, flow rate, interaction between solution concentration and electrospinning voltage, and interaction between flow rate and electrospinning voltage all had significant effects on the standard deviation of fiber diameter. The interaction between the flow rate and electrospinning voltage had the most significant effect on the standard deviation of fiber diameter. Since P-values for the quadratic effect of electrospinning voltage and solution concentration on the fiber diameter standard deviation were larger than the critical P-value of 0.1, their effects on standard deviation of fiber diameter can be considered linear. A regression model equation was generated for the standard deviation of fiber diameter as well. The prediction error of this regression model is rather high, and hence, the analysis should not solely depend on the regression model. The assessment of experimental data would be necessary. Using both the regression model analysis and experimental data analysis, it was ascertained that the fiber diameter standard deviation was lowest when the solution concentration was fixed at a specific level while both electrospinning voltage and flow rate were set to their highest levels.

Based on the analysis results of the DOE study, the mechanical properties characterization of Nylon 6 nanofiber mat was performed for three solution concentration levels (15wt%, 17.5wt%, 20wt%) and choosing the highest viable levels for both the electrospinning voltage (24kV) and flow rate (5µl/min).

Tensile testing results revealed that the elongation at break and tensile strength of electrospun Nylon 6 nanofiber mat strip increased with the increase of solution concentration from 15wt% to 20wt%. This increase in mechanical properties was accompanied by an increase in average fiber diameters. For the elastic modulus, based on comparatively high standard deviations for the elastic modulus and t-test results, it can be concluded that there is no significant change of elastic modulus with the increase of solution concentration from 15wt% to 20wt%.

6.2 Future directions

1. Mechanical property of single fibers

The present study yielded tensile test results for electrospun Nylon 6 fiber mat specimens. However, it was impossible to fully analyze the relationship between electrospinning parameters and mechanical properties for single Nylon 6 nanofibers. A number of factors affect fiber mat

mechanical properties, including number of fibers, fiber orientation and friction between fibers. It would be desirable to perform tensile testing of single fibers in order to obtain additional information on the effect of the electrospinning parameters on the actual fiber performance. For future work, it is thus recommended to conduct single fiber tensile testing and contrast experimental results with those from random fiber mats.

2. Adding nanoscale fillers to polymer solution

Adding nanoscale fillers to the polymer solution and subsequently electrospinning nanocomposite fiber may have beneficial effects on fiber properties or create a fiber material that has multifunctional properties. Nylon 6 has good mechanical properties and is a biocompatible polymer [35,36]. Hence, filler-modified Nylon 6 is a very promising material for advanced products such as conductive composite yarns for strain sensing applications, which can be accomplished adding conductive nanoparticles. It was already reported in the technical literatures that carbon nanotubes were successfully added to the Nylon 6 to fabricate electrospun Nylon 6/carbon nanotube nanofibers for strain sensing and other electronic applications [39,41]. Employing a DOE approach and suitable statistical methods is seen as an appropriate means to explore the design space for such materials, and this thesis provides a guideline for this process. It is therefore recommended to employ the present approach to achieve effective design guidance also for nanoparticle modified electrospun nanofibers.

3. Increasing the number of tensile testing fiber mat specimens

For this study, the electrospinning experiment for each solution concentration was finished in one day. Given the current electrospinning setup, only a limited amount of tensile testing fiber strips could be produced in a one-day electrospinning experiment. To increase the number of tensile testing fiber mat specimens is a possible future direction. There are mainly two possible solutions. The first solution is to improve the electrospinning setup, e.g. using a larger collector or using two needles to concurrently electrospin nanofibers. The main purpose of this solution is to collect a larger area of fiber mat during the one-day electrospinning. The second solution is to electrospin fiber mats in two separate days. Then, tensile tests would be done for all specimens collected from two days of electrospinning. Note that there are several important issues that need to be considered for this solution. When electrospinning for two days, it is critical to guarantee controlled/constant manufacturing parameters, i.e., temperature, humidity, needle size, syringe

type and electrospinning distance, to remain exactly the same for two-day experiments. If some variables change within a two-day electrospinning experiment, the final tensile testing results are not reliable because the effects of the changed variables are not considered. In addition, for the tensile testing fiber specimens that are electrospun on different days, the storage time before the tensile testing should remain constant.

Bibliography

[1] Jayesh Doshi and Darrell H. Reneker, "Electrospinning Process and Applications of Electrospun Fibers," Journal of Electrostatics, vol. 35, pp.l51-160, 1995.

[2] Pitt Supaphol, Chidchanok Mit-Uppatham and Manit Nithitanakul, "Ultrafine electrospun polyamide-6 fibers: Effect of emitting electrode polarity on morphology and average fiber diameter," *Journal of Polymer Science Part B: Polymer Physics*, vol. 43, pp. 3699-3712, 2005.

[3] C. J. Luo, Simeon D. Stoyanov, E. Stride, E. Pelan and M. Edirisinghe, "Electrospinning versus fibre production methods: from specifics to technological convergence," *Chem Soc Rev*, vol. 41, pp. 4708–4735, 2012.

[4] Seeram Ramakrishna, Kazutoshi Fujihara, Wee-Eong Teo, Teik-Cheng Lim, & Zuwei Ma, "An Introduction to Electrospinning and Nanofibers," World Scientific Publishing Company, Singapore, 2005.

[5] Dennis Edmondson, Ashleigh Cooper, Soumen Jana, David Wood and Miqin Zhang, "Centrifugal electrospinning of highly aligned polymer nanofibers over a large area," *J. Mater. Chem.*, vol.22, pp. 18646-18652, 2012

[6] Zheng-Ming Huang, Y.-Z. Zhang, M. Kotaki, S.Ramakrishna, "A review on polymer nanofibers by electrospinning and their applications in nanocomposites," *Composites Science And Technology,* vol. 63, pp. 2223-2253, 2003.

[7] W E Teo and S Ramakrishna, "A review on electrospinning design and nanofibre assemblies," *Nanotechnology*, vol. 17, pp. R89-R106, 2006.

[8] Ali Eftekhari, "Nanostructured Conductive Polymers," John Wiley & Sons, Ltd, 2010, ISBN: 978-0-470-74585-4.

[9] J.M. Deitzel, J.D. Kleinmeyer, J.K. Hirvonen, N.C. Beck Tan, "Controlled deposition of electrospun poly(ethylene oxide) fibers," *Polymer*, vol. 42, pp. 8163-8170, 2001.

[10] Huan Pan, Luming Li, Long Hu, Xiaojie Cui, "Continuous aligned polymer fibers produced by a modified electrospinning method," *Polymer*, vol.47, pp.4901-4904, 2006.

[11] I. S. Chronakis, "Novel nanocomposites and nanoceramics based on polymer nanofibers using electrospinning process – A review," *J. Mater. Proc. Technol.*, vol. 167, pp. 283–293, 2005.

[12] Sureeporn Koombhongse, Wenxia Liu and Darrell H. Reneker, "Flat polymer ribbons and other shapes by electrospinning," *Journal of Polymer Science Part B: Polymer Physics*, vol.39, pp.2598-2606, 2001.

[13] E. Zussman, M. Burman, A. L. Yarin, R. Khalfin and Y. Cohen, "Tensile Deformation of Electrospun Nylon-6,6 Nanofibers," *Journal of Polymer Science Part B: Polymer Physics,* Vol. 44, pp. 1482-1489, 2006

[14] Darrell H. Reneker, Alexander L. Yarin, Hao Fong, and Sureeporn Koombhongse, "Bending instability of electrically charged liquid jets of polymer solutions in electrospinning," *Journal of Applied Physics, Vol.87,* pp. 4531-4547, 2000.

[15] D.H. RENEKER, A.L. YARIN, E.ZUSSMAN and H.XU, "Electrospinning of Nanofibers from Polymer Solutions and Melts," *Advanced In Applied Mechanics*, vol. 41, pp. 43-195, 2007.

[16] Jun-Seo Park, "Electrospinning and its applications," *Advances in Natural Sciences: Nanoscience and Nanotechnology*, vol. 1, pp. 1-5, 2010.
[17] Seema Agarwal, Joachim H. Wendorff, Andreas Greiner, "Use of electrospinning technique for biomedical applications," *Polymer,* vol. 49, pp. 5603–5621, 2008.
[18] Taylor, G. I., "Disintegration of water drops in an electric field," *Proc. R. Soc. A*, vol.280 pp.383–397, 1964.
[19] Thandavamoorthy Subbiah, G. S. Bhat, R. W. Tock, S. Parameswaran, S. S. Ramkumar, "Electrospinning of Nanofibers," *Journal of Applied Polymer Science*, vol.96, pp.557-569, 2005.
[20] Xinhua Zong, Kwangsok Kim, Dufei Fang, Shaofeng Ran, Benjamin S. Hsiao, Benjamin Chu, "Structure and process relationship of electrospun bioabsorbable nanofiber membranes," *Polymer*, vol. 43, pp. 4403–4412, 2002.
[21] J.M Deitzel, J Kleinmeyer, D Harris, N.C Beck Tan , "The effect of processing variables on the morphology of electrospun nanofibers and textiles," *Polymer*,vol.42, pp.261-272, 2001.
[22] Silke Megelski, Jean S. Stephens, D. Bruce Chase and John F. Rabolt, "Micro- and Nanostructured Surface Morphology on Electrospun Polymer Fibers," *Macromolecules*, vol.35, pp.8456-8466, 2002.
[23] Christopher J. Buchko, Loui C. Chen, Yu Shen, David C. Martin, "Processing and microstructural characterization of porous biocompatible protein polymer thin films," *Polymer*, vol.40, pp. 7397-7407, 1999.
[24] Yvette S. Castillo, "Design of experimentation to systematically determine the interaction between electrospinning variables and to optimize the fiber diameter of electrospun poly (d,l-lactide-co-glycolide) scaffolds for tissue engineered constructs," Master of Science Thesis, California Polytechnic State University, San Luis Obispo, 2012.
[25] Haiqing Liu and You-Lo Hsieh, "Ultrafine fibrous cellulose membranes from electrospinning of cellulose acetate," *Journal of Polymer Science Part B: Polymer Physics*, vol.40, pp.2119-2129, 2002.
[26] Ladawan Wannatong, Anuvat Sirivat and Pitt Supaphol, "Effects of solvents on electrospun polymeric fibers: preliminary study on polystyrene," *Polymer International*, vol.53, pp.1851-1859, 2004.
[27] Md. Fazley Elahi, Wang Lu, Guan Guoping and Farzana Khan, "Core-shell Fibers for Biomedical Applications-A Review," *Journal of Bioengineering & Biomedical Science*, vol. 3, pp.1-14, 2013.
[28] Mahboubeh Maleki, Masoud Latifi, Mohammad Amani-Tehran and Sanjay Mathur, "Electrospun core–shell nanofibers for drug encapsulation and sustained release," *Polymer Engineering & Science*, vol.53, pp.1770-1779, 2013.
[29] Jesse T. McCann, Dan Li and Younan Xia, "Electrospinning of nanofibers with core-sheath, hollow, or porous structures," *Journal of Materials Chemistry*, vol.15, pp.735-738, 2005.
[30] Michael Bognitzki, Wolfgang Czado, Thomas Frese, Andreas Schaper, Michael Hellwig, Martin Steinhart, Andreas Greiner, and Joachim H. Wendorf, "Nanostructured Fibers via Electrospinning," *Advanced Materials*, vol.13, pp.70-72, 2001

[31] M. Bognitzki, H. Hou, M. Ishaque, T. Frese, M. Hellwig, C. Schwarte, A. Schaper, J. H. Wendorff and A. Greiner, "Polymer, Metal, and Hybrid Nano- and Mesotubes by Coating Degradable Polymer Template Fibers (TUFT Process)," *Advanced Materials*, vol.12, pp.637-640, 2000.

[32] Yanzhong Zhang, Zheng-Ming Huang, Xiaojing Xu, Chwee Teck Lim and Seeram Ramakrishna, "Preparation of Core−Shell Structured PCL-r-Gelatin Bi-Component Nanofibers by Coaxial Electrospinning," *Chem. Mater.*, vol.16, pp.3406-3409, 2004.

[33] Z. Sun, E. Zussman, A.L. Yarin, J.H. Wendorff andA. Greiner, "Compound Core–Shell Polymer Nanofibers by Co-Electrospinning," *Advanced Materials*, vol.15, pp.1929-1932, 2003.

[34] Search conducted in database "SCOPUS" on date 06-01-2014 using the keyword "electrospinning".

[35] Jean S. Stephens, D. Bruce Chase, and John F. Rabolt, "Effect of the Electrospinning Process on Polymer Crystallization Chain Conformation in Nylon-6 and Nylon-12," *Macromolecules*, vol.37, pp.877-881, 2004.

[36] Gopal Panthi, Nasser A.M. Barakat, Prabodh Risal, Ayman Yousef, Bishweshwar Pant, Afeesh R. Unnithan and Hak Yong Kim, "Preparation and Characterization of Nylon-6/Gelatin Composite Nanofibers Via Electrospinning for Biomedical Applications," *Fibers and Polymers*, vol.14, pp.718-723, 2013.

[37] Laleh MALEKNIA, Ramin KAYALI, Majid MONTAZER, "Preparation Conductive Nylon 6 Nanofiber for Medical Application," Nanocon 2013: 5th International Conference.

[38] James E. Mark, "Polymer Data Handbook," *Oxford University Press*, pp.180, 1999

[39] Jie Li, Long Tian, Ning Pan and Zhi-juan Pan, "Mechanical and electrical properties of the PA6/SWNTs nanofiber yarn by electrospinning," *Polymer Engineering & Science*, Online Version of Record published before inclusion in an issue.

[40] Byoung-Sun Lee, Woong-Ryeol Yu, "PA6/MWNT Nanocomposites Fabricated Using Electrospun Nanofibers Containing MWNT," *Macromolecular Research*, vol. 18, pp. 162-169, 2010.

[41] Hyun Suk Kim, Hyoung-Joon Jin, Seung Jun Myung, Minsung Kang and In-Joo Chin, "Carbon Nanotube-Adsorbed Electrospun Nanofibrous Membranes of Nylon 6," *Macromolecular Rapid Communications*, vol. 27, pp. 146-151, 2006.

[42] Giriprasath Gururajan, S. P. Sullivan, T. P. Beebe, D. B. Chase and J. F. Rabolt, "Continuous electrospinning of polymer nanofibers of Nylon-6 using an atomic force microscope tip," *Nanoscale*, vol.3, pp.3300-3308, 2011.

[43] R. Nirmala, Jin Won Jeong, Hyun Ju Oh, R. Navamathavan, Mohamed El-Newehy, Salem S Al-Deyab, and Hak Yong Kim, "Electrical Properties of Ultrafine Nylon-6 Nanofibers Prepared Via Electrospinning," *Fibers and Polymers*, vol.12, pp.1021-1024, 2011.

[44] Gui-Bo Yin, "Analysis of Electrospun Nylon 6 Nanofibrous Membrane as Filters," *Journal of Fiber Bioengineering and Informatics*, vol. 3, pp.137-141, 2010.

[45] Mohamed H. El-Newehy, Salem S. Al-Deyab, El-Refaie Kenawy and Ahmed Abdel-Megeed, "Nanospider Technology for the Production of Nylon-6 Nanofibers for Biomedical Applications," *Journal of Nanomaterials*, pp.1-8, 2011.

[46] Mohammad Chowdhury and George Stylios, “Effect of Experimental Parameters on the Morphology of Electrospun Nylon 6 fibres,” *International Journal of Basic & Applied Sciences*, vol. 10, pp. 70-78, 2010.
[47] Amirreza Sohrabi, Parmiss Mojir Shaibani and Thomas Thundat, “The Effect of Applied Electric Field on the Diameter and Size Distribution of Electrospun Nylon6 Nanofibers,” *Scanning*, vol.35, pp.183-188, 2013.
[48] Mohamed B. Bazbouz and George K. Stylios, “Alignment and optimization of nylon 6 nanofibers by electrospinning,” *Journal of Applied Polymer Science*, vol.107, pp.3023-3032, 2008.
[49] Shamim Zargham, Saeed Bazgir, Amir Tavakoli, Abo Saied Rashidi, Rogheih Damerchely, “The Effect of Flow Rate on Morphology and Deposition Area of Electrospun Nylon 6 Nanofiber,” vol.7, pp.42-49, 2012.
[50] Pirjo Heikkilä, Ali Harlin, “Parameter study of electrospinning of polyamide-6,” *European Polymer Journal*, vol. 44, pp.3067-3079, 2008.
[51] DOUGLAS C. MONTGOMERY, “Design and Analysis of Experiments (Seventh Edition),” *John Wiley & Sons,Inc.*, 2008.
[52] Stuart R. Coles, Daniel K. Jacobs, James O. Meredith, Guy Barker, Andrew J. Clark, Kerry Kirwan, Jon Stanger and Nick Tucker, “A design of experiments (DoE) approach to material properties optimization of electrospun nanofibers,” *Journal of Applied Polymer Science*, vol. 117, pp. 2251-2257, 2010
[53] S. Anandhan, K. Ponprapakaran, T. Senthil, Gibin George, “Parametric study of manufacturing ultrafine polybenzimidazole fibers by electrospinning,” *International Journal of Plastics Technology*, vol.16, pp.101-116, 2012.
[54] K. Desai, C.Sung, “DOE Optimization and Phase Morphology of Electrospun Nanofibers of PANI/PMMA Blends ,” *Nanotech*, vol.3, pp.429-432, 2004.
[55] Wenguo Cui, Xiaohong Li, Shaobing Zhou and Jie Weng, “Investigation on process parameters of electrospinning system through orthogonal experimental design,” *Journal of Applied Polymer Science*, vol.103, pp.3105-3112, 2007.

Appendix A

Fiber diameter distribution analysis for the screening test of the DOE study

Concentration(wt%)	Voltage(kV)	Flow rate （μl/min）	The size distribution of Nylon 6 nanofibers
15	**12**	**2**	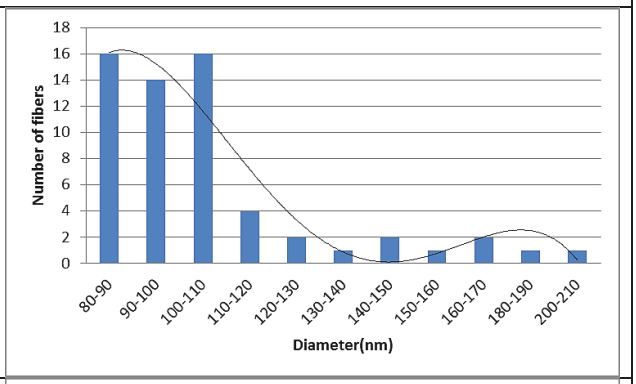
15	**24**	**2**	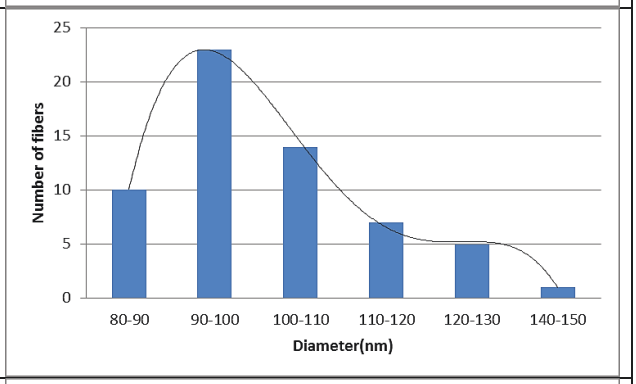
15	**12**	**5**	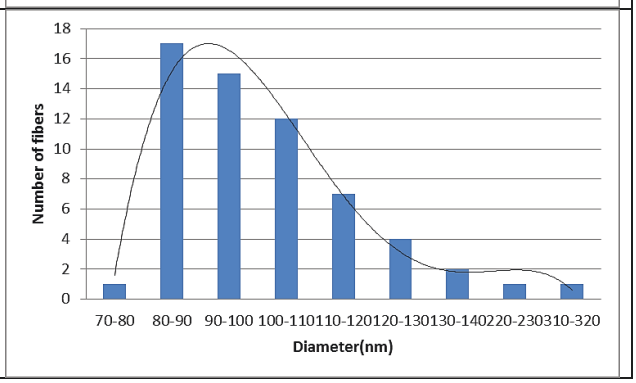

15	**24**	**5**	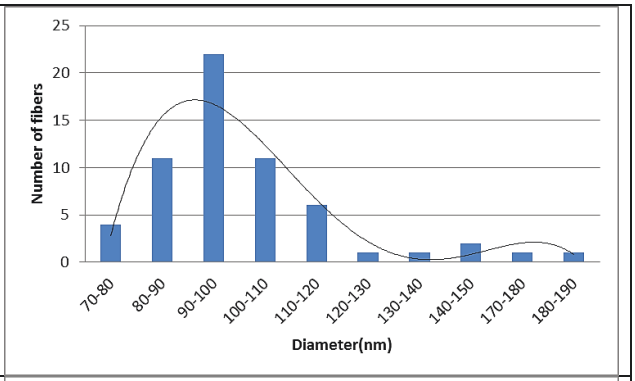
20	**12**	**2**	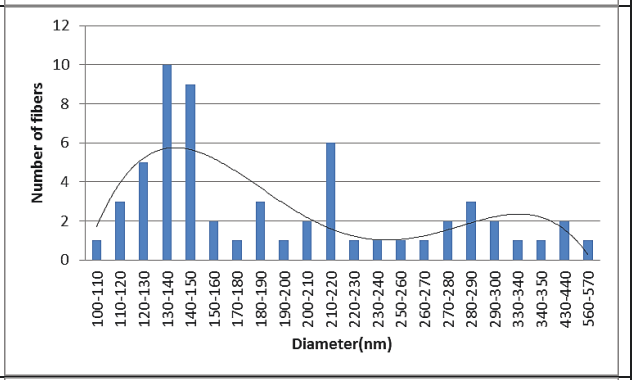
20	**24**	**2**	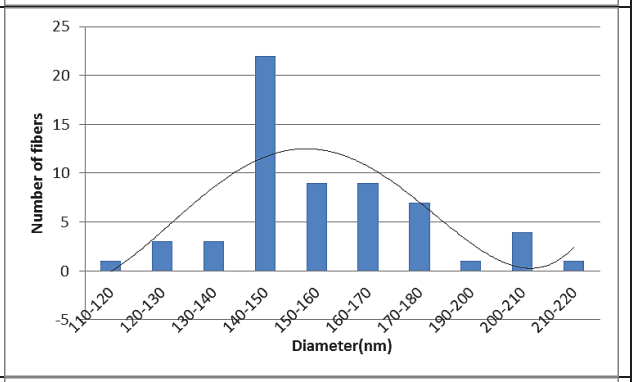
20	**12**	**5**	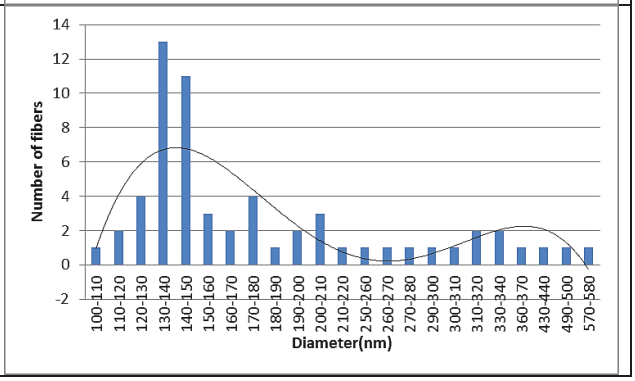

20	**24**	**5**	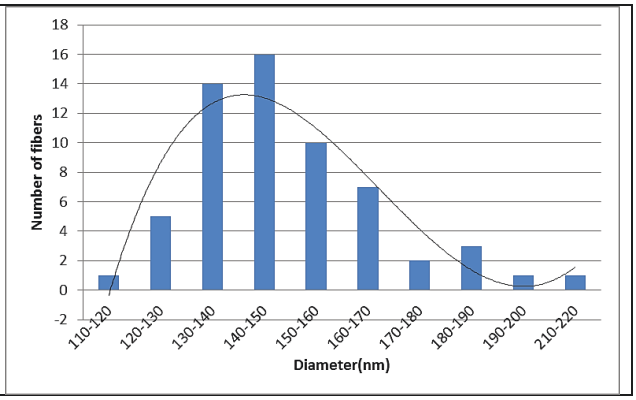

Appendix B

Fiber diameter distribution analysis for the second step of the DOE study (original group)

Concentration(wt%)	Voltage(kV)	Flow rate （μl/min）	The size distribution of Nylon 6 nanofibers
15	**16**	**2**	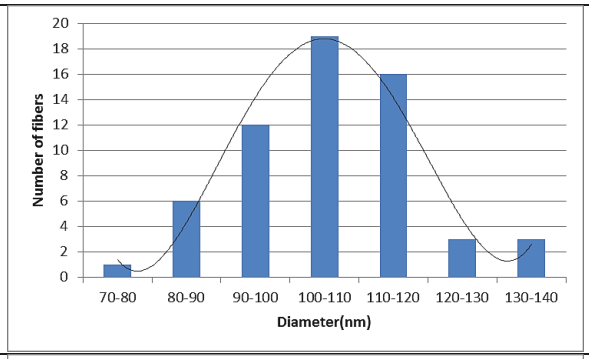
15	**20**	**2**	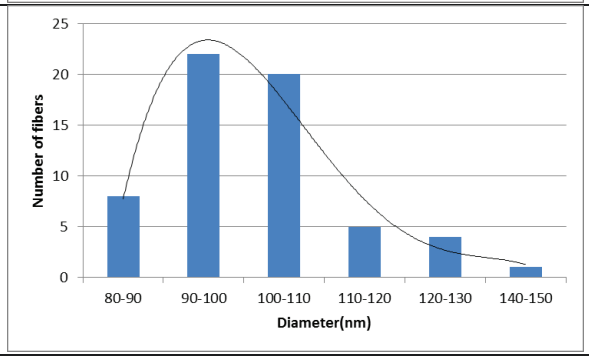

15	**24**	**2**	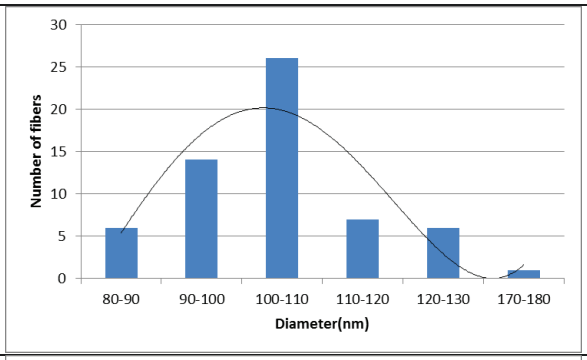
17.5	**16**	**2**	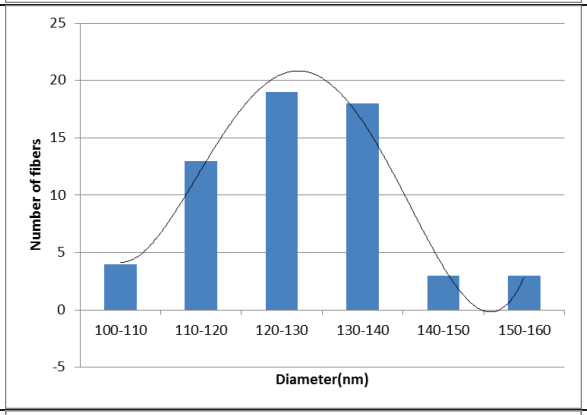
17.5	**20**	**2**	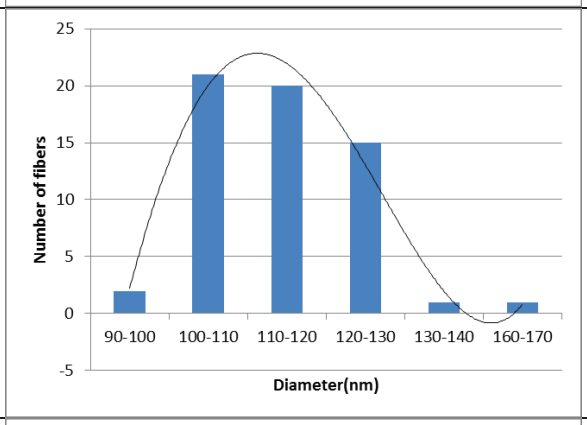
17.5	**24**	**2**	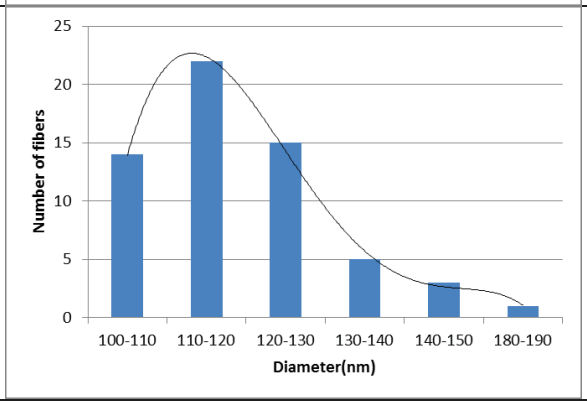

20	**16**	**2**	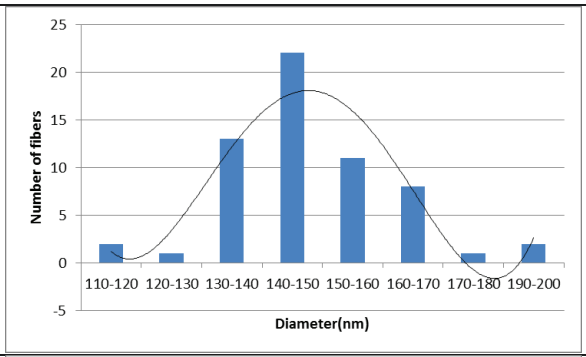
20	**20**	**2**	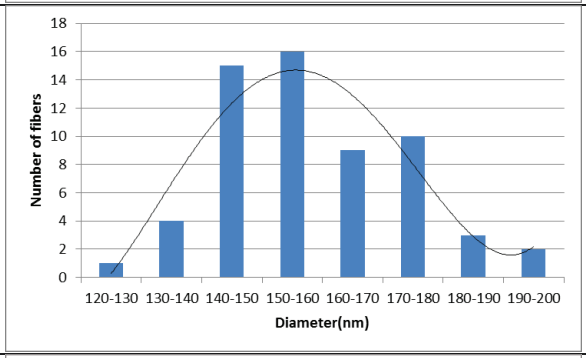
20	**24**	**2**	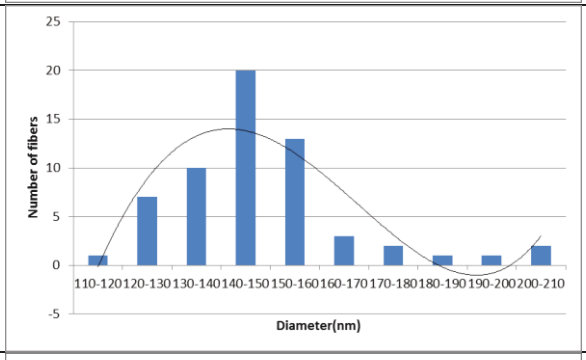
15	**16**	**5**	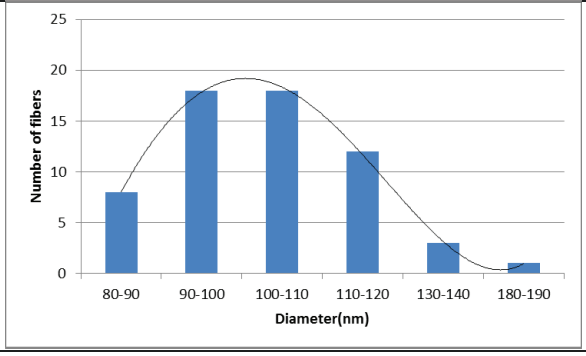

15	**20**	**5**	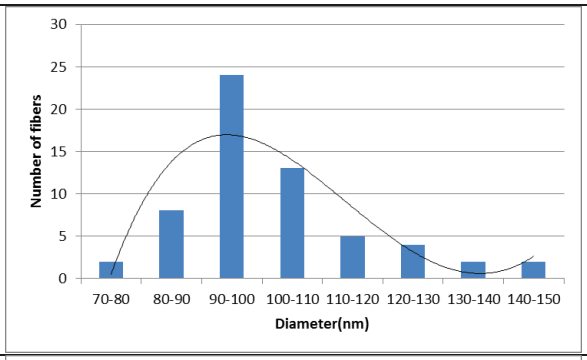
15	**24**	**5**	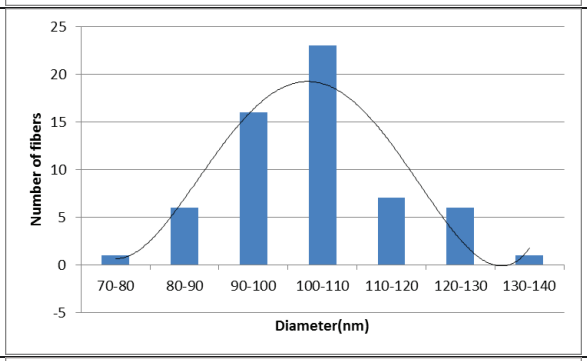
17.5	**16**	**5**	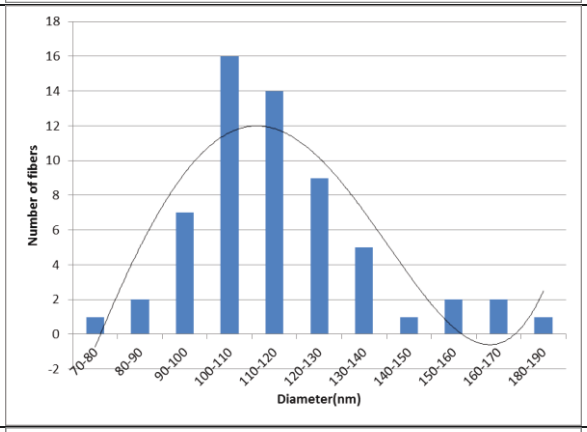
17.5	**20**	**5**	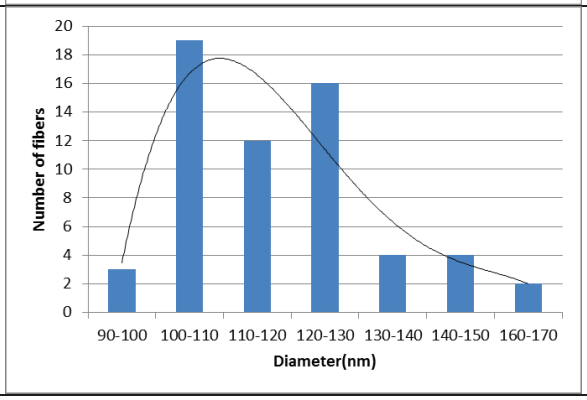

17.5	**24**	**5**	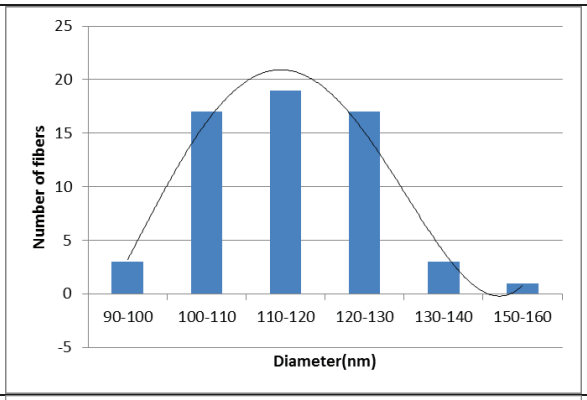
20	**16**	**5**	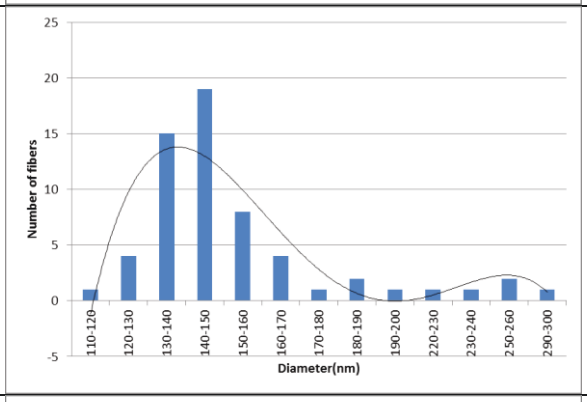
20	**20**	**5**	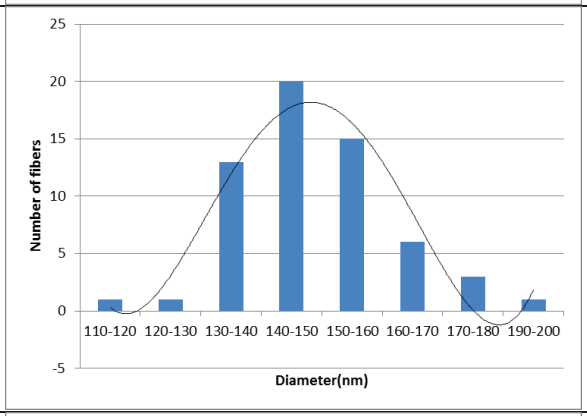
20	**24**	**5**	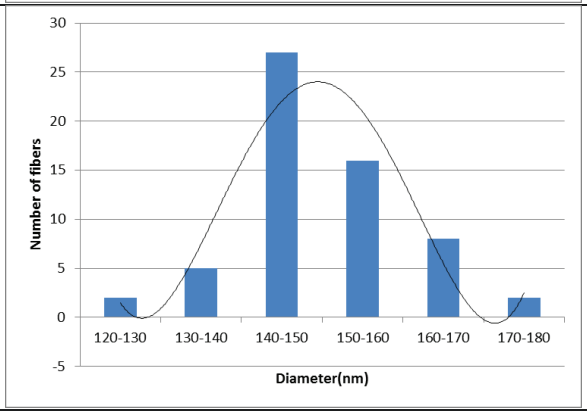

Appendix C

Effect estimate tables for the screening test and the second step of the DOE study

(1)Effect estimate table of fiber diameter for the screening test

Factor	Effect Estimates; Var.:Fiber Diameter; R-sqr=.99996; Adj:.99972 (Spreadsheet1) 2**(3-0) design; MS Residual=.494598 DV: Fiber Diameter									
	Effect	Std.Err.	t(1)	p	-95.% Cnf.Limt	+95.% Cnf.Limt	Coeff.	Std.Err. Coeff.	-95.% Cnf.Limt	+95.% Cnf.Limt
Mean/Interc.	139.3861	0.248646	560.5810	0.001136	136.2268	142.5455	139.3861	0.248646	136.2268	142.5455
(1)Solution Concentration	71.1494	0.497292	143.0739	0.004450	64.8308	77.4681	35.5747	0.248646	32.4154	38.7341
(2)Electrospinning Voltage	-24.4529	0.497292	-49.1722	0.012945	-30.7716	-18.1342	-12.2265	0.248646	-15.3858	-9.0671
(3)Flow rate	-3.2702	0.497292	-6.5760	0.096073	-9.5889	3.0485	-1.6351	0.248646	-4.7944	1.5242
1 by 2	-19.8717	0.497292	-39.9598	0.015928	-26.1903	-13.5530	-9.9358	0.248646	-13.0952	-6.7765
1 by 3	-2.9288	0.497292	-5.8895	0.107073	-9.2475	3.3899	-1.4644	0.248646	-4.6237	1.6949
2 by 3	0.2896	0.497292	0.5824	0.664243	-6.0290	6.6083	0.1448	0.248646	-3.0145	3.3042

(2) Effect estimate table of the standard deviation of fiber diameter for the screening test

Factor	Effect Estimates; Var.:Standard Deviation; R-sqr=.99927; Adj:.99489 (Spreadsheet1) 2**(3-0) design; MS Residual=5.689511 DV: Standard Deviation									
	Effect	Std.Err.	t(1)	p	-95.% Cnf.Limt	+95.% Cnf.Limt	Coeff.	Std.Err. Coeff.	-95.% Cnf.Limt	+95.% Cnf.Limt
Mean/Interc.	39.7568	0.843320	47.1432	0.013502	29.0414	50.4722	39.7568	0.843320	29.0414	50.4722
(1)Solution Concentration	33.2844	1.686640	19.7342	0.032232	11.8536	54.7152	16.6422	0.843320	5.9268	27.3576
(2)Electrospinning Voltage	-43.3819	1.686640	-25.7209	0.024739	-64.8127	-21.9511	-21.6910	0.843320	-32.4064	-10.9756
(3)Flow rate	5.2541	1.686640	3.1151	0.197747	-16.1767	26.6849	2.6271	0.843320	-8.0883	13.3425
1 by 2	-29.3368	1.686640	-17.3936	0.036560	-50.7676	-7.9060	-14.6684	0.843320	-25.3838	-3.9530
1 by 3	-3.4726	1.686640	-2.0589	0.287846	-24.9034	17.9582	-1.7363	0.843320	-12.4517	8.9791
2 by 3	-2.1302	1.686640	-1.2630	0.426350	-23.5610	19.3006	-1.0651	0.843320	-11.7805	9.6503

(3)Effect estimate table of fiber diameter for the second step of the DOE study

Factor	Effect Estimates; Var.:Fiber diameter; R-sqr=.97979; Adj:.97381 (Spreadsheet47) 1 2-level factors, 2 3-level factors, 36 Runs DV: Fiber diameter; MS Residual=10.42544									
	Effect	Std.Err.	t(27)	p	-95.% Cnf.Limt	+95.% Cnf.Limt	Coeff.	Std.Err. Coeff.	-95.% Cnf.Limt	+95.% Cnf.Limt
Mean/Interc.	124.0328	0.538141	230.4838	0.000000	122.9286	125.1369	124.0328	0.538141	122.9286	125.1369
(1)Solution Concentration(L)	46.4133	1.318171	35.2104	0.000000	43.7086	49.1179	23.2066	0.659085	21.8543	24.5590
Solution Concentration(Q)	-8.4771	1.141569	-7.4259	0.000000	-10.8194	-6.1348	-4.2386	0.570785	-5.4097	-3.0674
(2)Electrospinning Voltage(L)	-3.4233	1.318171	-2.5970	0.015038	-6.1279	-0.7186	-1.7116	0.659085	-3.0640	-0.3593
Electrospinning Voltage(Q)	-1.7044	1.141569	-1.4930	0.147021	-4.0467	0.6379	-0.8522	0.570785	-2.0234	0.3189
(3)Flow rate(L)	-2.3268	1.076282	-2.1618	0.039658	-4.5351	-0.1184	-1.1634	0.538141	-2.2676	-0.0592
1L by 2L	-1.1718	1.614423	-0.7259	0.474170	-4.4844	2.1407	-0.5859	0.807211	-2.2422	1.0703
1L by 3L	0.2170	1.318171	0.1646	0.870450	-2.4876	2.9217	0.1085	0.659085	-1.2438	1.4608
2L by 3L	0.2865	1.318171	0.2174	0.829564	-2.4181	2.9912	0.1433	0.659085	-1.2091	1.4956

(4)Effect estimate table of standard deviation of fiber diameter for the second step of the DOE study

Factor	Effect Estimates; Var.:Standard deviation of fiber diameter; R-sqr=.75966; Adj:.68845 (Spreadsheet47) 1 2-level factors, 2 3-level factors, 36 Runs DV: Standard deviation of fiber diameter; MS Residual=8.392252									
	Effect	Std.Err.	t(27)	p	-95.% Cnf.Limt	+95.% Cnf.Limt	Coeff.	Std.Err. Coeff.	-95.% Cnf.Limt	+95.% Cnf.Limt
Mean/Interc.	14.38209	0.482823	29.78750	0.000000	13.39142	15.37276	14.38209	0.482823	13.39142	15.37276
(1)Solution Concentration(L)	5.01366	1.182670	4.23927	0.000234	2.58702	7.44029	2.50683	0.591335	1.29351	3.72015
Solution Concentration(Q)	-1.38052	1.024222	-1.34787	0.188901	-3.48205	0.72101	-0.69026	0.512111	-1.74102	0.36051
(2)Electrospinning Voltage(L)	-4.78070	1.182670	-4.04229	0.000396	-7.20733	-2.35406	-2.39035	0.591335	-3.60367	-1.17703
Electrospinning Voltage(Q)	-1.66117	1.024222	-1.62189	0.116449	-3.76270	0.44036	-0.83059	0.512111	-1.88135	0.22018
(3)Flow rate(L)	2.32568	0.965646	2.40842	0.023119	0.34434	4.30702	1.16284	0.482823	0.17217	2.15351
1L by 2L	-4.58044	1.448469	-3.16226	0.003846	-7.55245	-1.60843	-2.29022	0.724235	-3.77623	-0.80421
1L by 3L	1.45479	1.182670	1.23009	0.229275	-0.97185	3.88143	0.72739	0.591335	-0.48593	1.94071
2L by 3L	-6.39842	1.182670	-5.41015	0.000010	-8.82506	-3.97178	-3.19921	0.591335	-4.41253	-1.98589

Appendix D

Strain/stress curves for electrospun Nylon 6 nanofibers with 15wt%, 17.5wt% and 20wt% concentrations

(1)Strain/stress curves for electrospun Nylon 6 nanofibers with 15wt% concentration

Note that red lines shown in the stress/strain curves are the linear parts used to calculate the elastic modulus.

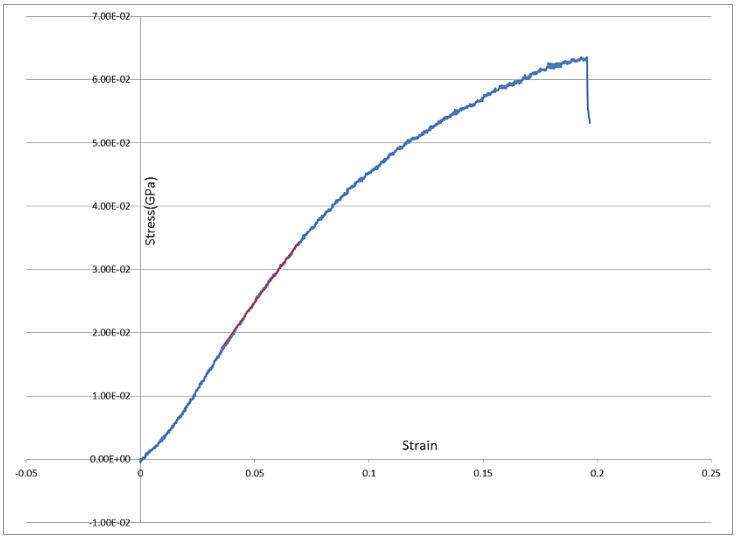

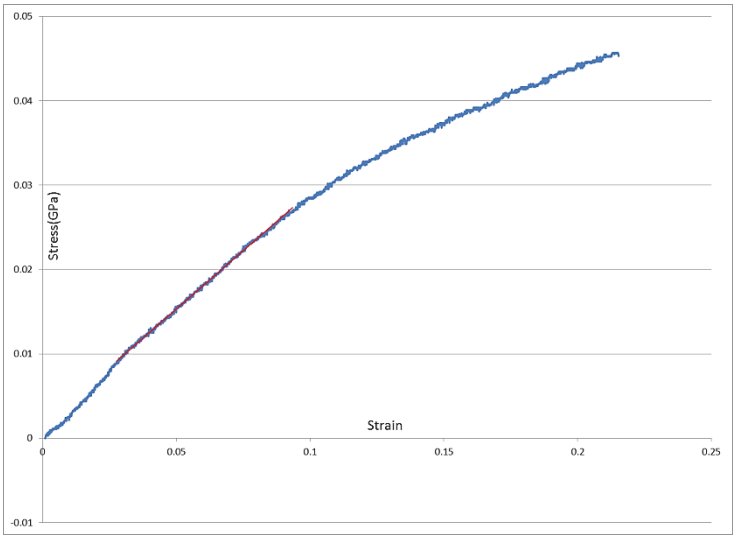
0.05
0.04
0.03
0.02
0.01
0
-0.01
Stress(GPa)
Strain
0
0.05
0.1
0.15
0.2
0.25

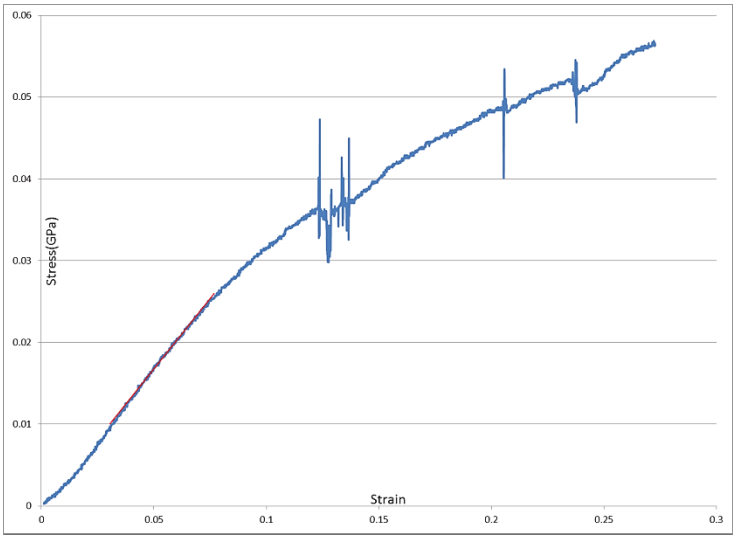
0.06
0.05
0.04
0.03
0.02
0.01
0
Stress(GPa)
Strain
0
0.05
0.1
0.15
0.2
0.25
0.3

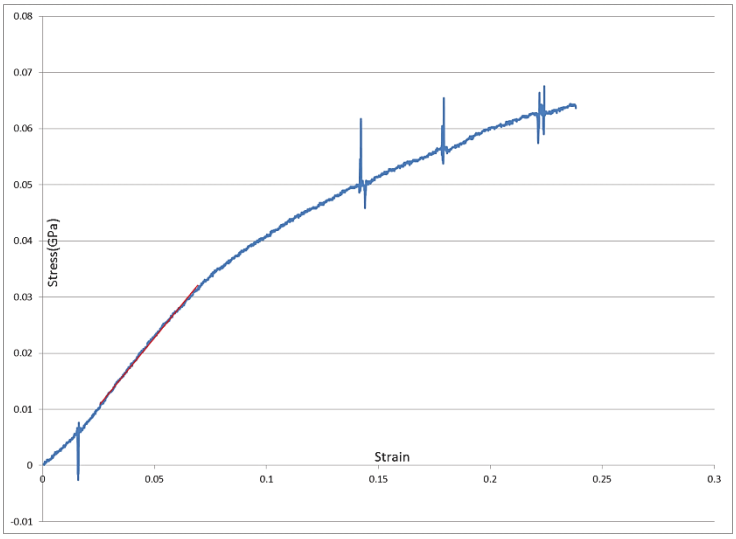
0.08
0.07
0.06
0.05
0.04
0.03
0.02
0.01
0
-0.01
Stress(GPa)
Strain
0
0.05
0.1
0.15
0.2
0.25
0.3

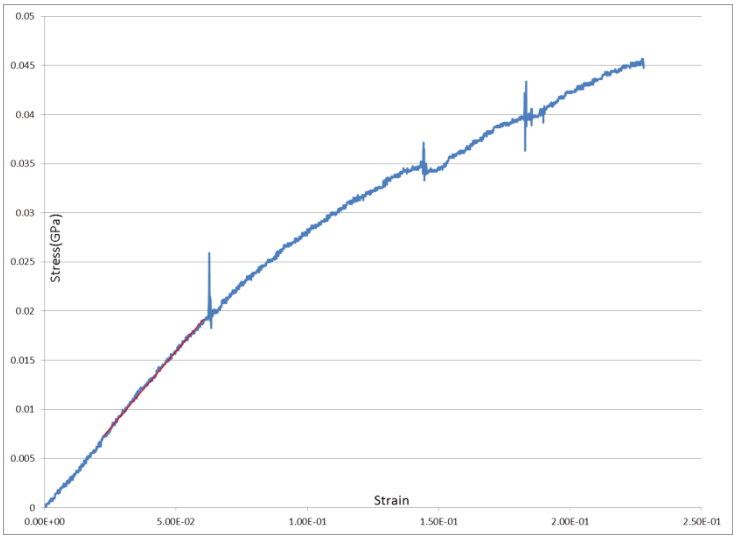
0.05
0.045
0.04
0.035
0.03
0.025
0.02
0.015
0.01
0.005
0
Stress(GPa)
Strain
0.00E+00
5.00E-02
1.00E-01
1.50E-01
2.00E-01
2.50E-01

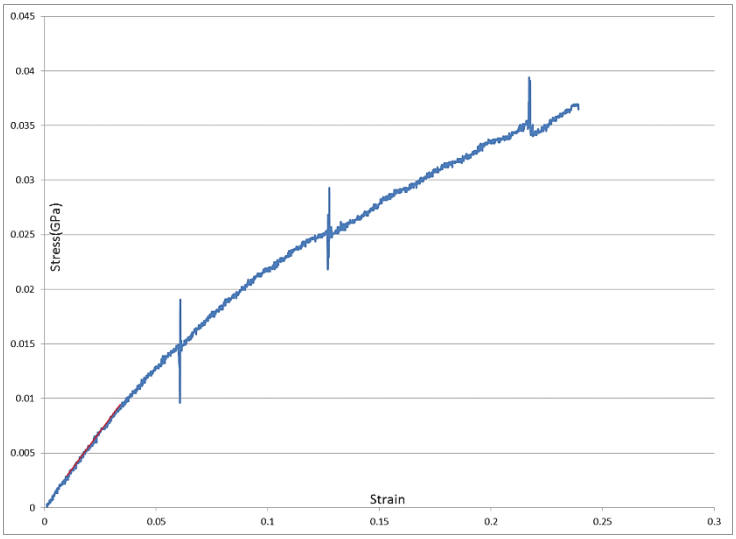
0.045
0.04
0.035
0.03
0.025
0.02
0.015
0.01
0.005
0
Stress(GPa)
Strain
0
0.05
0.1
0.15
0.2
0.25
0.3

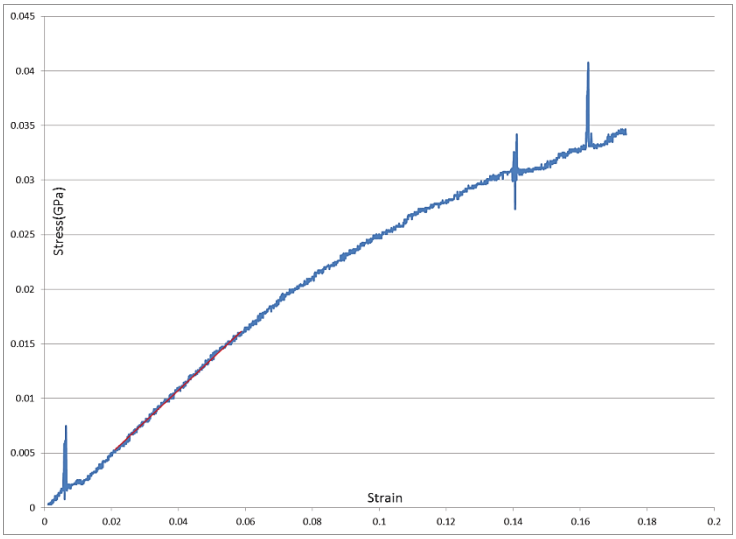
0.045
0.04
0.035
0.03
0.025
0.02
0.015
0.01
0.005
0
Stress(GPa)
Strain
0
0.02
0.04
0.06
0.08
0.1
0.12
0.14
0.16
0.18
0.2

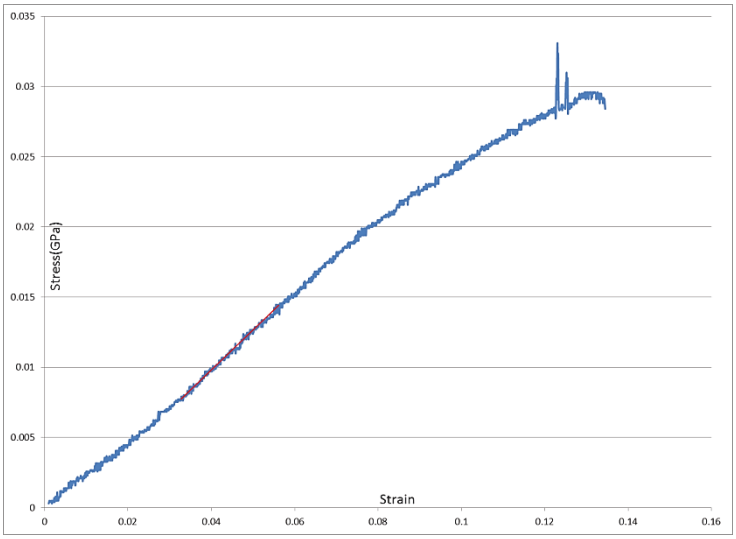
0.035
0.03
0.025
0.02
0.015
0.01
0.005
0
Stress(GPa)
Strain
0
0.02
0.04
0.06
0.08
0.1
0.12
0.14
0.16

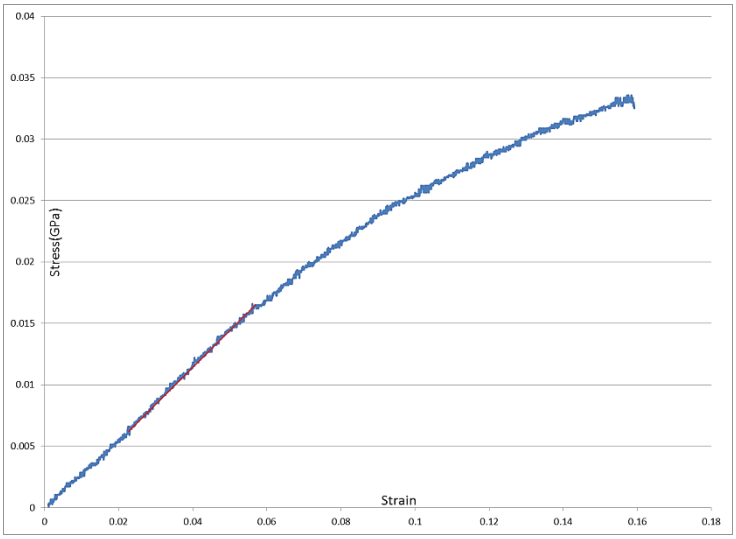
0.04
0.035
0.03
0.025
0.02
0.015
0.01
0.005
0
Stress(GPa)
Strain
0
0.02
0.04
0.06
0.08
0.1
0.12
0.14
0.16
0.18

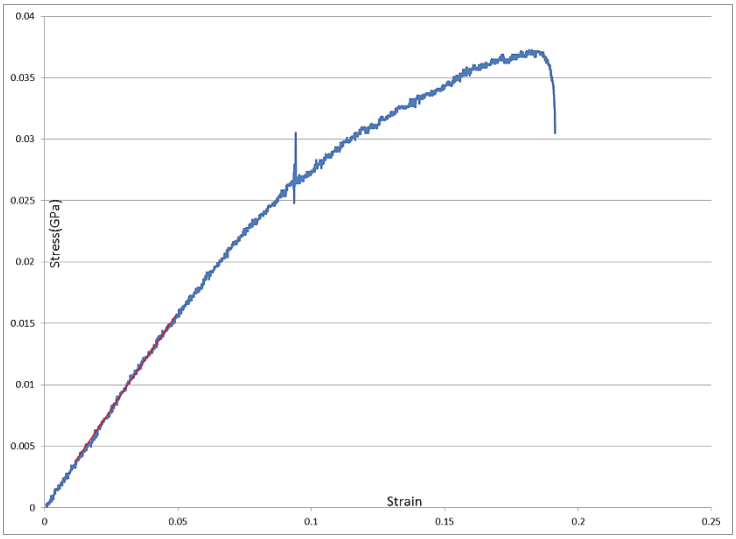
0.04
0.035
0.03
0.025
0.02
0.015
0.01
0.005
0
Stress(GPa)
Strain
0
0.05
0.1
0.15
0.2
0.25

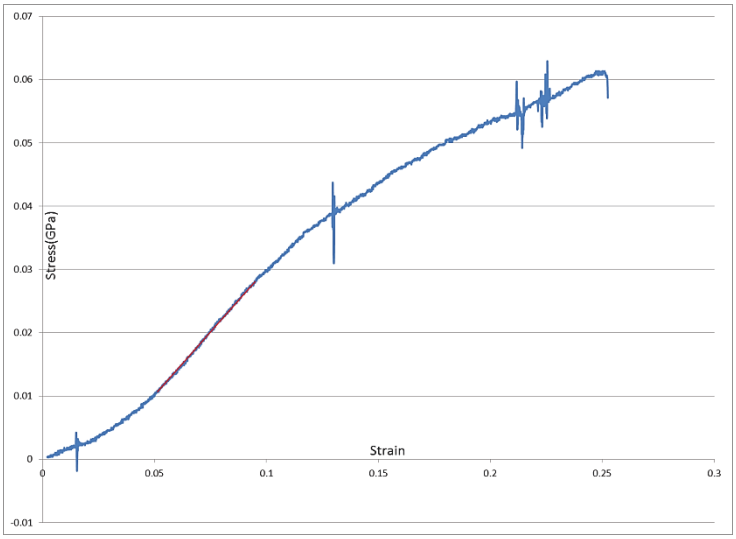
0.07
0.06
0.05
0.04
0.03
0.02
0.01
0
-0.01
Stress(GPa)
Strain
0
0.05
0.1
0.15
0.2
0.25
0.3

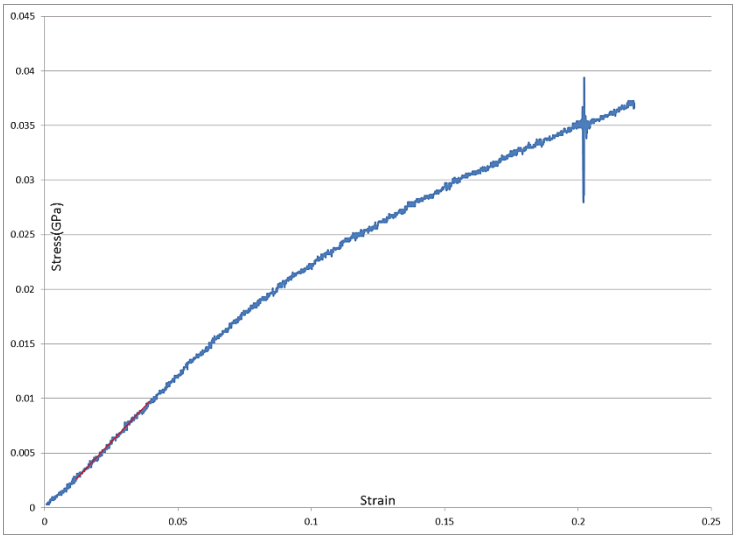
0.045
0.04
0.035
0.03
0.025
0.02
0.015
0.01
0.005
0
Stress(GPa)
Strain
0
0.05
0.1
0.15
0.2
0.25

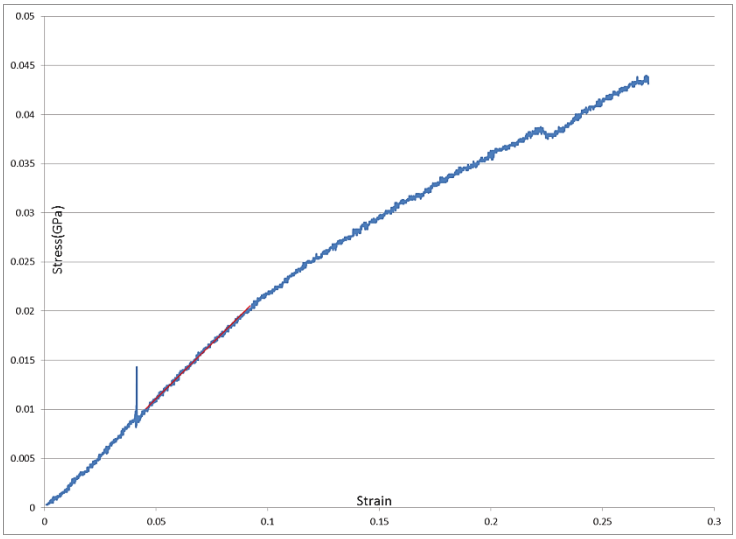
0.05
0.045
0.04
0.035
0.03
0.025
0.02
0.015
0.01
0.005
0
Stress(GPa)
Strain
0
0.05
0.1
0.15
0.2
0.25
0.3

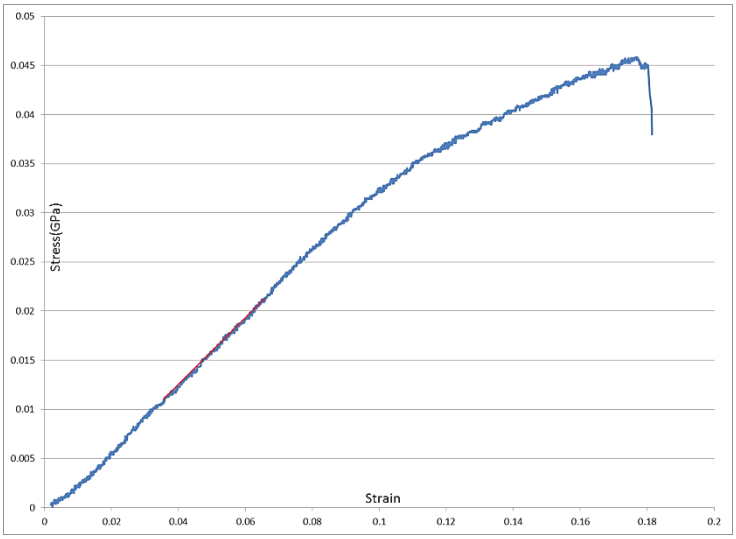

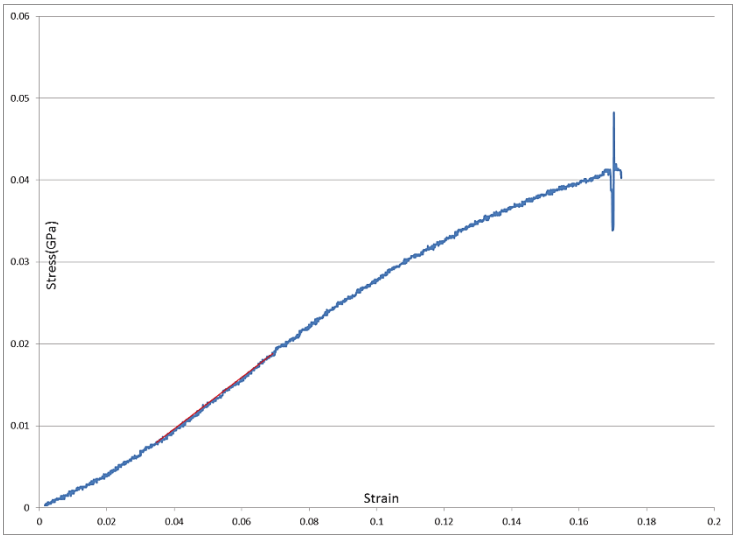

(2)Strain/stress curves for electrospun Nylon 6 nanofibers with 17.5wt% concentration

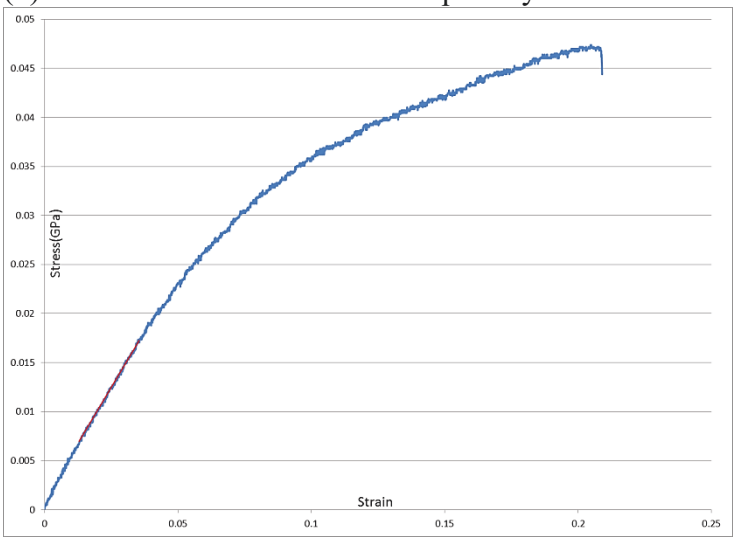

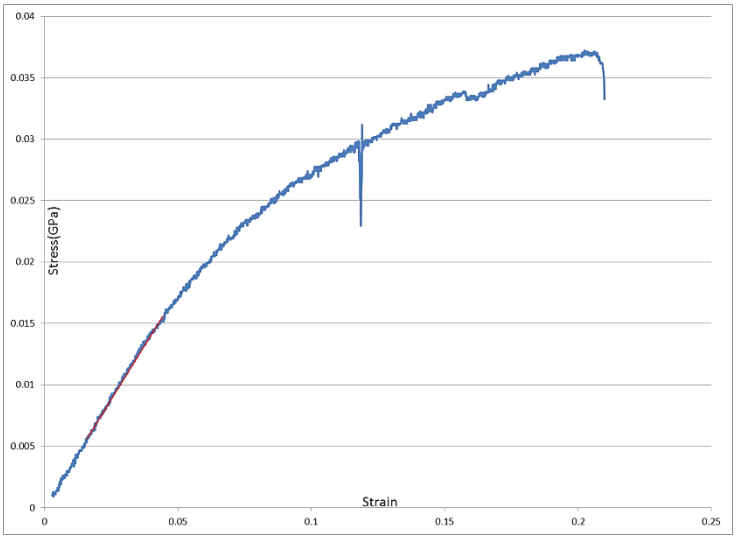
0.04
0.035
0.03
0.025
0.02
0.015
0.01
0.005
0
Stress(GPa)
Strain
0
0.05
0.1
0.15
0.2
0.25

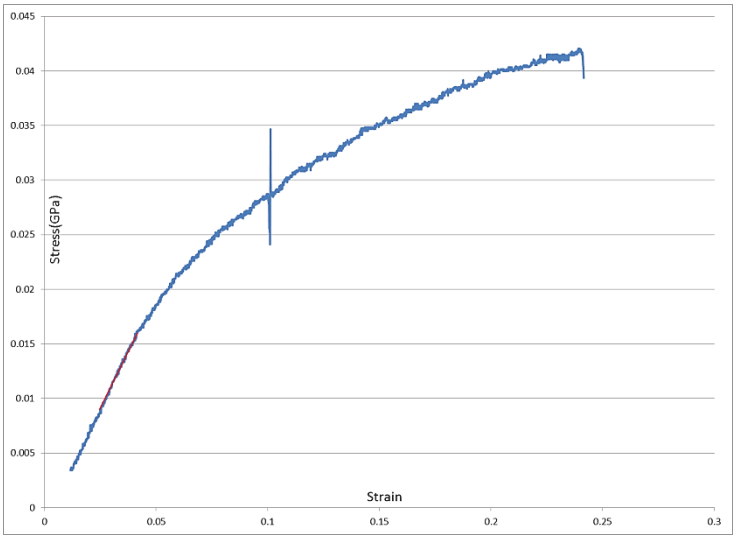
0.045
0.04
0.035
0.03
0.025
0.02
0.015
0.01
0.005
0
Stress(GPa)
Strain
0
0.05
0.1
0.15
0.2
0.25
0.3

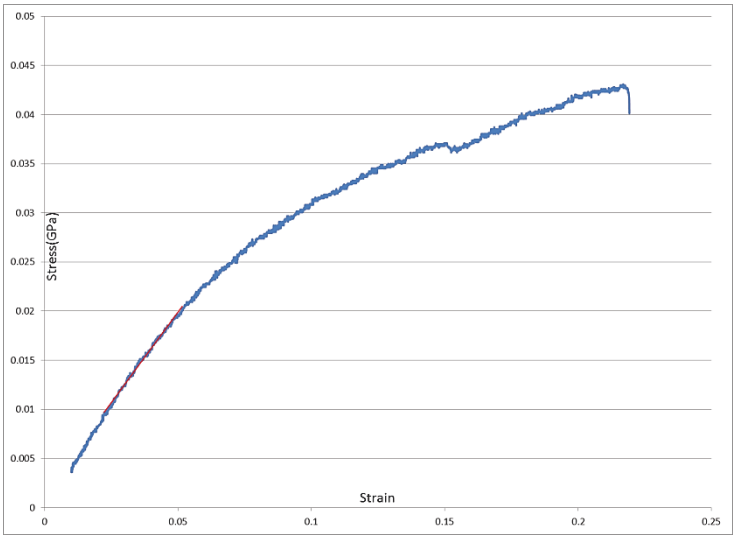
0.05
0.045
0.04
0.035
0.03
0.025
0.02
0.015
0.01
0.005
0
Stress(GPa)
Strain
0
0.05
0.1
0.15
0.2
0.25

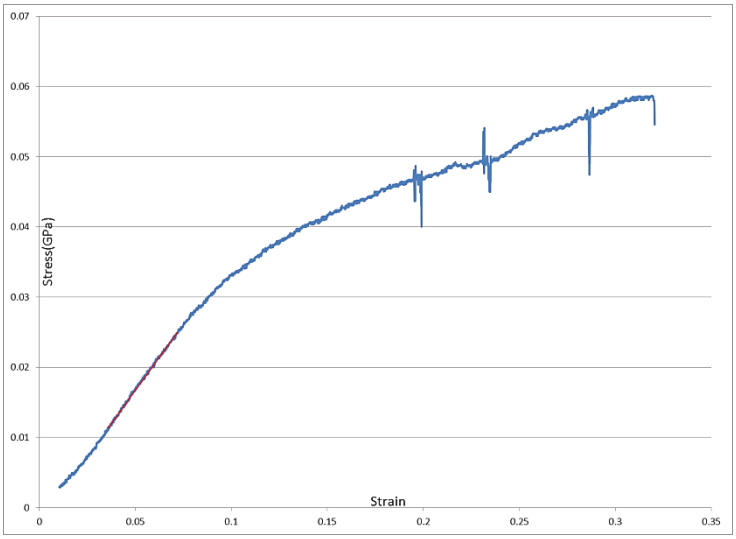
0.07
0.06
0.05
0.04
0.03
0.02
0.01
0
Stress(GPa)
0
0.05
0.1
0.15
0.2
0.25
0.3
0.35
Strain

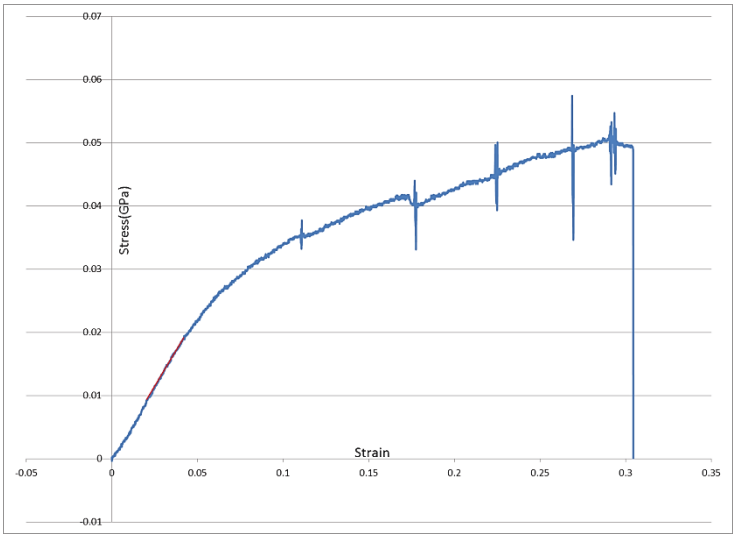
0.07
0.06
0.05
0.04
0.03
0.02
0.01
0
-0.01
Stress(GPa)
-0.05
0
0.05
0.1
0.15
0.2
0.25
0.3
0.35
Strain

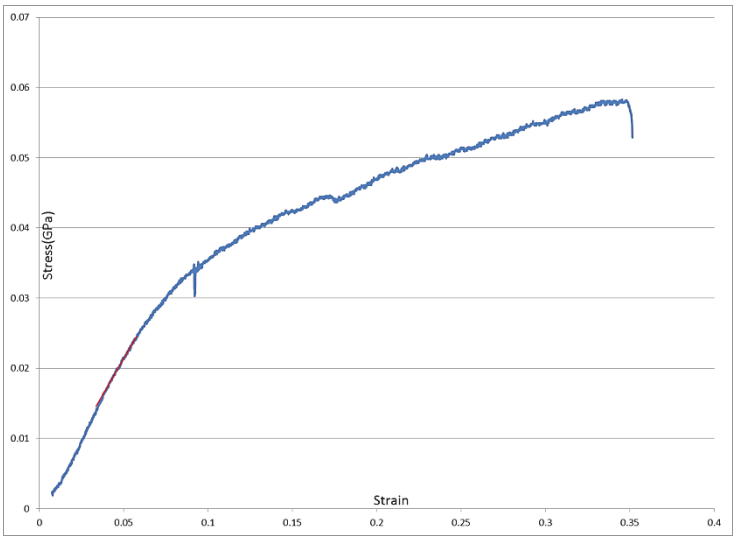
0.07
0.06
0.05
0.04
0.03
0.02
0.01
0
Stress(GPa)
0
0.05
0.1
0.15
0.2
0.25
0.3
0.35
0.4
Strain

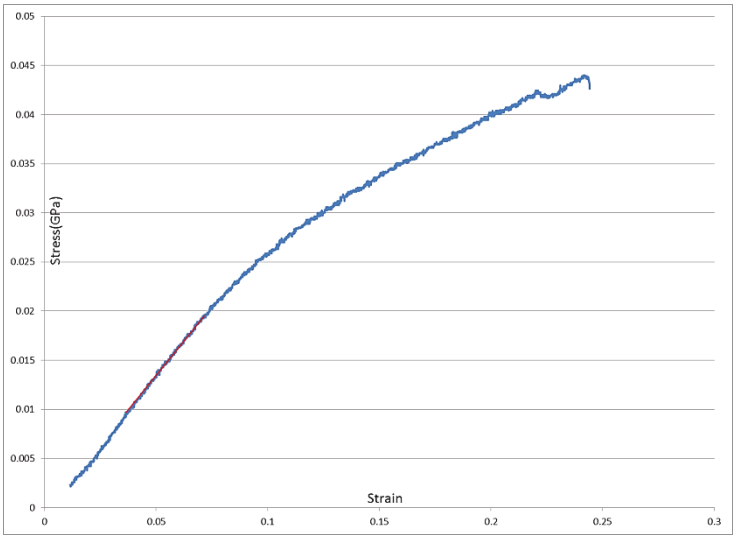
0.05
0.045
0.04
0.035
0.03
0.025
0.02
0.015
0.01
0.005
0
Stress(GPa)
Strain
0
0.05
0.1
0.15
0.2
0.25
0.3

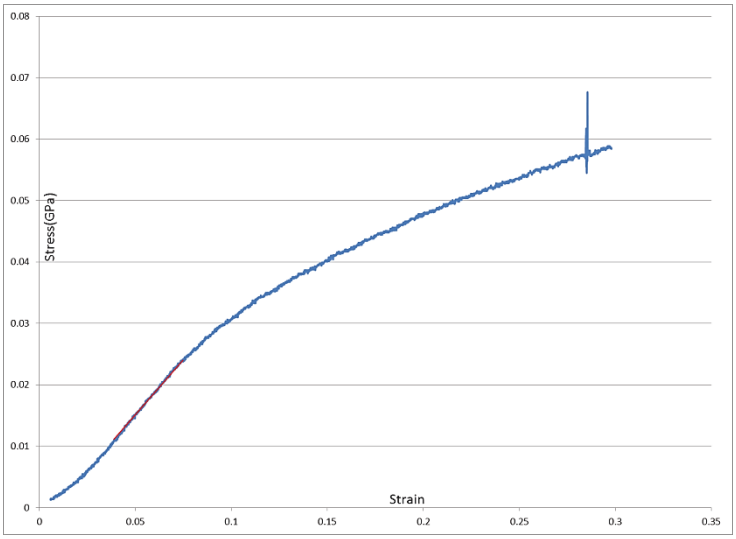
0.08
0.07
0.06
0.05
0.04
0.03
0.02
0.01
0
Stress(GPa)
Strain
0
0.05
0.1
0.15
0.2
0.25
0.3
0.35

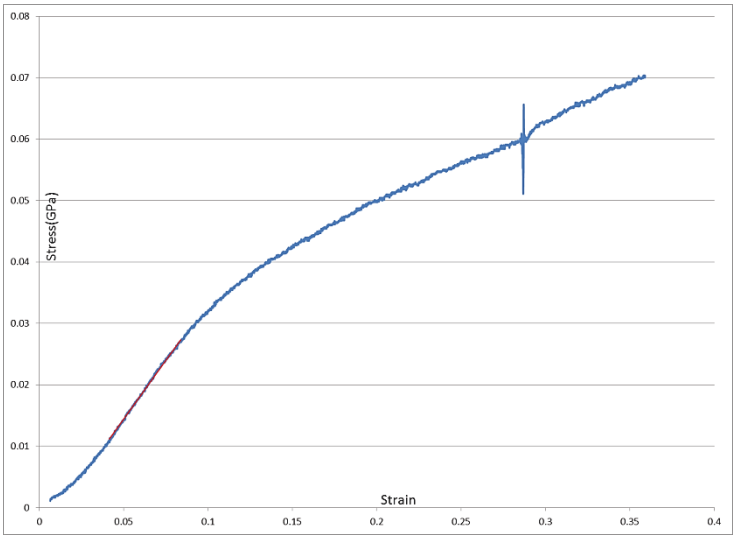
0.08
0.07
0.06
0.05
0.04
0.03
0.02
0.01
0
Stress(GPa)
Strain
0
0.05
0.1
0.15
0.2
0.25
0.3
0.35
0.4

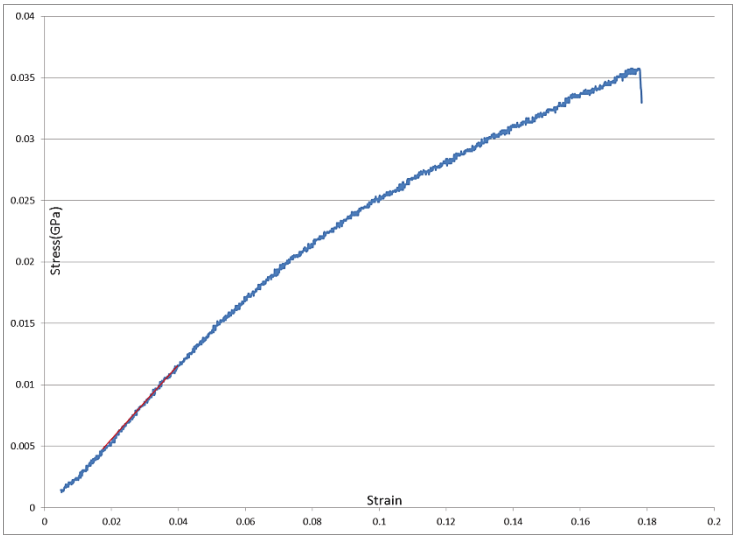
Stress(GPa)
Strain
0.04
0.035
0.03
0.025
0.02
0.015
0.01
0.005
0
0
0.02
0.04
0.06
0.08
0.1
0.12
0.14
0.16
0.18
0.2

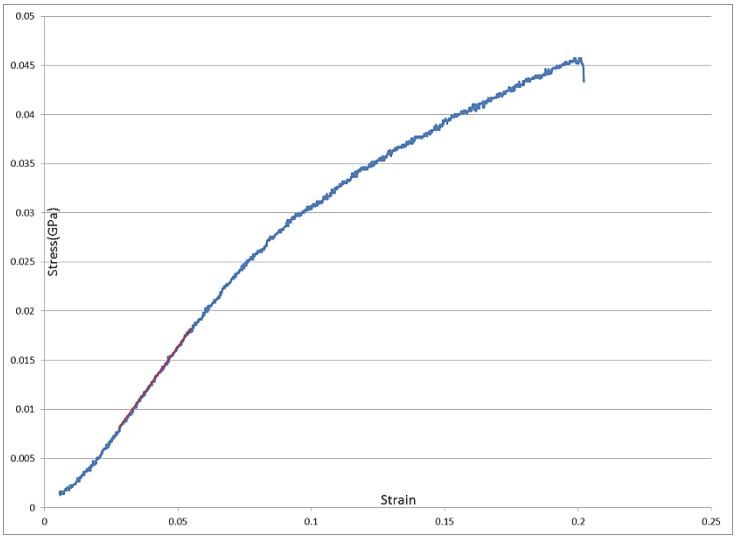
Stress(GPa)
Strain
0.05
0.045
0.04
0.035
0.03
0.025
0.02
0.015
0.01
0.005
0
0
0.05
0.1
0.15
0.2
0.25

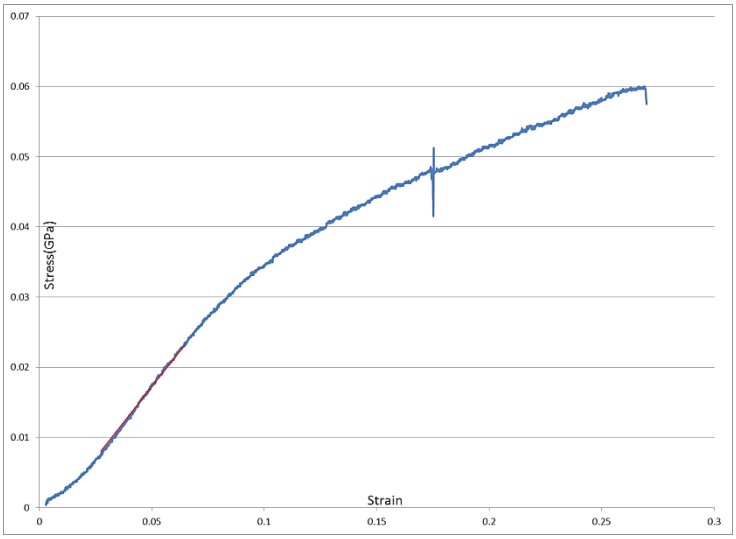
Stress(GPa)
Strain
0.07
0.06
0.05
0.04
0.03
0.02
0.01
0
0
0.05
0.1
0.15
0.2
0.25
0.3

(3)Strain/stress curves for electrospun Nylon 6 nanofibers with 20wt% concentration

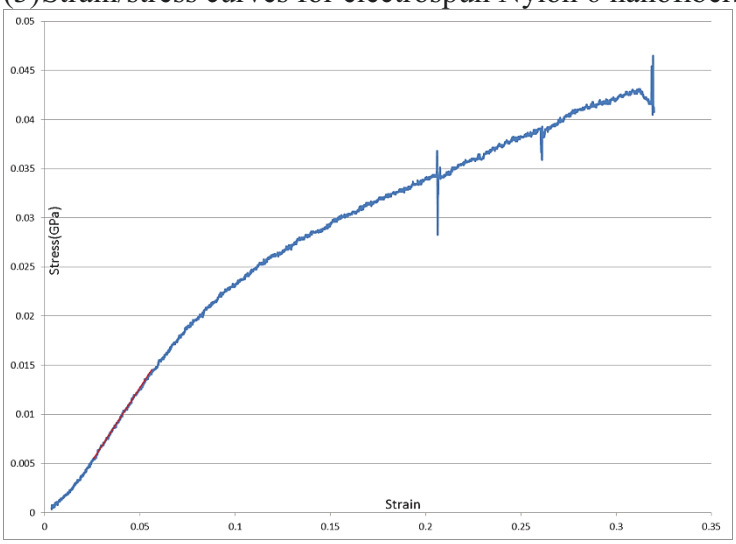

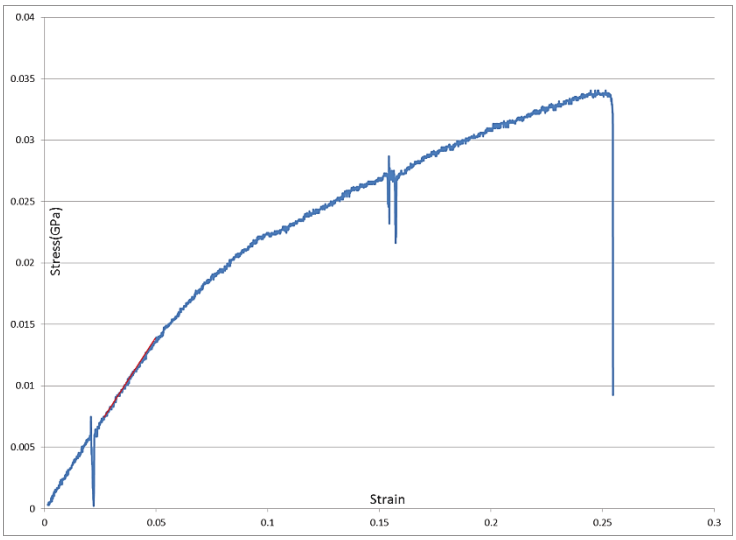

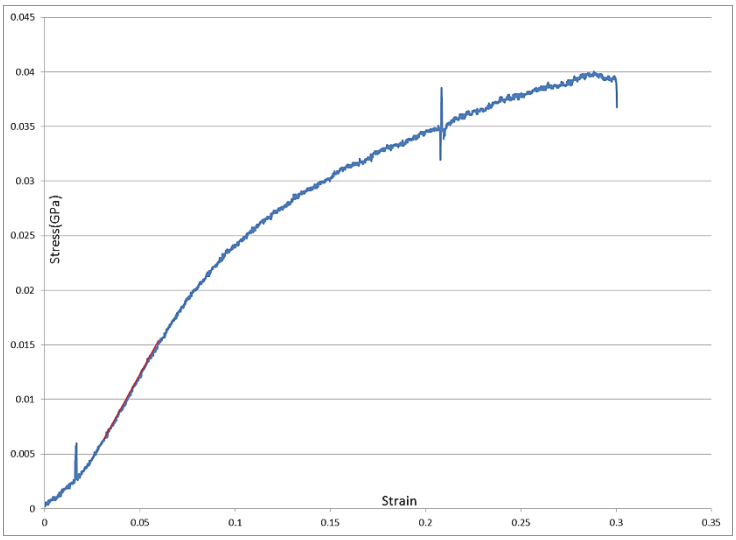

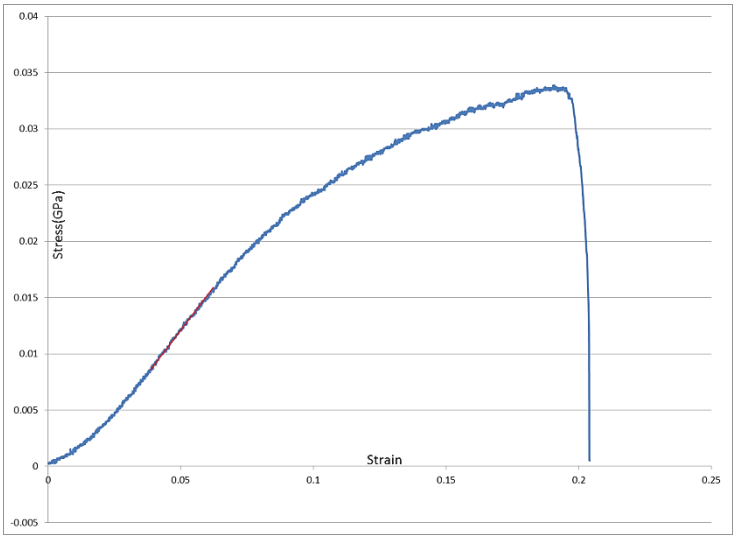
0.04
0.035
0.03
0.025
0.02
0.015
0.01
0.005
0
-0.005
Stress(GPa)
Strain
0
0.05
0.1
0.15
0.2
0.25

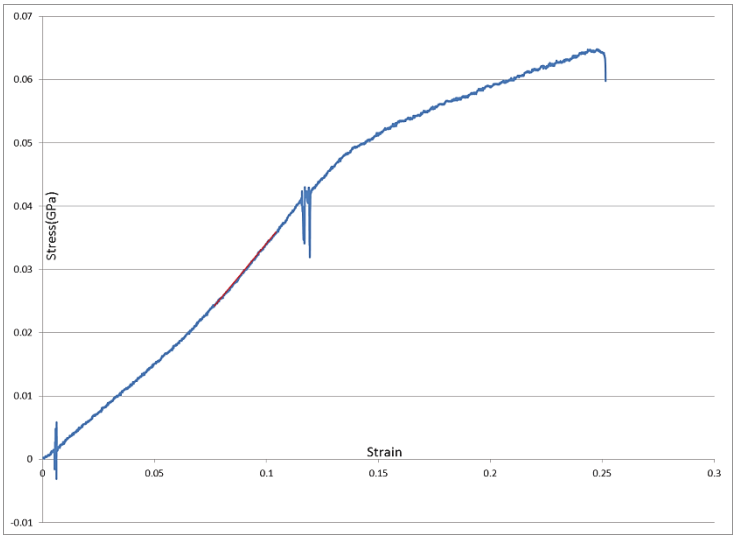
0.07
0.06
0.05
0.04
0.03
0.02
0.01
0
-0.01
Stress(GPa)
Strain
0
0.05
0.1
0.15
0.2
0.25
0.3

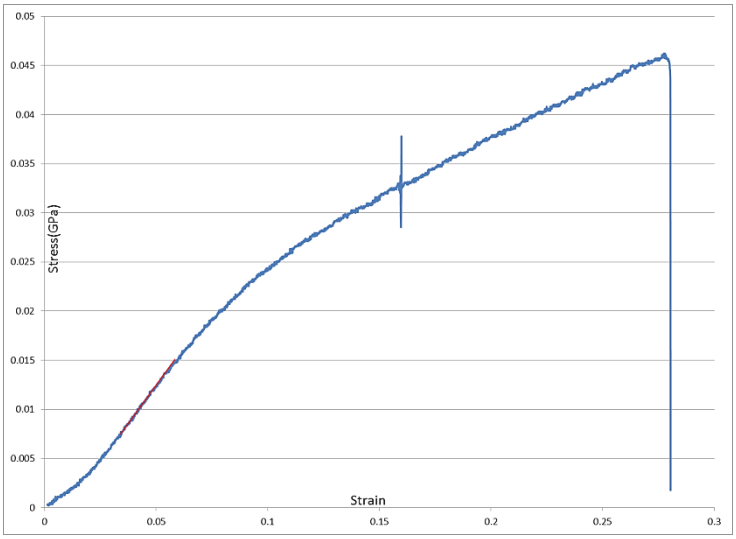
0.05
0.045
0.04
0.035
0.03
0.025
0.02
0.015
0.01
0.005
0
Stress(GPa)
Strain
0
0.05
0.1
0.15
0.2
0.25
0.3

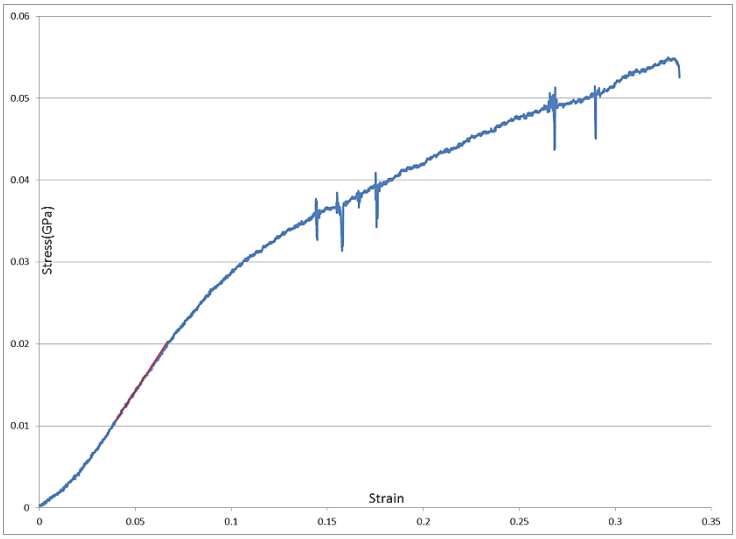
0.06
0.05
0.04
0.03
0.02
0.01
0
Stress(GPa)
Strain
0
0.05
0.1
0.15
0.2
0.25
0.3
0.35

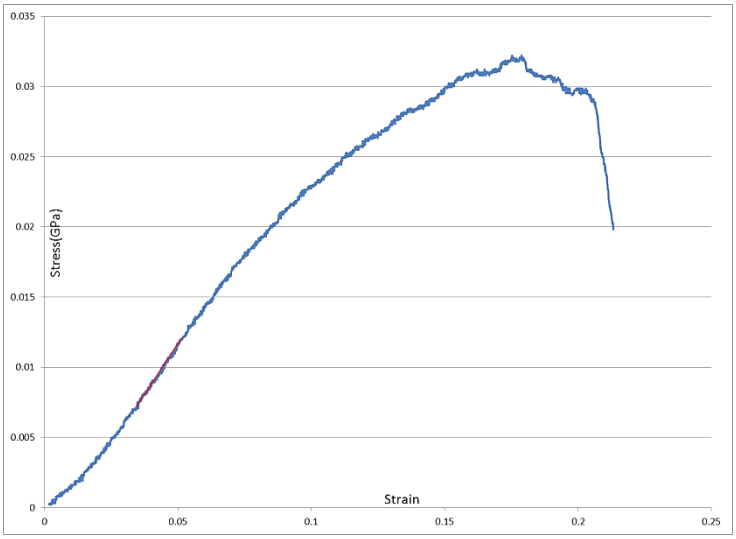
0.035
0.03
0.025
0.02
0.015
0.01
0.005
0
Stress(GPa)
Strain
0
0.05
0.1
0.15
0.2
0.25

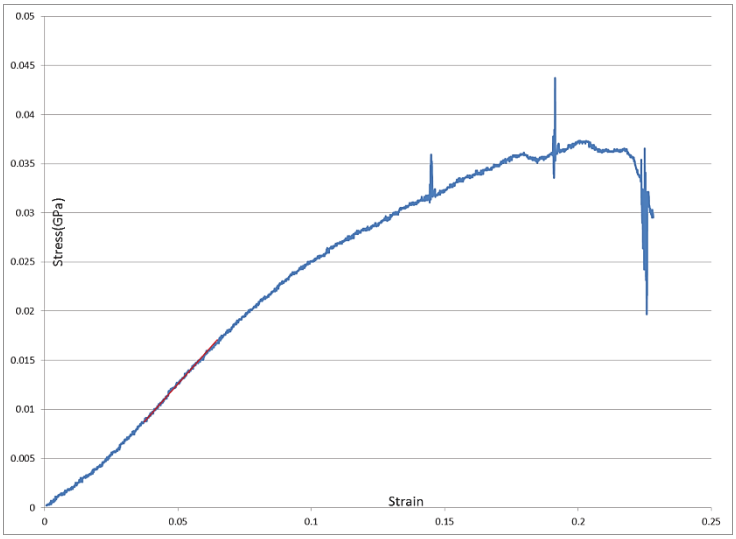
0.05
0.045
0.04
0.035
0.03
0.025
0.02
0.015
0.01
0.005
0
Stress(GPa)
Strain
0
0.05
0.1
0.15
0.2
0.25

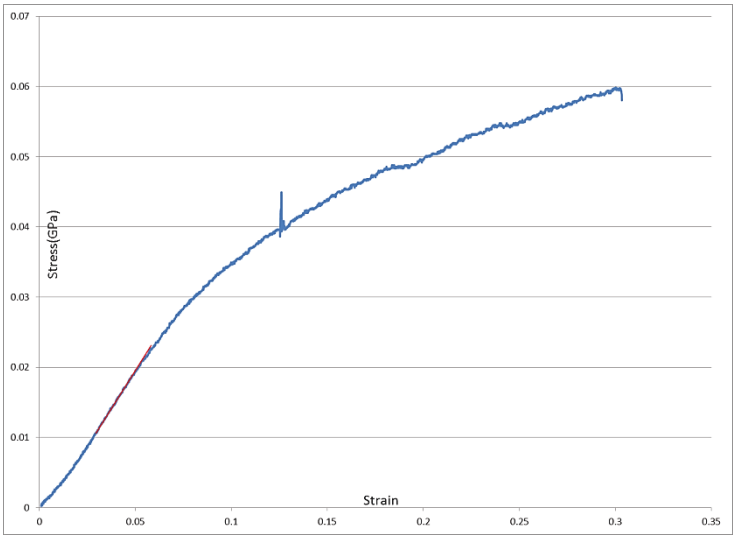
0.07
0.06
0.05
0.04
0.03
0.02
0.01
0
Stress(GPa)
Strain
0
0.05
0.1
0.15
0.2
0.25
0.3
0.35

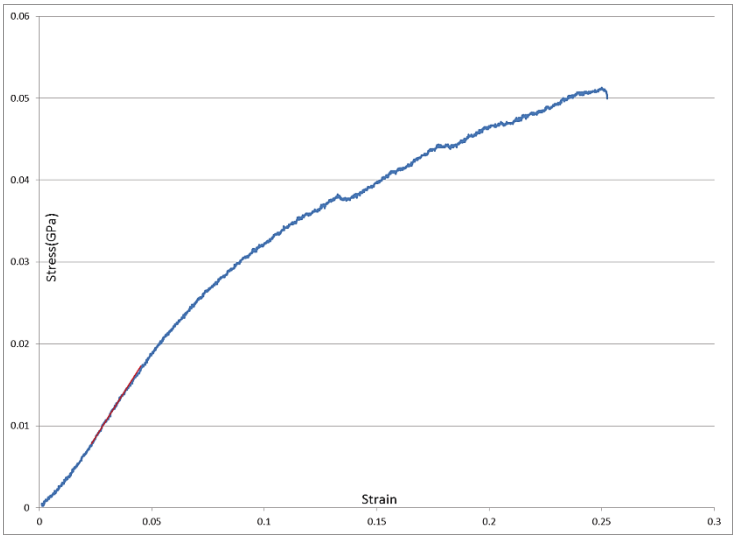
0.06
0.05
0.04
0.03
0.02
0.01
0
Stress(GPa)
Strain
0
0.05
0.1
0.15
0.2
0.25
0.3

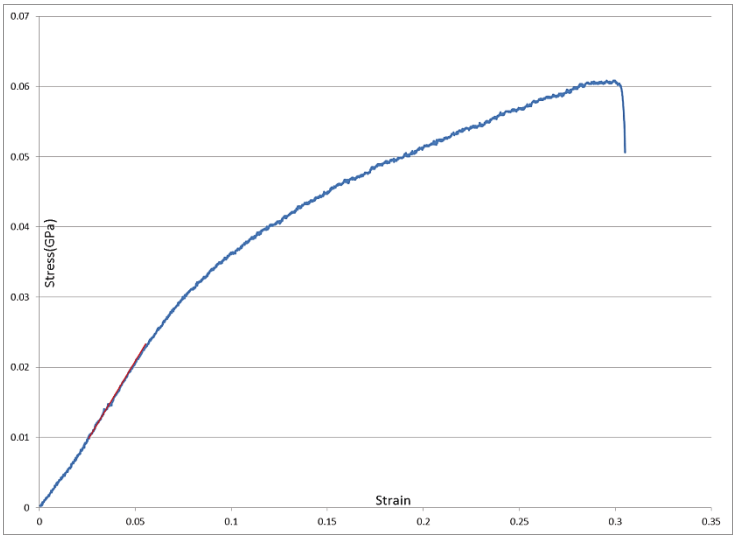
0.07
0.06
0.05
0.04
0.03
0.02
0.01
0
Stress(GPa)
Strain
0
0.05
0.1
0.15
0.2
0.25
0.3
0.35

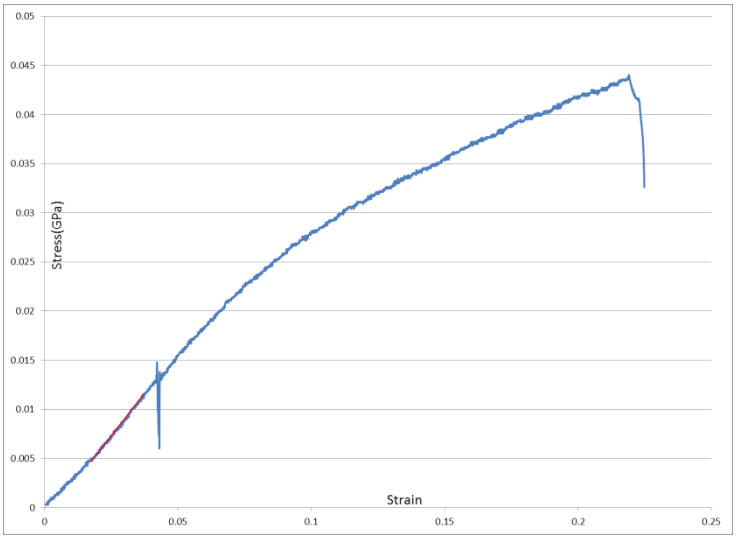
0.05
0.045
0.04
0.035
0.03
0.025
0.02
0.015
0.01
0.005
0
Stress(GPa)
0
0.05
0.1
0.15
0.2
0.25
Strain